METALLOPROTEIN ELECTRON TRANSFER MECHANISMS

Thesis by

Scot Edward Wherland

In Partial Fulfillment of the Requirements

For the Degree

of

Doctor of Philosophy

California Institute of Technology

Pasadena, California

1977

(Submitted September 10, 1976)

ACKNOWLEDGMENTS

This is a welcome opportunity to express to my parents my appreciation for the love, preparation, and encouragement they have given me. The preparation they gave me in values and work attitudes, and their unselfish encouragement to pursue my dreams, whatever they might be, have been my most basic strength and support.

Four people have been especially influential in my scientific education. From Leona Metzger I gained my first appreciation of the order in nature, and experienced a sincere encouragement to pursue a career in science. Wendell McCain provided a careful introduction to chemistry and effectively discouraged sloppy thinking. Ed Deutsch taught me to appreciate careful experimentation, a lesson which is easily missed. Harry Gray has taught me about the selection of scientific problems to study, and the importance of matching experiments to the level of knowledge.

I wish to express my particular and personal appreciation to Diane and Phil Cummins for their friendship, sensitivity, and encouraging example. Through our friendship I have matured and gained the personal confidence that I could never have gained through my work.

I acknowledge the National Science Foundation for a Graduate Fellowship (1973-76) which allowed me to complete this work in three years.

ABSTRACT

The rates of oxidation and reduction of various metalloproteins (several cytochromes c, azurin, plastocyanin, stellacyanin, and HiPIP) by inorganic reagents (including $Fe(EDTA)^{2-}$, $Co(phen)_3^{3+}$, $Fe(CN)_6^{3-/4-}$, derivatives of the latter two reagents, and $Ru(NH_3)_6^{2+}$) have been analyzed within the framework of the relative Marcus theory of outer-sphere electron transfer. This approach has allowed contributions to the overall free energy of activation (the specific activation of the reagent, the thermodynamic driving force for the reaction, and the general coulombic interactions of the reactants) to be factored out, leaving a quantity which is characteristic of the activation process the protein must undergo in order to transfer an electron with each reagent. These analyses have led to the definition of the "kinetic accessibility" of the electron transfer sites of several proteins, the order being stellacyanin $\gg$ plastocyanin $>$ horse heart cytochrome c $>$ Pseudomonas cytochrome c_{551} $>$ HiPIP $\cong$ Pseudomonas azurin. As the kinetic accessibility of the proteins decreases, the variety of apparent electron transfer mechanisms increases. It is concluded that the two most important factors in controlling the reactivity of redox proteins with inorganic reagents (after the three previously mentioned contributions are eliminated) are the availability of extended π orbital systems to facilitate orbital overlap and thus adiabaticity, and the capacity of the reagents to

penetrate the hydrophobic residues surrounding the metal sites in many proteins. Protein-protein electron transfer reactions are also considered, as are ionic strength and pH influences on the rate constants.

TABLE OF CONTENTS

TABLE OF CONTENTS (Continued)

CHAPTER 1. ELECTRON TRANSFER MECHANISMS EMPLOYED BY METALLOPROTEINS

I. Introduction

The electron transfer reactivities of metalloproteins are of current interest for several reasons. The biological function of the simple electron carriers, long recognized for the cytochromes[1] and more recently elucidated for some of the blue copper proteins,[2] is being further investigated in terms of the mechanism of the specificity between physiological redox partners; in addition, the more complex reaction-pathway problems of the multi-electron accepting, multi-substrate oxidases are beginning to be explored. The simple one electron carriers have been singled out for study as they are not expected to have as much of a substrate-accepting role as the oxidases or enzymes catalyzing covalent changes; furthermore, there are often only two forms of the protein which must be considered (oxidized and reduced). Although structural differences between these two forms may be expected, these may be studied conveniently by standard physical and chemical techniques. The workers in the field have come from different disciplines and have provided different approaches to the problems, but many recent advances have come from the laboratories of bioinorganic chemists[3] and others who have studied the reactions of electron transfer proteins with small inorganic redox reagents as well as with other redox-active biomolecules.

Three general classes of metalloproteins, the c type cytochromes, the iron-sulfur proteins, and the blue, type 1 copper only, proteins, have been frequently and extensively studied. A brief summary of the available three dimensional and electronic

structural information is appropriate. X-ray studies by Dickerson and coworkers[1] have established the essential features of the structures of both oxidized and reduced forms of horse heart cytochrome c. Further, some structural information on ferricytochrome c_{551} from Pseudomonas aeruginosa is also available.[1] In the structure of horse heart ferricytochrome c, a heme c group (Figure 1) is bound to the polypeptide chain through covalent sulfur linkages at Cys-17 and Cys-14, as well as by the axial iron ligands His-18 imidazole and Met-80 sulfur. A schematic representation of the structure in the vicinity of the heme group is shown in Figure 2. The heme group is buried in the hydrophobic interior of the protein, except for one edge (shown in boldface in Figure 2; rings 2 and 3 in Figure 1) which is near the surface. In the present discussion we shall refer to the 2,3-ring system as the "exposed heme edge". However, we hasten to note that the exact extent of exposure of this edge to solvent molecules and redox agents is a matter for speculation. Examination of the models of the ferricytochrome c structure suggests that the 2,3-edge is at least 1 Å below the protein surface and access to the region may be difficult for certain molecules. Both oxidized and reduced cytochromes c possess low-spin electronic ground states, corresponding to the metal orbital configurations $(t_{2g})^5$ and $(t_{2g})^6$, respectively. Outer sphere electron transfer of a t_{2g} electron is known to be facile, as minimal inner sphere reorganizational activation is required (vide infra). Thus, both steric and electronic considerations favor outer

Figure 1. Structural formula of heme c, showing the attachment to the protein from rings 1 and 2.

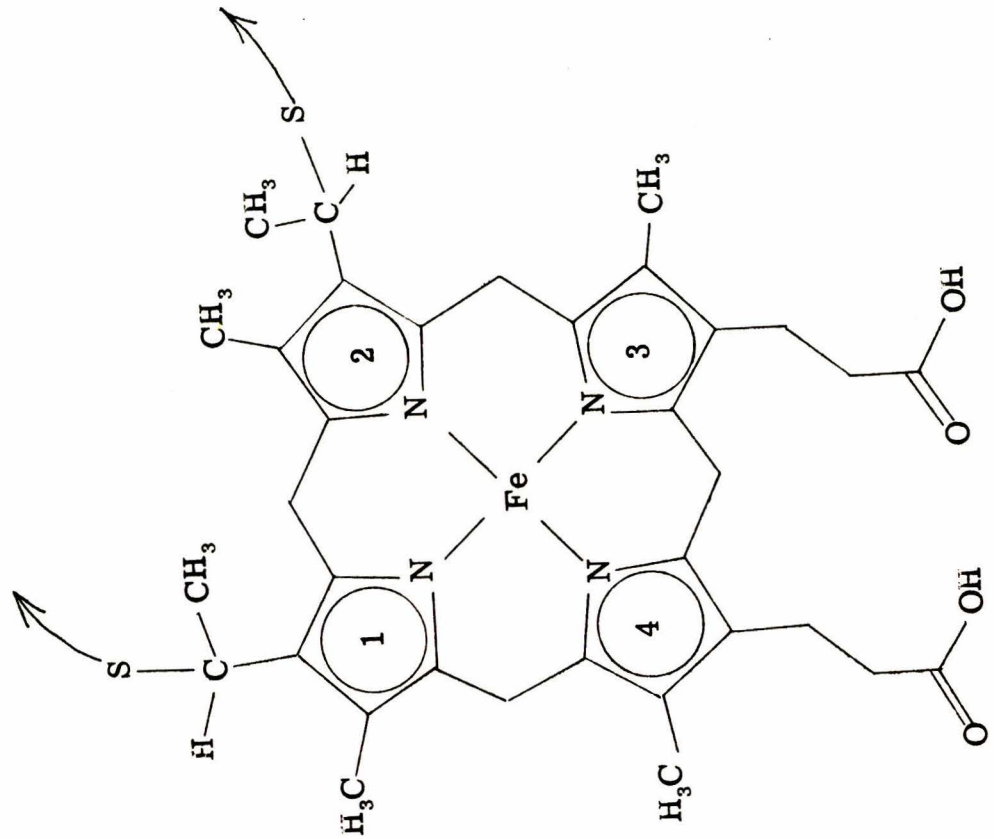
S
CH3
C
H
CH3
CH3
2
N
3
N
OH
O
Fe
S
CH3
C
H
1
N
N
4
OH
O
H3C
H3C

Figure 2. A schematic representation of cytochrome c in the vicinity of the heme (see ref. 1 for structural details).

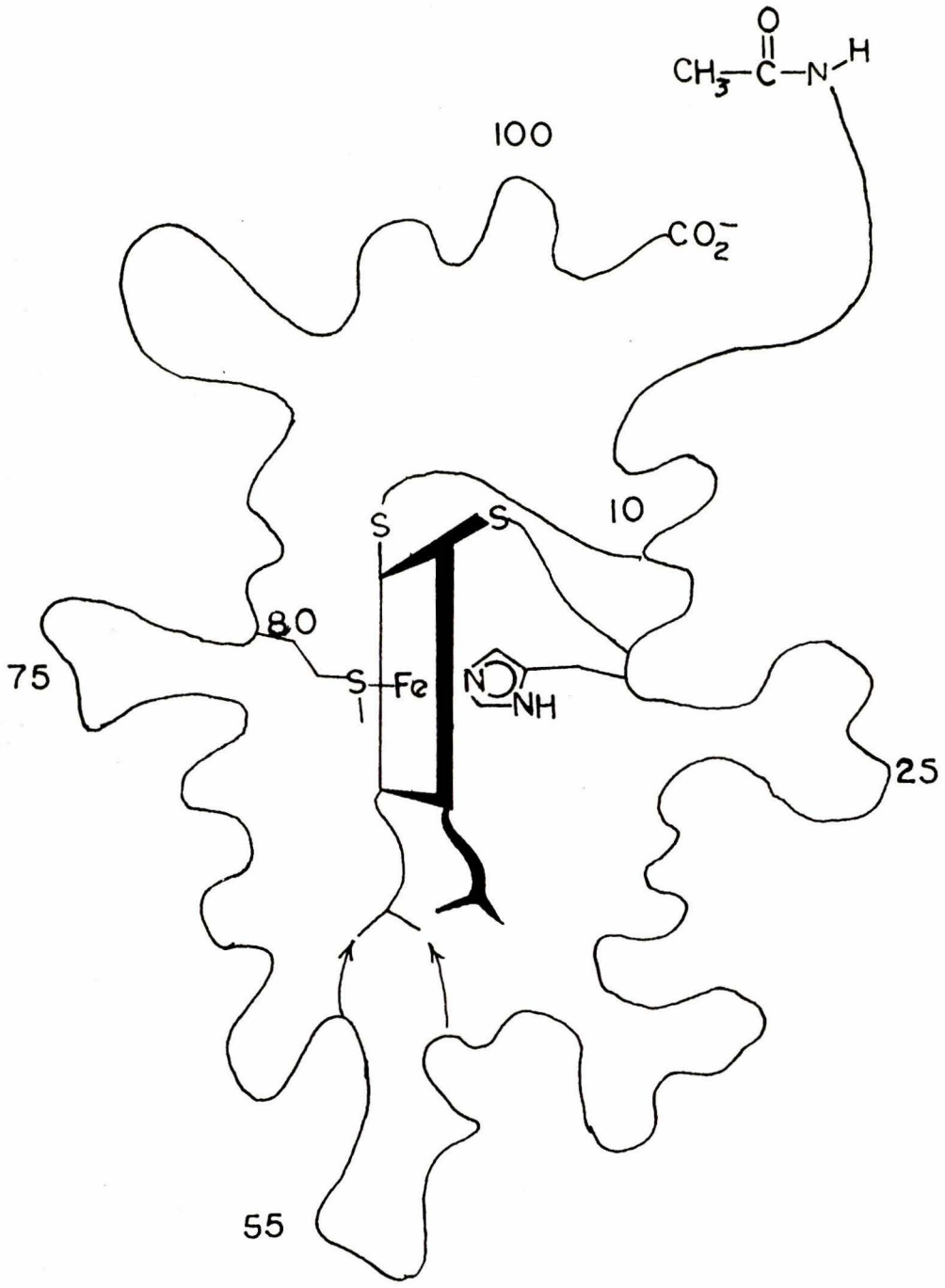
O
CH3—C—N—H
100
CO2−
10
S
S
80
75
S
Fe
N
NH
1
25
55

sphere electron transfer to and from the exposed heme edge as the mechanism of choice for cytochromes c. However, adjacent inner or outer sphere attack is not precluded, but must necessarily be accompanied by some type of conformational change in which the heme crevice is exposed to small molecules.

X-ray studies of the high potential-iron sulfur protein from Chromatium vinosum (HiPIP) show that the cube-like $Fe_4S_4S_4$* cluster is completely buried[4,5] with the closest distance from a protein surface to the edge of the cluster being about 3.5 Å (Figure 3).[6] HiPIP utilizes relatively nonbonding (e-type) orbitals[7] of the distorted tetrahedral FeS_4 centers (each Fe in the $Fe_4S_4S_4$* cluster is tetrahedrally coordinated to four S atoms) for electron transfer, and thus the activation requirements owing to inner sphere rearrangement are not expected to be large. As was the case for cytochrome c, therefore, structural considerations greatly favor outer sphere electron transfer as a pathway of choice in redox reactions involving HiPIP and other iron-sulfur proteins that contain tetrahedral FeS_4 centers.

X-ray crystal structure analysis has not been completed to date for any blue copper protein. The probability that the copper coordination environment is highly unusual, however, has long been recognized, as a result of various spectroscopic studies. A typical blue copper protein is characterized by an intense visible absorption band system,[2] which peaks at about 600 nm, as well as by an extremely small $A_{||}$ EPR spectral parameter. Neither of these

Figure 3. Illustration of the relatively buried Fe_4S_4* cluster in HiPIP (see ref. 4 for structural details).

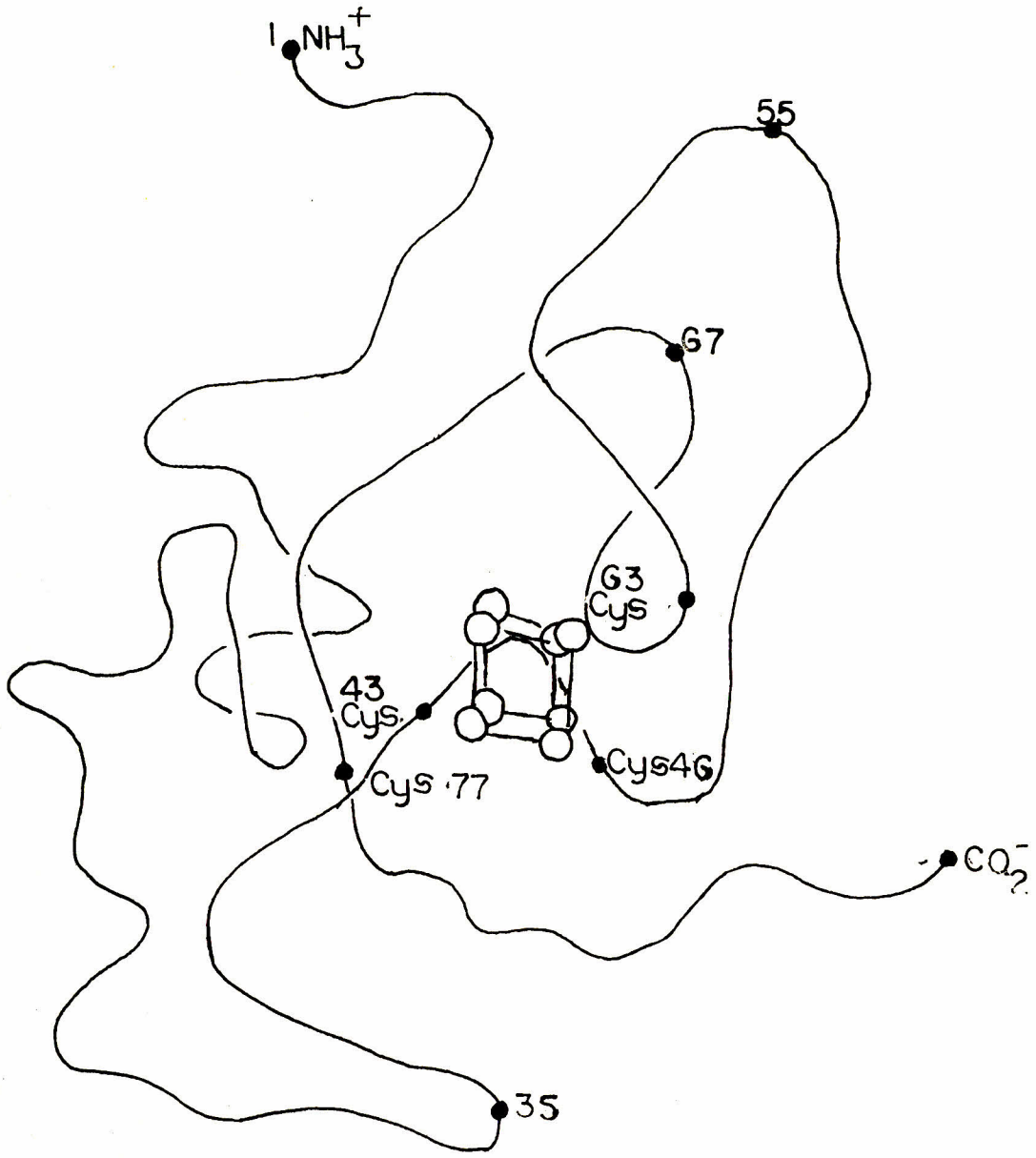
1 NH_3^+
55
G7
G3
Cys
43
Cys
Cys 77
Cys4G
CO_2^-
35

spectral properties has been duplicated satisfactorily in low molecular weight copper(II) complexes. As square planar copper(II) centers, in particular, exhibit optical and EPR spectra that are much different from those observed for the blue proteins, most models have featured geometries based on tetrahedral or five coordination. Two explanations of the intense, 600-nm absorption have been proposed. One treats the band as arising from one or more allowed d-d transitions in a noncentrosymmetric center, and the other attributes the strong absorption to a charge transfer process, probably of the ligand-to-metal type. Spectroscopic studies of cobalt(II) derivatives of Rhus vernicifera stellacyanin, bean plastocyanin, and Pseudomonas aeruginosa azurin have established that the charge transfer interpretation is to be preferred, as intense bands analogous to the 600-nm band system are observed between 300 and 350 nm in the cobalt(II) derivatives.[8,9,10] Furthermore, visible and near infrared absorption, circular dichroism (CD), and magnetic circular dichroism (MCD) spectra of the cobalt(II) derivatives of stellacyanin, plastocyanin, and azurin have been interpreted[11] successfully in terms of the d-d transitions expected for a high-spin d^7 ion in a distorted tetrahedral binding site. In recent work, the d-d transitions have been observed for the first time in near infrared absorption, CD, and MCD studies of the native copper forms of all three proteins.[10] The positions of the near infrared d-d transitions are fully consistent with a slightly flattened tetrahedral structure for the blue copper centers in the native proteins.

Research aimed at the identification of the ligands comprising the flattened tetrahedral blue copper center has been particularly intense in the case of plastocyanin. Direct evidence for a sulfur ligand has come from X-ray photoelectron spectral experiments on bean plastocyanin, where a large shift of the S2p core energy of a single cysteine (Cys-85) residue in the protein upon metal incorporation has been observed.[11] The two histidines in spinach plastocyanin have been found in NMR titration experiments to exhibit pK values below 5,[12] suggesting that they are coordinated to copper. It is reasonable to assume, therefore, that the analogous two residues in the bean protein, His-38 and His-88, are also ligands.[10] The fourth ligand in the proposed donor set for bean plastocyanin has been identified in extensive infrared spectral studies.[13] These experiments have revealed that a short section of helix in apoplastocyanin is strongly perturbed upon metal (Cu(II) or Co(II)) incorporation, thereby implicating a backbone peptide nitrogen or oxygen as a ligand. The preference of copper for nitrogen donors, as well as evidence from charge transfer spectra, favor coordination by a deprotonated peptide nitrogen. Consideration of the bean plastocyanin sequence places the helix, and therefore the backbone peptide nitrogen, a few residues above His-38.[14]

A model for the blue copper site in bean plastocyanin based on the available spectroscopic evidence is shown in Figure 4.[10] The other blue proteins are expected to have similar (although not necessarily identical) coordination environments. The observed

Figure 4. Proposed model of the blue copper site in bean plastocyanin (see ref. 10 for structural details).

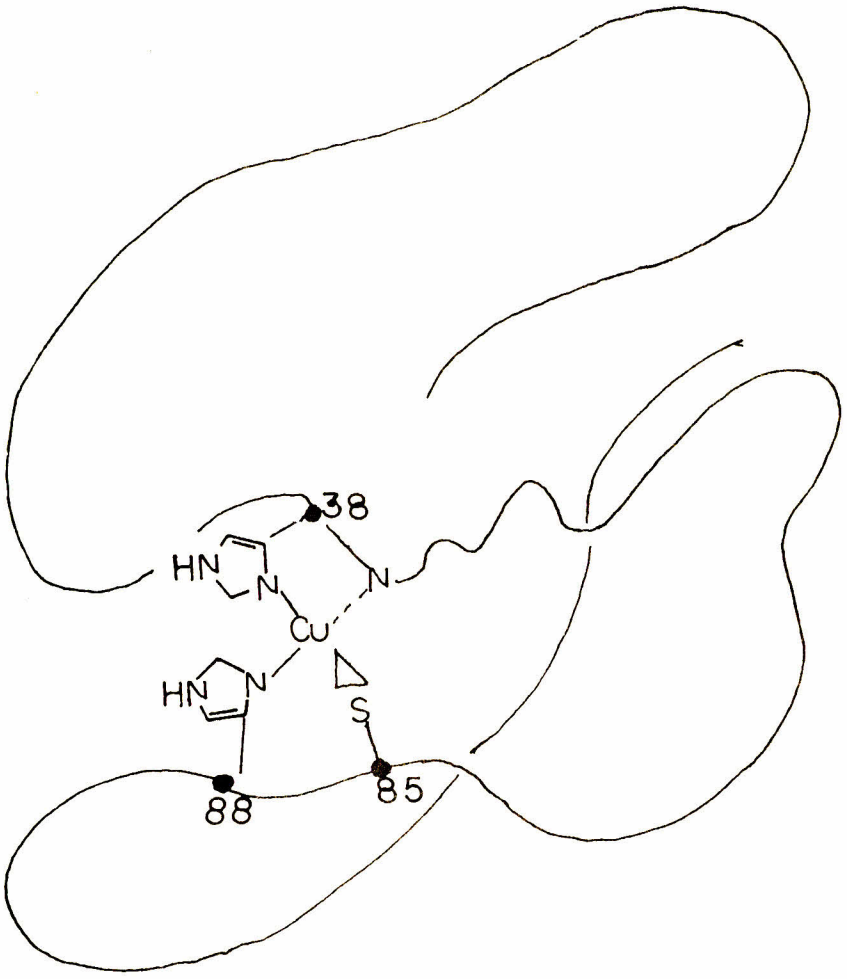
38
HN
N
N
Cu
HN
N
S
88
85

variation in spectroscopic parameters and reduction potentials could be accounted for by minor variations in ligand composition or coordination geometry of the blue copper center.[14] If the flattened tetrahedral geometry is correct for blue copper proteins, then once again we have a situation in which inner-sphere reorganization associated with electron transfer (between Cu(II) and Cu(I) states) is minimized, and facile outer-sphere electron transfer is to be expected. Furthermore, there is reason to believe that certain blue copper sites (especially that of azurin[15-17]) are substantially buried in hydrophobic protein interiors, and are therefore relatively inaccessible to solvent and other small molecules.

Before discussing the available kinetic data on these proteins, certain problems need to be considered. One problem that arises when comparing the reactions of a single protein with different reagents is associated with variations in the thermodynamic driving force. As free energy/reactivity relationships are expected to exist, the question of the type of correlation between rate constants and driving force must be considered. This correlation may be expected to be quite different for coupled systems (e.g., cytochrome oxidase), which are designed to use the excess free energy available from an oxidation-reduction cycle, than for the simple electron carriers. The enthalpy and entropy components of the free energy difference should also be considered. The nature of the interaction between the oxidant and reductant must be appraised, and evidence for binding sought ; whether or not the interaction is such as to lead to measurable binding, electrostatic and non-electrostatic interactions

between the reactants are expected to lead to differences in rates, and these differences might be correlated with trends in the enthalpy and entropy of activation as well as with the overall rate constant. Further variables include steric constraints, affecting the distance over which the electron may be transferred, which for a protein may be dynamic and part of the reaction path (and therefore reflected in the rate law and activation parameters), or static but still variable with changes in pH of the medium or salt content. Other effects of changing the medium may also be important; the coulombic interaction between the reactants is expected to vary with the salt content of the solvent, specific activators or inhibitors for the proteins may exist, the pH and the buffer type may be influential, and the availability of bridging anions, even in outer sphere cases, is expected to have an influence on the rate which may be interpreted. The symmetry of the redox orbitals of the electron donor and acceptor and the match between them should be considered, and may be varied. The inherent protein reactivity is also a variable, and with the help of the above considerations this variable (for the same protein with different reagent as well as for different proteins) should also be considered and might be isolated.

The above problems are greatly compounded when both the oxidant and reductant are proteins; therefore, several workers have used small molecule oxidants and reductants to probe the reactivity of redox proteins. The small molecule reagents are generally more readily available in quantity than the proteins, and many

changes can be made in their structures with predictable effects. By a careful selection of reagents, inner or outer sphere reactivity may be selected or at least favored, the redox potential of the reagent and thus the free energy change of the reaction may be controlled, the size and hydrophobic or hydrophilic nature of the reagent may be varied by introducing changes in the structure, the charge of the reagent, and the reactivity of the reagent (as measured by its electron self-exchange rate) may be varied. Although both inorganic and organic reagents are available, inorganic complexes are somewhat more convenient, as they have characteristic spectral changes and usually are one electron donors or acceptors (many commonly-used organic systems are two electron reagents and produce reactive free radicals on one electron transfers). After separating protein from reagent effects by judicious choices of reagents and conditions, the results of protein-protein reactions may be more critically examined.

II. Theory

A. Inner and Outer Sphere Mechanisms

The distinction between inner sphere (including remote attack) and outer sphere mechanisms is a classical one in inorganic chemistry and there are several monographs and review articles available,[18,19] including one by Bennett which discusses bio-inorganic examples up to 1973.[3] A requirement for a strictly inner sphere reaction is that one of the reactants must possess an open coordination position and the other center must have a first coordination sphere ligand atom accessible for bridging. The

requirements for remote attack are not so stringent in that all must be available on the second reactant is a coordination position somewhere on a ligand. Outer sphere reactions are those that involve an electron transfer in which no ligands are shared between the two redox centers. An outer sphere reaction is virtually assured if the protein metal center is buried and does not include a ligand which reaches to the protein surface. Even if there is such a ligand (like a heme) there still must be an available coordination site on it and an available position on the attacking reagent.

B. Marcus Theory

Outer sphere electron transfer reactions are among the simplest to consider theoretically because no bonds are made or broken; accordingly, several theories for treating such reactions from first principles are available. The most useful theory is due to Marcus.[20] The result from this treatment that will be used here is not the one for an a priori calculation of rate constants but rather a correlation equation for relating the cross reaction rate constant between two species to the equilibrium constant, the self-exchange rate constants for the two reactants, and a term which evaluates to about one for reactions with small driving force. This equation is

$$k_{12} = \sqrt{k_{11}k_{22}Kf} \qquad (1)$$

where K is the equilibrium constant, k_{11} and k_{22} the two self-exchange rate constants, k_{12} the cross reaction rate constant, and

$$\ln f = (\ln K)^2/4\,(\ln (k_{11}k_{22}/Z^2)) \qquad (2)$$

The value of Z, the collision frequency of neutral molecules in solution may be estimated from the simple kinetic theory of gases, if diffusion is truly random,[21] and is found to be roughly constant for the reactions of interest. The theory can include corrections for adiabaticity by substituting k_{12}/p_{12}, k_{11}/p_{11}, and k_{22}/p_{22} for k_{12}, k_{11}, and k_{22}, respectively, where p is 1 for an adiabatic reaction and less than 1 for nonadiabatic reactions. Equation 1 is valid if all reactions are adiabatic ($p_{12} = p_{11} = p_{22}$) or if all are uniformly non-adiabatic ($p_{12}^2/p_{11}p_{22} = 1$). The Marcus relationship has been extensively applied in the inorganic literature, especially by Sutin and coworkers,[22] and found to be generally valid except in some cases involving cobalt amine and aquo complexes. As it will be used here, the Marcus relationship will allow compensation for differences in driving force and differences in the inherent reactivity of the reagents being used. For this purpose, the equation may be rearranged to give (for 25 °)

$$k_{11} = k_{12}^2/k_{22}K = k_{12}^2/k_{22} \exp (38.94 (\Delta E)) \qquad (3)$$

where ΔE is the potential difference in volts

As used here and from this point on, the subscript 2 will refer to the small molecule reagent or the protein for which a self-exchange rate constant is assumed, and the subscript 1 will be for the protein for which a self-exchange rate constant is calculated. As presented above, the correlation is essentially one of free energies of activation, but with enough information the individual enthalpy and entropy

components of the activation and equilibrium components may be treated separately.

As k_{11} values calculated using the Marcus theory equations will be used extensively in the data treatment, some more discussion of what this parameter means is warranted. First, assuming to begin with that the equation is valid, the result is only as good as the parameters which go into calculating it. The precision of the parameters will be discussed later, but it should be reiterated here that each small molecule reagent is assumed to have only one mechanism of electron transfer available, the one that is characterized by its self-exchange rate constant and activation parameters. The k_{11} calculated, then, is a quantity that characterizes the activation process (including inherent activation of the protein metal center and certain contributions from the interaction of the protein and the reagent) the protein must undergo to transfer an electron, assuming no other limiting process is involved. Thus if the redox reaction of two different reagents with the same protein leads to the same predicted k_{11} (and its activation parameters), it follows that the electron transfer mechanism is the same for the two reactions, barring fortuitous compensation. If k_{11} values vary significantly, the electron transfer mechanisms are expected to differ correspondingly.

Predicted protein self-exchange rate constants above the diffusion controlled limit may (and do) occur; diffusion control would of course set in and prevent such high rates from being attained; however, if two predicted exchange rate constants are significantly different and both above the diffusion limit, the conclusion is still

that the two mechanisms are different. The actual protein exchange rate, in those few cases where it has been measured does not "prove" or "disprove" the predictions made from other reactions, it merely represents a mechanism that may or may not be the same as the others that have been studied.

C. Electrostatic Interactions

The electrostatic interaction between the two reacting species has been ignored in the above presentation of the Marcus equations, as is the custom for simple inorganic reactions. The justification for this in the simpler systems is that reactions between reagents of similar charge type require little if any correction and most simple inorganic reactions are between ions of similar radius and charge (often $+2/+3$). For the protein reactions, however, the protein often is not of the same charge type as the reagent, and the electrostatic interactions can no longer be ignored. In the discussion below, several alternative analyses of the problem of electrostatic interaction will be presented. These theories will in general be quite simplified, and it should be possible, given the large amount of structural and ion binding information available for several of the proteins under consideration (especially horse heart cytochrome c) and using more precise equations than those of simple Debye-Hückel theory, to make a much more detailed analysis; however, the primary goal at this point is the development of an approximate calculational method for charge effects, using experimentally available data, which may be applied to proteins for which little structural data are available.

The most often discussed manifestation of electrostatic interactions is the ionic strength dependence of reactions between ions. In the most common theoretical treatment, the transition state formalism is used and the ionic strength dependence is treated as the result of the changing activity coefficients of the reactants and the transition state with ionic strength.[23] Assuming the Debye-Hückel treatment for these activity coefficients, the resulting equation is

$$\ln k = \ln k_0 - \frac{Z_1^2 \alpha\sqrt{\mu}}{1 + \beta R_1\sqrt{\mu}} - \frac{Z_2^2 \alpha\sqrt{\mu}}{1 + \beta R_2\sqrt{\mu}} + \frac{(Z_1 + Z_2)^2 \alpha\sqrt{\mu}}{1 + \beta R_{\ddagger}\sqrt{\mu}} \quad (4)$$

where k is the rate constant at ionic strength μ, the Z's are the charges on the reactants, the R's are the radii of the reactants (1 and 2) and the transition state ($\ddagger$), and α and β are constants with values 1.17 (water, 25°) and 0.329 Å^{-1}, respectively. If it is assumed that the radii of the protein and the activated complex are the same, ($R_1 = R_{\ddagger}$) the equation reduces to

$$\ln k = \ln k_0 + \frac{(2Z_1Z_2 + Z_2^2)\alpha\sqrt{\mu}}{1 + \beta R_1\sqrt{\mu}} - \frac{Z_2^2 \alpha\sqrt{\mu}}{1 + \beta R_2\sqrt{\mu}} \quad (5)$$

This reduces to the oft-quoted equation

$$\ln k = \ln k_0 + 2Z_1Z_1\alpha\sqrt{\mu} \quad (6)$$

only if all radii are assumed to be the same and the ionic strength is such that $1 \gg \beta R\sqrt{\mu}$.

Another approach to treating the ionic strength dependence of electron transfer reactions is to use the equations of Marcus theory and an appropriate function for the coulombic interaction.[24] First, the free energy change for the cross reaction, ΔG_{12}^{0}, can be separated into an electrostatic contribution, w^{0}, and a term independent of electrostatic interactions, ΔG_{r}^{0}, and thus

$$\Delta G_{12}^{0} = \Delta G_{r}^{0} + w^{0} \tag{7}$$

The w^{0} term in turn may be expressed as the difference between the electrostatic work to bring the reactants together, w_{12}, and that to bring the products together, w_{21},

$$\Delta G_{12}^{0} = \Delta G_{r}^{0} + w_{12} - w_{21} \tag{8}$$

Similarly, the three activation free energies, ΔG_{12}^{*} for the cross reaction, and ΔG_{11}^{*} and ΔG_{22}^{*} for the two electron exchange rate constants may be expressed as the sum of work and electrostatics-independent terms

$$\Delta G_{11}^{*} = \Delta G_{11}^{**} + w_{11} \tag{9}$$

$$\Delta G_{22}^{*} = \Delta G_{22}^{**} + w_{22} \tag{10}$$

$$\Delta G_{12}^{*} = \Delta G_{12}^{**} + w_{12} \tag{11}$$

For the cross reaction, the part of the activation energy that is independent of electrostatic effects is expressed

$$\Delta G_{12}^{**} = (\Delta G_{11}^{**} + \Delta G_{22}^{**} + \Delta G_r^{0})/2 \qquad (12)$$

$$= (\Delta G_{11}^{*} + \Delta G_{22}^{*} + \Delta G_{12}^{0} - w_{12} + w_{21} - w_{11} - w_{22})/2$$

The predicted cross reaction activation free energy is then

$$\Delta G_{12}^{*} = \Delta G_{12}^{**} + w_{12}$$

$$= (\Delta G_{11}^{*} + \Delta G_{22}^{*} + \Delta G_{12}^{0} + w_{12} + w_{21} - w_{11} - w_{22})/2 \qquad (13)$$

Solving for the predicted protein self-exchange activation energy results in the equation

$$\Delta G_{11}^{*} = 2\Delta G_{12}^{*} - \Delta G_{22}^{*} - \Delta G_{12}^{0} - w_{21} - w_{12} + w_{11} + w_{22} \qquad (14)$$

This formalism can also include the correction term f, which in this treatment is expressed through a term $1 + \alpha^{**}$

$$\Delta G_{12}^{**} = \tfrac{1}{2}(\Delta G_{11}^{**} + \Delta G_{22}^{**} + \Delta G_r^{0} (1 + \alpha^{**})) \qquad (15)$$

where α^{**} is defined by Eq. 16:

$$\alpha^{**} = \frac{\Delta G_0{}^{r}}{4(\Delta G_{11}^{**} + \Delta G_{22}^{**})} \qquad (16)$$

Solving for ΔG_{11}^{**} gives an equation of the form

$$A(\Delta G_{11}^{**})^2 + B(\Delta G_{11}^{**}) + C = O \qquad (17)$$

where

$$A = 4 \tag{18}$$

$$B = 8\Delta G_{22}^{**} + 4\Delta G_0^{r} - 8\Delta G_{12}^{**} \tag{19}$$

$$C = 4\Delta G_{22}^{**} + \Delta G_0^{r} - 2\Delta G_{12}^{**}) + (\Delta G_r^{0})^2 \tag{20}$$

which can be solved for ΔG_{11}^{**}, using the substitutions from above for ΔG_{11}^{**}, ΔG_{22}^{**}, and ΔG_0^{r}, thus k_{11}. In order to calculate free energies from rate constants and potential differences (and vice versa), the following equations are useful

$$\Delta G^* = RT[23.76 - \ln(R/T)] \tag{21}$$

$$= 592.1\ (29.45 - \ln k)\ (T = 298\ K)$$

$$\Delta G_{12}^{0} = -23.06\ (\Delta E)\ \text{kcal/mole}\ (\Delta E \text{ in volts}) \tag{22}$$

$$k = 6.21\ (10^{12})\ \exp\ (-\Delta G^*/0.5921)\ (T = 298\ K)$$

The terms that must be calculated in order to evaluate the above equations represent the work required to bring the two reactants from infinite separation to the separation in the activated complex. As this problem will prove difficult enough to handle, further refinements, such as protein conformation and charge distribution changes on forming the activated complex, will not be considered. The possible importance of changes in charge distribution and dipole interactions is documented[25] and should be considered in more detailed calculations.

The simplest model for making this calculation considers the protein to be a sphere with a totally symmetric charge distribution. The dielectric within the sphere is lower than that of the medium, but its value is not required, nor is the actual detailed charge distribution required as long as it is totally symmetric, concentric with, and located within the region of low dielectric.[26] The equation for the potential is[27]

$$V = \tfrac{1}{2}\left[\frac{e^{\kappa R_1}}{1 + \kappa R_1} + \frac{e^{\kappa R_2}}{1 + \kappa R_2}\right] \frac{Z_1 Z_2 e^2}{\epsilon} \frac{e^{-\kappa r}}{r} \qquad (23)$$

where $\kappa = \alpha \mu^{\frac{1}{2}} \text{Å}$ at 25° in water.

R_1 = radius of the protein at the distance of closest approach by the average small ion in solution

R_2 = radius of reagent, defined as is R_1

Z_1 = charge on the protein

Z_2 = charge on the reagent

ϵ = dielectric constant of the medium (78.3 for water at 25°)

r = distance between the centers of the reagent and protein in the activated complex

e = charge on an electron

This equation reduces to

$$V = 2.1175 \left[\frac{e^{\kappa R_1}}{1 + \kappa R_1} + \frac{e^{\kappa R_2}}{1 + \kappa R_2}\right] \frac{Z_1 Z_2}{R_1 + R_2} e^{-\kappa(R_1 + R_2)} \qquad (24)$$

when the values of the constants are substituted. For the calculations to be done in subsequent sections, r is approximated as the sum of

the radii of the protein and reagent. Figure 5 illustrates the free energy terms according to this model.

The remaining problem that must be solved before the equations may be evaluated is the selection of the R and Z parameters; for the small molecule reagents, these values are easily determined from the molecular formula and X-ray structural data or model building. For proteins, the radius may be estimated from Eq. 25[28]:

$$R^3 = \frac{3}{4\pi} \frac{M}{N} (\bar{\nu}_2 + \delta_1 \nu_1^0) \qquad (25)$$

where

R	= radius	$\bar{\nu}_2$	= partial specific volume (recriprocal of the density)
M	= molecular weight		
N	= Avogadro's number	ν_1^0	= partial specific volume of water
δ	= effective solvation		

The protein partial specific volume is taken as 0.73 cm^3/g unless a measured value is available, the solvent partial specific volume is 1.0 cm^3/g, and the effective solvation is 0.2. With these substitutions, the radius in angstroms is

$$R = 0.717\, M^{\frac{1}{3}} \qquad (26)$$

The charge on the protein may be crudely estimated from the amino acid composition. The maximum number of charged groups (at pH 7) is estimated assuming all of the glutamates and aspartates are ionized, that all the lysines are protonated, and that arginine is in its monopositive form. It is further assumed that

Figure 5. The free energy terms in the Marcus calculation. The circles represent the hard sphere, smeared-out charge models used in the electrostatic calculation. The M terms represent the different in free energy between the actual species and those assumed in the electrostatic calculation. These terms have been assumed to be zero in the calculation.

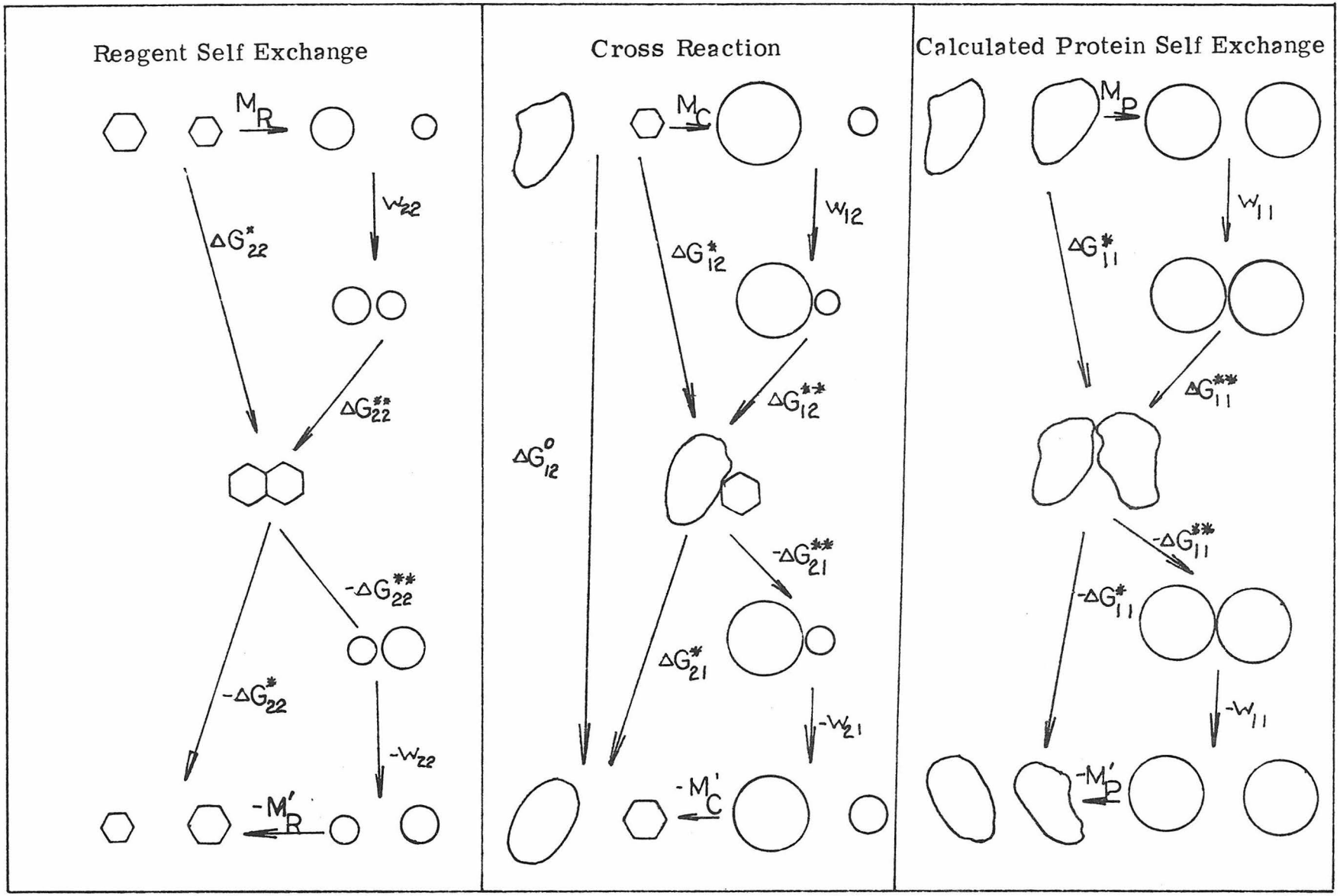
Reagent Self Exchange
M_R
w_{22}
ΔG^{*}_{22}
ΔG^{**}_{22}
$-\Delta G^{**}_{22}$
$-\Delta G^{*}_{22}$
$-w_{22}$
$-M'_R$
Cross Reaction
M_C
w_{12}
ΔG^{*}_{12}
ΔG^{**}_{12}
ΔG^{o}_{12}
$-\Delta G^{**}_{21}$
ΔG^{*}_{21}
$-w_{21}$
$-M'_C$
Calculated Protein Self Exchange
M_P
w_{11}
ΔG^{*}_{11}
ΔG^{**}_{11}
$-\Delta G^{**}_{11}$
$-\Delta G^{*}_{11}$
$-w_{11}$
$-M'_P$

half of the histidines are protonated; this last assumption may be somewhat of an overestimate but will be retained for simplicity in the light of the approximate nature of the whole approach. Further charged groups could include amino sugars (if they are not acetylated), the propionate side chains and deprotonated nitrogens on the heme group, the sulfides in the iron-sulfur proteins, any residues that have their pK's shifted by coordination to the metal or as a result of being located in a hydrophobic region (for the polar residues), and the metal itself. The contribution to the total charge from the metal and its ligands can be expected to be small, as is the case for well known examples. Such sites are constituted with low charges, as they are usually buried in the low dielectric of the protein interior. For example, the iron center in a heme protein is effectively neutralized by the two deprotonated nitrogens of the heme; in HiPIP with four thiolates and four sulfides, the oxidized cluster (assuming a charge of +11 from the four irons) has a charge of -1 on the oxidized and -2 on the reduced form. The copper proteins are less well characterized, but assuming a cysteine sulfur, the charge is at most +1 on the oxidized form and may be zero if a deprotonated amide is one of the ligands. The principle that the coordination site is formed so as to neutralize the charge on the metal ion may well be of general validity, at least for sites which prove to be buried, because of the high thermodynamic cost of having charged sites in a low dielectric medium.

An expression for the ionic strength dependence of the rate constant will now be derived. The free energy of activation for the cross reaction is

$$\Delta G_{12}^{*} = \tfrac{1}{2}(\Delta G_{11}^{**} + \Delta G_{22}^{**} + \Delta G_{r}^{0}) + w_{12} \quad (27)$$

where the only ionic strength dependent term is w_{12}. Substituting from Eq. 24 for the work terms and converting to rate form this becomes

$$\ln k = \ln k_0 - 3.576 \left[\frac{e^{-\kappa R_2}}{1 + \kappa R_1} + \frac{e^{-\kappa R_1}}{1 + \kappa R_2} \right] \frac{Z_1 Z_2}{R_1 + R_2} \quad (28)$$

(where the radii of both the reagent and the protein are assumed invariant and k_0 is the rate constant at infinite ionic strength). This equation can be compared with Eqs. 5 and 6. The expression for the ionic strength dependence that originates from the Marcus theory treatment is preferable in terms of internal consistency when the value of the charge on the protein is sought (from ionic strength dependence data) in order to correct for the work terms in the calculation of protein self-exchange rate constants (k_{11}) from cross reaction data.

In the discussions above, the protein has been considered as a sphere of uniformly distributed charge; another model that could be considered when adequate information exists to parametrize it includes provision for an active site. In this model, the whole protein charge is divided between the site, with a given charge and radius, and the rest of the protein with the remaining charge and the full radius. Each of these spheres is treated independently with the

same functions presented above.

It should be mentioned here that the general approach of treating the effects of ions using the ionic strength as the relevant variable is inaccurate away from the low ionic strength regime where the Debye-Hückel expressions are rigorously valid. Data at higher ionic strengths (above 0.1 M) have been successfully treated[29] when interaction parameters between all anion-cation pairs are included in the expressions, and with the use of ion association constants. These latter treatments involve many parameters and would be studies unto themselves if they were to be extended to the protein systems. They are only mentioned to emphasize the highly approximate nature of the ionic strength treatment and indicate a possible direction for future investigation.

In the discussion of electron transfer reactions, the overall reaction is often broken into three steps: (1) the formation of the precursor complex, (2) the electron transfer within this complex to form the successor complex, and (3) the dissociation of the successor complex to give the individual products. The formation constants for the precursor complexes are often too small to appear in the rate law (i.e., no saturation behavior is observable), but under the assumption that the binding is purely electrostatic, these constants may be estimated from the equation[22]

$$K = \frac{4\pi N r^3}{3000} \exp(-U(r)/RT) \quad (29)$$

$$U(r) = \frac{Z_1 Z_2}{\epsilon r(1 + \kappa r)} \quad (30)$$

where r is the distance between the centers of the reactants and the rest of the symbols have already been defined. When the precursor complex is formed quickly compared to the electron transfer rate, so that the equilibrium between reactants and the precursor complex is maintained throughout the reaction, the observed rate constant may be written

$$k_{obsd} = K k_{et} \quad (31)$$

where k_{et} is the unimolecular electron transfer rate constant for the conversion of the precursor to the successor complex. This method of treating the electrostatic effects is required in the extreme case of a long-lived precursor complex, whereas the previously-presented work term description is proper when the precursor complex is extremely short-lived. The dividing line between the two cases is not a clear one, except in those cases where saturation is observed in the kinetics. As with the work term formulation, if the precursor and successor complex theory is used, it must be used consistently for all rate constants being considered. When this is done the Marcus cross reaction equation becomes[20]

$$k_{12} = \left[\frac{P_{12}P_{21}k_{11}k_{22}K_{12}f}{P_{11}P_{22}}\right]^{\frac{1}{2}} \qquad (32)$$

$$\ln f = (\ln K_{12}P_{21}/P_{12})^2/4 \ln(k_{11}k_{22}/P_{11}P_{22}Z^2) \qquad (33)$$

where P_{11}, P_{22}, and P_{12} are the stability constants for the three precursor complexes and P_{21} is the stability constant for the cross reaction successor complex (the precursor complex for the reaction in the opposite direction). Equation 32 reduces to Eq. 1 when $P_{12}P_{21} \cong P_{11}P_{22}$.

D. Hydrophobic Effects

Another category of possible interactions between the reactants in an electron transfer reaction will be referred to as hydrophobic effects. For the purposes of this discussion this category will include most of the interactions that are not coulombic, including the nonpolar interactions between hydrophilic groups as well as the more important solvent interactions of nonpolar groups with water, the "freezing out" phenomenon associated with water molecules at the interface between the bulk solvent and nonpolar solutes. Hydrogen bonding is another form of interaction that may be of some importance and is also hard to analyze for or predict. Any of these interactions would affect the rate through stabilization or destabilization of the precursor and successor complexes, and would thus enter into the calculations in the same manner as discussed above. Because these interactions are less well understood

than the simple coulombic ones, no attempt will be made to formulate an analogue to the work term treatment.

E. Specific Ion Effects

There are other effects that may be caused by ions (and sometimes uncharged solutes) other than the general ones discussed above. The most dramatic of these are the specific ion effects, especially specific inhibition. An example of this is the inhibition of type 2 copper containing proteins by azide. In those cases, the azide is thought to bind to the copper and thus block the binding of a substrate or modify the reactivity of the copper.[30] A somewhat different type of anion inhibition is shown by the interaction of azide with cytochrome c; in this case the azide causes a major change in the structure of the cytochrome by replacing an axial (Met-80) ligand of the iron.[31] Both of these types of inhibition are the result of the specific interaction of an inhibitor with the protein; a more subtle effect, and one that is usually smaller in magnitude than the previous examples, is anion assistance of outer sphere reactions. This effect has been studied by Sutin and coworkers in inorganic systems and the conclusions that have been reached are that the added anion catalyzes electron transfer by acting as a bridge.[32] The effectiveness of the bridge is related to the symmetry of the available bridging ligand and metal orbitals. The most effective bridges are of the same symmetry as the acceptor and donor orbitals; for example, azide is a good π bridging ligand and is especially effective between ruthenium or iron centers and reagents with π orbitals, whereas

chloride is a good σ bridge and is more effective between chromium and cobalt centers and between reagents with only σ orbitals available on the ligands. The effectiveness of the bridge is also dependent on the ability of the potential bridging anion to associate with one or the other of the reactants in order to be brought into the transition state (discounting any significant number of effective ternary collisions). Even less specific is the effect of a more general binding of anions or cations to a protein surface or association with the small molecule reagents. If there is a reason to suspect such binding, a general electrostatic correction could be attempted for it by correcting the total charge on the reagent or protein for the suspected number of bound ions. Such interactions are not just speculation, as binding constants for several anions with cytochrome c have been measured[33,34] and the electron exchange rate for $Fe(CN)_6^{3-/4-}$ is strongly affected by cations,[35] whereas the $Co(phen)_3^{3+/2+}$ exchange is anion dependent.[36]

Another topic that may be considered under the general title of ion and medium effects is the effect of varying pH. Once the pH dependence is available (it should be as wide a range as possible within the capabilities of a single buffer, or separate, overlapping buffer systems may be used) attempts may be made to fit the data to one or more titration curves and pK values may be assigned. If titration data are available for the protein and the reagent, this information can first be consulted in interpreting the pH dependence of an electron exchange rate and thus it can usually be decided if the

reagent or protein is involved. Usually the reagent can be eliminated as a source of a pH dependence, or at least a reagent may be found that does not have a pK in the region being analyzed if the protein pH behavior is especially important to isolate. The most probable origin of a pH dependence that originates from a pK of the small molecule reagent is electrostatic interaction, but protein proton equilibria will often involve conformational changes as well as changes in charge. Changes in conformation are especially well documented at extremely low pH values, where proteins often assume much more open structures (a good example here again is cytochrome c for which several forms have been characterized[1]). Conformational changes may strongly involve the metal center, for example, the ligation of cytochrome c changes at high pH with a large decrease in the potential,[1] and blue proteins bleach at higher pH values,[2] indicating structural modification of the copper site. The particular residues responsible for a transition with a given pK are difficult to assign because of the problems associated with multiple equilibria and because the pK's of the individual side chains are often shifted by their environments. A further warning that should be made is that although a large pH dependence may be confidently interpreted, small changes of rate with pH (less than a factor of two overall) are hazardous to analyze, as there could be many reasons for such a dependence, including changes in the medium because of the changing ionic forms of the buffer and the concentration of added salt.

F. Steric Effects

Another variable that must be considered and may be controlled in the selection of small molecule reactants is molecular size and steric constraint. The steric constraints and predicted effects from changes in the size of the reagent will vary for different proteins and different proposed mechanisms. Common examples would include a metal site that is buried at the bottom of a pit or groove of the protein; in this case, reagents much larger than the size of the opening should react more slowly, and there should be a discontinuity in the rate above a certain size reagent. If the metal site of the protein is on the surface, then there should be no such discontinuity but other factors might be expected to change the rate with increasing size of the reagent. Electrostatic effects would be small, but such interactions would decrease with increasing size, thereby leading to an increase in the rate if the reagents are like-charged, or to a decrease if the two reagents have opposite charges. If tunnelling is suspected, the rate is expected to be approximately proportional to e^{-r}, where r is the distance between the donor and acceptor (which may be the metal ions or the edges of π systems, for example).[37] Strong dependences on distance are also to be expected if changing the size of the reagent strongly affects the orbital overlap in the transition state, thus possibly changing a case of good overlap (adiabatic) to a case of poor overlap (possibly nonadiabatic).

G. Symmetry Aspects

As was hinted at before in the discussion of bridging ligand effects, the match of symmetry between the donor and acceptor orbitals has been found to correlate with electron transfer reactivity; when the donor and acceptor orbitals are both of the same symmetry type, the rate constant is higher than when one is σ and the other π, all else being equal. This generalization can be used and tested by varying the reagent as was considered when bridging anions were discussed. Some of the variation that arises from the symmetry properties will be compensated for in the Marcus calculation through the self-exchange rate constant. Thus, the generally higher rate constants found for reagents with π symmetry redox orbitals will be compensated for by the k_{22} parameter. If the extent of orbital overlap (and thus the adiabaticity that is assumed to parallel this overlap) between the protein and reagent redox orbitals varies so as to invalidate the assumption of an adiabatic or uniformly nonadiabatic reaction (see Section II-B), then symmetry effects will directly affect the calculated k_{11} val ue. As there is no way to measure the adiabaticity, variations in k_{11}/p_{11} are all that can really be compar ed; p_{11} could always be artificially chosen such that $p_{12}^2 = p_{11}p_{22}$, and thus all of the variation placed on changes in k_{11} (as is implicitly done when the calculations are done without the adiabaticity factors); but from a conceptual viewpoint the two terms, k and p, should be kept distinct and variations in the adiabaticity of the cross reaction (relative to the adiabaticity of the reagent self-exchange reaction) should be considered in terms of p factors.

H. Activation Parameters

Activation parameters are available for many of the electron transfer reactions to be considered. As large differences in activation parameters are sometimes found when there is little difference in rate constants, it may be expected that analysis of these parameters will show differences in reaction pathways and that these differences may be interpreted mechanistically. The Marcus theory of electron transfer reactions provides a prediction for activation parameters as well as just free energies of activation (rate constants), so this treatment will now be given.[20] The temperature dependence for an outer sphere reaction used in the Marcus presentation is given by

$$k_r = pZ^{-\Delta G^*/RT} \tag{34}$$

where p is the probability of electron transfer in the activated complex (transmission coefficient) and Z is the temperature dependent collision frequency between two uncharged particles in solution. Using the equations previously given for the cross reaction rate

$$k_{12} = \sqrt{k_{11}k_{22}K_{12}f} \tag{1}$$

$$\ln f = (\ln K)^2/(4 \ln (k_{11}k_{22}/Z^2)) \tag{2}$$

and the following expression for the free energy can then be derived

$$\Delta G_{12}^* = \frac{\Delta G_{11}^* + \Delta G_{22}^*}{2} + \Delta G_{12}^{0}(1 + \alpha) \tag{15}$$

$$\alpha = \frac{\Delta G_{12}^*}{4(\Delta G_{11}^* + \Delta G_{22}^*)} \tag{16}$$

By using the expressions

$$\Delta S = -\frac{\partial \Delta G}{\partial T} \qquad \Delta H = \frac{\partial \Delta G/T}{\partial 1/T} \tag{35}$$

Eqs. 36 and 37 may be derived:

$$\Delta S_{12}^* = \frac{\Delta S_{11}^*}{2} + \frac{\Delta S_{22}^*}{2}(1 - 4\alpha^2) + \frac{\Delta S_{12}^{\,0}}{2}(1 + 2\alpha) \tag{36}$$

$$\Delta H_{12}^* = \frac{\Delta H_{11}^*}{2} + \frac{\Delta H_{22}^*}{2}(1 - 4\alpha^2) + \frac{\Delta H_{12}^{\,0}}{2}(1 + 2\alpha) \tag{37}$$

These activation parameters are not the same as those calculated normally from temperature dependence data, because the Eyring expression from transition state theory

$$k_r = p\frac{kT}{h} e^{-\Delta G^{\ddagger}/RT} \tag{38}$$

is different from Eq. 36, which was assumed in the Marcus derivations. Therefore the following conversions are necessary to relate the two types of activation parameters (in deriving these relationships it is assumed that Z, the collision frequency, is proportional to $T^{\frac{1}{2}}$);[21]

$$\Delta G^{\ddagger} = \Delta G^* - RT \ln(hZ/kT) \tag{39}$$

$$\Delta S^{\ddagger} = \Delta S^* + R \ln(hZ/kT) - \tfrac{1}{2}R \tag{40}$$

$$\Delta H^{\ddagger} = \Delta H^* - \tfrac{1}{2}RT \tag{41}$$

The terms with hZ/kT are dependent on the value selected for Z; when 10^{11} $\underline{M}^{-1}$ sec^{-1} is used, hZ/kT is about 62 and RTln(hZ/kT) is 2.56 kcal/mole at 298 K. As there is not an entirely satisfactory method for estimating Z, the correction will be left indeterminate.

The dependence of electron transfer rate on temperature in systems where a tunnelling mechanism is operating is characterized by a curved Arrhenius plot (or Eyring plot) which levels off at low temperature.[37]

Considering the possible importance of electrostatic (i.e., coulombic) interactions, some consideration must be given to the enthalpy and entropy components of the work term contributions. The temperature dependence of the work terms (see Eq. 25) is the result of the temperature dependence of κ

$$\kappa = 50.3\ \text{Å}\ \left(\frac{\mu}{\epsilon T}\right)^{\frac{1}{2}} \tag{42}$$

The dielectric constant of water is somewhat temperature dependent, varying from 87.9 at 0° to 69.9 at 100°; thus, $1/\epsilon T$ varies only from $4.17(10^5)$ at 0° to $4.82(10^5)$ at 100°, and is $4.37(10^5)$ at 20°. Assuming, then, that $\epsilon = \epsilon_0 + \epsilon_1/T$, the expression for a work term

$$V = \frac{e^2}{2}\left[\frac{-\kappa R_2}{1 + \kappa R_1} + \frac{-\kappa R_1}{1 + \kappa R_2}\right]\frac{Z_1 Z_2}{\epsilon(R_1 + R_2)} \tag{23}$$

may be solved for the entropy component using the relationship

$$\frac{\partial V}{\partial T} = -\Delta S \tag{43}$$

Carrying out the partial differentiation and substituting back for ϵ

$$-\Delta S = V\{25.15\ \mu^{\frac{1}{2}}\ \epsilon_0\ (\frac{\epsilon}{T})^{-3/2}[\frac{1}{r\epsilon} + \frac{(1 + \kappa R_1)R_2 + R_1}{(1 + \kappa R_1)^2} + \frac{(1 + \kappa R_2)R_1 + R_2}{(1 + \kappa R_2)^2}] + \frac{\epsilon_1}{rT^2\epsilon}\} \quad (44)$$

$$\text{and } \Delta H = \Delta G + T\Delta S \quad (45)$$

$$= V + T\Delta S$$

can be used to solve for the enthalpy component.

If the overall electron transfer rate constant is best represented as the product of an equilibrium constant for formation of a precursor complex and an intracomplex electron transfer rate constant ($k = Kk_{et}$), then the enthalpy and entropy contributions to K and k_{et} may be extracted from the kinetics. If Eq. 29 is used to estimate a precursor or successor complex formation constant, then under the same assumption that $\epsilon = \epsilon_0 + \epsilon_1/T$

$$K = 2.52(10^{-3})r^3 \exp\left(-\frac{Z_1Z_2}{\epsilon(1 + \kappa r)(RT)}\right) \quad (46)$$

$$\Delta G = -RT\ln K \quad (47)$$

$$= -RT\ln 2.52(10^{-3})r^3 + \frac{Z_1Z_2}{\epsilon(1 + \kappa r)r}$$

$$-\Delta S = \frac{\partial \Delta G}{\partial T} \quad (35)$$

$$-\Delta S = -R\ln 2.52(10^{-3})r^3 - \frac{Z_1Z_2}{T^2 r\epsilon(1 + \kappa)}\left[\frac{\epsilon_1}{\epsilon} + \frac{25.15\ \mu^{\frac{1}{2}}\epsilon_0 T^{\frac{1}{2}}}{\epsilon^{3/2}(1 + \kappa)}\right] \quad (48)$$

and $\Delta H = \Delta G + T\Delta S$.

One hazard in the interpretation of activation parameters is the possibility that in solution one of the reagents is an equilibrium mixture of several forms. This should not be a problem for the small molecule reagents but is a significant consideration for proteins. The origin of this problem may be illustrated for the case of two forms of a protein which differ by a proton and react at different rates, with the assumption that the proton transfer is fast enough with respect to the electron transfer that the two forms of the protein A and B are always in equilibrium, that there is a first order excess of the other reagent, and that the two forms of the protein are indistinguishable at the wavelength being followed.

$$A + H^+ \overset{K}{\rightleftharpoons} B \qquad K = \frac{B}{(A)(H^+)} \tag{49}$$

$$A \overset{k_1}{\rightarrow} P \tag{50}$$

$$B \overset{k_2}{\rightarrow} Q \tag{51}$$

$$k_{obsd} = \frac{k_1 + k_2K(H^+)}{1 + K(H^+)} \tag{52}$$

As k_1, k_2, and K each have their own thermodynamic parameters, it is clear that the standard plot of $\ln(k/T)$ vs. $1/T$ will constitute a complex, nonlinear combination of the various contributions (this is most easily seen in the numerator where the added terms are seen to mingle under the operation of taking the logarithm). Such a plot cannot be separated into its components, except by working at pH's where only one path contributes, and by finding the temperature

dependence of the equilibrium constant by doing the temperature dependence of the pH dependence. The problem of obtaining the individual enthalpies and entropies is clearly a difficult one, even in the simple case described above, and then it requires that the protein be stable at the extreme pH values where only one form (A or B) exists. The whole situation is compounded if there are overlapping proton equilibria, ion binding, and more general ionic strength dependent conformational changes. Another problem of heterogeneity involves different structural forms of the protein, resulting from partial denaturation, or from such common differences as slight variations in the sugars of glycoproteins. In general, however, these latter examples should not give clean kinetics (the different forms are not in rapid equilibrium and thus will exhibit parallel first order behavior under pseudo-first order conditions). The problem of heterogeneity of forms when they are in equilibrium must be assumed at this time to be one which cannot be solved exhaustively by studying each species independently; and it must be hoped that the different redox forms follow similar enough mechanisms so that the average activation parameters actually obtained are representative. If some case of an especially clean pH dependence as described in the example is available, it would be interesting to perform the full analysis, but this would be a time-consuming task.

Once the activation parameters for a given reaction are obtained, they can be compared with others available. Within the Marcus theory formalism, the contribution to the activation parameters owing to the protein may be isolated. One of the most

important questions to consider is whether the mechanisms of various reagents (small molecule or protein) reacting with a given protein are the same or different. Previously this question was considered in terms of free energies in the comparison of the calculated k_{11} values for the protein. With the additional information available in activation parameters, it may be found that rates that are similar are actually the result of coincidence (or compensation) in that the enthalpies and entropies changed drastically but the free energy remained constant.

The phenomenon of compensation (the observation of a linear relationship between the enthalpy and entropy of activation across a series of reactions) is well documented, especially for organic reactions. Under certain assumptions,[38] compensation is predicted when there is only one interaction between the reactants which varies within the series of reactions being considered, the remainder of the mechanism being invariant. Although the microscopic basis for compensation is not well understood,[39] it can be rationalized in a simple case where the difference in a given series of reactions has its origin in the binding of the two reactants. If this binding becomes stronger, the activation enthalpy will decrease, but at the same time the entropy is expected to decrease because of the more restricted orientation produced by the tighter binding. The whole situation is further complicated if the solvent is considered, as the stronger binding of the two reactants will release bound solvent (an increase in enthalpy attributable to breakage of solvent-reagent hydrogen bonds; a decrease in enthalpy for the new solvent-solvent

hydrogen bonds; and an increase in entropy for the freed solvent).[39] Under the assumption that the observation of a linear compensation plot indicates that only one interaction varies within the series of reactions being considered, a range of activation parameters which might otherwise be considered to indicate rather complex differences in mechanism may be more confidently considered in terms of one type of interaction. The lack of compensation similarly reinforces the conclusion that there is more than one difference among the mechanisms of the reactions being compared. In considering just the contribution from the protein activation (the calculated enthalpies and entropies derived for the protein self-exchange reaction), compensation might also be considered.

In concluding the discussion of activation parameters, it should be emphasized that comparing cross reaction activation parameters is quite hazardous without some concept of the extent to which these activation parameters are the result of the free energy change for the reaction or contributions from the different reagent self-exchange mechanisms. The best comparison, within the Marcus theory formalism, is between the activation parameters for the calculated protein self-exchange. Other comparisons should be made only with extreme caution.

I. Protein-Protein Reactions

Most of the above discussion has been directed at the interpretation of reactions between a protein and a small molecule reagent because these are easier to treat and there are more data available; this last part of the Theory section will discuss some of

the problems in analyzing data on the reactions between two proteins. The main problem in analyzing protein-protein reactions is that, with present knowledge, both reactants must be considered as unknowns. The great advantage of using a small molecule reagent is that its kinetic properties can be considered to be fixed and known, and, through the Marcus theory analysis, these can be factored out to yield a quantitative description of the reactivity of the protein. It must be kept in mind that protein-protein interactions may well be of a character significantly different from those protein-small molecule interactions that are used as models. Good examples of interactions that should exist between proteins (especially specific physiological partners), and that are predicted from certain calculations to be influential in reactions, are those of the ion-ion and dipole-dipole types.[25] The model for these interactions, besides including a "good fit" between the two proteins that would line up opposite charges and opposite dipoles in the sense of static configurations, is involved with the induced changes in charge distribution and dipoles that can occur when two protein surfaces interact. In this model ion-ion (or dipole-dipole) binding may be induced between sites that were not necessarily charged (or dipolar) in the two proteins taken individually. Single interactions of this type might not be large enough to give a significant rate constant differential and thus may be missed even if a small reagent that interacts in such a way is found, but a large reagent that can induce many such interactions is likely to reap enormous benefits and react at a significantly

different rate. For such reasons as these, the proteins, no matter how well understood with small molecules, must not be taken for granted in their interactions with other proteins.

III. Data Reliability

The most basic parameter under consideration is the electron transfer rate constant. In the best of cases (clean pseudo-first order kinetics giving a linear plot with a zero intercept for the concentration dependence on the reagent in excess), the second order rate constants under a given set of experimental conditions should be known to be better than ± 10%. The further uncertainty involved because of possible medium dependences should always be considered. Ionic strength and pH dependences should be determined; if they are small, it may be assumed safely that small differences in pH or μ in, say, the various solutions used for concentration dependence, do not introduce significant error. The other possible small effects (changes in buffer, changes in salt, rigorous elimination of trace ions and product inhibition) are usually ignored because of the time required to check for them and the difficulty in analyzing the small differences (if any) usually found on varying them when there is not a reason to specifically suspect a problem (sometimes an ion, such as perchlorate, may be suspected of denaturing the protein, or a pH dependence that fits the pK of the buffer may raise suspicions). A large dependence on any parameter (pH or a specific ion concentration) should lead to the consideration

of the protein under the different conditions as separate species to be treated independently. This is easier if the relationship between the species is clearly defined by an equilibrium constant of some kind, but it is not so easy if the variation does not fit such a simple analysis, as discussed in Section II-H. Some dependences are usually ignored in preference to taking a standard state for comparison (e.g., pH 7, μ 0.1 M) and the variability is relegated to increased error limits. For the purposes of the analyses to be performed in the rest of this paper, error limits of ± 10% will be used when there is no evidence that they should be larger.

A second category of problems that may be encountered when trying to assign error limits may be associated with rate laws that are more complicated than the simple second order one considered in the previous paragraph. The first problem is to accurately define the rate law and all of the parameters involved. If saturation is indicated or if the data may be fit by a parallel first order scheme, this is not difficult. However, much more data must be collected than in the simple case of a second order process. In more complicated situations, the data may be quite difficult to analyze and the various equilibrium and kinetic parameters may not be easily separable. For the later use of these parameters in a Marcus theory analysis, saturation may be handled by considering precursor complex formation and parallel paths may indicate some sort of heterogeneity of protein forms in solution, but anything more complicated may make the application of the Marcus equations

inappropriate. For problems involving protein-protein reactions, it is often difficult to obtain the range of concentrations of the species required to test for binding.

Next to be considered are the reduction potentials for the proteins and reagents. For the Marcus theory calculations, the potentials are used as an indirect way of measuring the equilibrium constant between the oxidant and reductant. If this value has been measured directly for any given reaction, it is always more accurate to use the direct determination, but as such measurements are seldom performed the measured potential values must be relied on.

For the small molecule reagents of interest, the potentials have often been measured by direct means because the reagents react directly with electrodes at acceptable rates, but more often than not the determination has been done under conditions significantly different from the conditions of the kinetic experiments. For example, many values are available for reagents that have been used in standard inorganic electron transfer studies but these are usually measured at ionic strengths from 1 to 4 M and at 0.1 M or higher acid concentration to match the conditions of the experiments then under consideration. For some classic cases, careful medium dependences have been performed (the best example here is the $Fe(CN)_6^{3-/4-}$ couple); these studies show strong dependences on the identity and concentration of ions. Although the lower charged ions are not expected to be so medium dependent in their electrochemistry, the possibility in general remains unexplored. For these reasons,

error limits for most reagent potentials are set at ± 20 mV, or ± 10 mV in the best of cases.

The situation for the protein potentials is even less encouraging. The potentials cannot be measured directly because the proteins do not react quickly at electrodes, and therefore either titrations must be done or electrode techniques using mediators must be used. Most of the data in the literature have been obtained by titration with $Fe(CN)_6^{3-/4-}$, because this is a simple technique. There are problems with this technique, however; these include the need to know the $Fe(CN)_6^{3-/4-}$ potential under the experimental conditions, and the problem of the interaction between the reagent and the protein, which is especially severe with such a highly charged reagent. Besides the problem of the method used, many available potentials for metalloproteins are determined in only one medium, and thus the same problem of an unknown medium dependence is involved here as was involved with the reagent potentials; one advantage here is that the differences between the medium of interest and the medium for which the measurement was done is less in the case of the protein data, as the proteins often are not stable under a wide range of conditions. The best data available have been obtained with a mediator technique (the mediator being kept at a low enough concentration that binding problems are minimized). With this technique data can be taken with an optically transparent electrode, thereby allowing direct monitoring of the concentrations of the oxidized and reduced protein species. Because of the problem of

the poor techniques used, most of the protein potentials will be given error limits of ± 20 mV.

The activation parameters determined from Eyring plots are seldom quoted with error limits; these limits are obtained from least squares fits only if the data are carefully weighted and the propagation of error is properly accounted for in the weighting; less care than might be proper is sometimes given to considering whether the plots are linear, and the range of temperatures that can be covered is usually so small (0 to 30°) that only extreme curvature would be apparent anyway. For these reasons, interpretations of activation enthalpy differences of less than two kcal/mol and entropy differences of less than five cal/mol-deg will not be attempted.

The individual components of the free energy changes for a reaction, ΔH^0 and ΔS^0, are evaluated most conveniently by the same method as is the equilibrium constant, i.e., by taking the sum of the thermodynamic changes for the oxidation and reduction of the reductant and oxidant, respectively. These data are especially scanty; as they are usually obtained by determining the temperature dependence of the reduction potential, all of the problems associated with determining potentials apply here also. When the data have been determined for the small molecules reagents, they are usually for the state of infinite dilution and medium dependences of enthalpy and entropy changes are even rarer than medium dependences of potentials. For the determination of potential parameters, the ferricyanide titration technique requires a knowledge of the enthalpy

and entropy changes for the $Fe(CN)_6^{3-/4-}$ couple instead of just its potential, and the influence of solvation on these highly charged ions is likely to result in compensation behavior. Thus the knowledge that the potential of the couple is insensitive to a certain medium change does not insure that the entropy and enthalpy components are similarly invariant. The conclusion here, as for the determination of the potentials, is that a great deal of careful work is necessary with techniques such as the optically transparent electrode approach described previously. No attempt will be made to give general error limits here as the few examples available will be treated individually as needed.

The next parameter to be discussed, which is of interest in some of the calculations that follow, is the measured electron exchange rate between the two oxidation states of small molecule reagent or a protein. One of the first problems in measuring the rate of such a reaction is finding a property to monitor, because the reactants and products are chemically identical. The most common approach used for the slower reactions of certain metal ion complexes is isotopic labelling, where one oxidation state of one reactant is originally a radioactive isotope; aliquots of the reaction mixture are taken periodically and the two oxidation states separated, and counted for label in each. This method is clearly limited to rather slow reactions, but great ingenuity has been used in fast separation techniques that allow rates as fast as that of the $Fe(CN)_6^{3-/4-}$ exchange to be measured by this method. For faster

reactions NMR and EPR line broadening measurements may be used if there is some magnetic resonance signal that is shifted by the change in oxidation state. There is a gulf between these two methods where reactions are too fast to be measured by labelling (given the separation methods that must be used) and too slow to be measured by magnetic resonance; some of the attempts to measure exchange rates have failed for this reason, whereas the difficulty of the isotopic labelling method has inhibited the collection of data by that method. Other methods for obtaining estimates of the true exchange rate involve making some sort of small change in one of the reactants that makes the reaction easier to follow, but presumably does not change the activation requirements and thus the rate appreciably. Such changes include making one of the reactants optically active (e.g., a substitution inert metal ion complex), or changing the ligand just enough to perturb the ultraviolet spectrum slightly. Such approaches as these are only as good as the assumption that the kinetics have not been changed by the modification, as the data usually become relatively easy to acquire with good accuracy. Even for those systems that have been studied, the now familiar problem of medium effects is again involved. Especially for the highly charged complexes, strong dependences on cations and anions have been observed. In general, when the available data are suspect because of the approach that had to be used (e.g., changing the ligand slightly) or if medium dependences are expected but not studied, a range of a factor of two to three is not an

unwarranted estimate of the possible error of the self-exchange rate constant.

The radii used for the reagents are evaluated from crystal structure data when possible, by taking the distance from the metal ion in the complex to a counter ion in the crystal, and subtracting the ionic radius of the counter ion. For $Fe(EDTA)^{2-/-}$ a larger value is required, as the complex is not actually spherical and the counter ion is especially close. As the radii of the protein and reagent are not accurately known (about ± 0.5 Å for the metal ion complexes), and as it is difficult to determine the average sizes of the other ions in solution, the small reagents have been given radii 0.2 or 0.3 Å larger than actually calculated and no correction has been made for the loss of solvating ions in going to the transition state. This procedure simplifies the calculations and does not decrease their accuracy, as the parameters are poorly defined in the first place.

Given the estimates of the reliability of the parameter values for the Marcus calculation, an overestimate of the error in k_{11} is

$$k_{11} = \frac{(1.1\ k_{12})^2}{\frac{1}{3}k_{22}\ 39.94(\Delta E - 0.03)} \text{ to } \frac{(0.9\ k_{12})^2}{3\ k_{22}\ 38.94(\Delta E + 0.03)} \qquad (53)$$

$$= 12 \text{ to } 0.08\ \frac{k_{12}^2}{k_{22}\ 38.94(\Delta E)}$$

thus the k_{11} values are determined to at least an order of magnitude.

IV. Properties of the Reactants

A. Small Molecule Reagents

This section presents a catalogue of the properties of the

reagents and the proteins of interest. For the small molecules, properties such as reduction potential, electron self-exchange rate, size, stability, and some discussion of reactivity characteristics (such as inner or outer sphere predilections) are given. For the proteins, the properties presented are molecular weight, size, isoelectric point, amino acid sequence, function, and the self-exchange rate, if it has been measured. Some indication of the reliability of the various parameters will be given.

Table 1 gives the available data[40-58] on the small molecule reagents of interest and some other information will be presented briefly now.

The three reagents chromium(II), dithionite, and hydroquinone are generally considered to use inner sphere mechanisms. Chromium(II) has been used for much of the inorganic electron transfer research available, especially the extensive work with various cobalt(III)pentammine derivatives that has defined bridging ligand effects.[18,19] One problem in the use of Cr(II) for studying metalloprotein electron transfer rates is the instability of the ion above about pH 4; as a result, this reagent has had only limited use. Both hydroquinone and dithionite can transfer one or two electrons. Dithionite can be a one electron reagent by producing a sulfur(IV) species and SO_2^-, the latter of which is in equilibrium with dithionite itself[59]:

$$S_2O_4^{2-} \overset{-e^-}{\rightleftharpoons} S(IV) + SO_2^- \qquad (54)$$

Table 1. Properties of the Small Molecule Reagents.

	E(mV, 25°)	μ(M)	Salt	$k_{22}(M^{-1}s^{-1}, 25°)$	$\Delta H^{\ddagger}$(kcal/mole)	$\Delta S^{\ddagger}$(eu)	pH	Buffer	μ(M)	Salt	R(Å)	Ref.
$Fe(EDTA)^{-/2-}$	120[a]	0.1	KCl	$3(10^4)$[b]	4.0	-25	4.5-6.5	A, L[c]			4	40-43
$Co(phen)_3^{3+/2+}$	370	0.1	P/Na_2SO_4	45[d]	5.1	-34			0.1	KNO_3	7	36,44-46
$Co(5\text{-Cl-phen})_3^{3+/2+}$	430	0.05	NaCl	$1.3(10^{-2})$[e]				P	0.1[e]	NaCl	8.5[f]	47
$Co(5,6\text{-}(Me)_2\text{-phen})_3^{3+/2+}$	420	0.05	NaCl	$5.0(10^{-2})$[e]				P	0.1[e]	NaCl	8.[f]	47
$Co(4,7\text{-}(Me)_2\text{-phen})_3^{3+/2+}$	340	0.05	NaCl	$7.7(10^{-1})$[e]				P	0.1[e]	NaCl	7[f]	47
$Co(4,7\text{-}(\phi\text{-}SO_3^-)_2\text{-phen})_3^{3-/4-}$	330	0.05	NaCl	$7.0(10^3)$[e]				P	0.1[e]	NaCl	11.5[fg]	47,48
	330	0.05	NaCl	$1.4(10^3)$[e]				P	0.1[e]	NaCl	7[g]	47,48
	330	0.05	NaCl	$3.5(10^2)$				P	0.1[e]	NaCl	7[g]	47,48
$Co(bipy)_3^{3+/2+}$	305	0.1	P/Na_2SO_4	18[d]	7.7	-27			0.1	KNO_3	7[o]	44,45,49
$Co(terpy)_2^{3+/2+}$	270	0.1	P/Na_2SO_4	$1.94(10^3)$[h]					0.1		7[o]	44,49,50
$Ru(NH_3)_6^{3+/2+}$	51	0.1	$NaBF_4$	$(8\pm1)(10^2)$	10±1	-11±3	~2	CF_3CO_2D (D_2O)	0.013		3.	51-53
$Fe(CN)_6^{3-/4-}$	416	0.1	K_2SO_4	$2.2(10^3)$[i]					0.02	KX[j]	4.5	35,54-56
	409	0.1	Na_2SO_4	$7.3(10^3)$					0.05	KX	4.5	35,54-56
	409	0.1	Na_2HPO_4	$1.5(10^4)$					0.1	KX	4.5	35,54-56
	424	0.1	KCl	$2.6(10^4)$					0.2	KX	4.5	35,54-56
	431	0.26	K_2SO_4	$3.3(10^4)$					0.3	KX	4.5	35,54-56

Table 1 (cont).

	E(mV, 25°)	μ(M)	Salt	$k_{22}(M^{-} s^{-1}, 25°)$	$\Delta H^{\ddagger}$(kcal/mole)	$\Delta S^{\ddagger}$(eu)	pH	Buffer	μ(M)	Salt	R(Å)	Ref.
$Fe(CN)_6^{3-/4-}$	431	0.26	K_2SO_4	$3.3(10^4)$					0.3	KX	4.5	35,54-56
	423	0.26	Na_2SO_4	$1.8(10^3)$	3.6	-23.7			3.2	$Fe(CN)_6^{3-/4-}$	4.5	35,54-56
	423	0.26	Na_2HPO_4								4.5	35,54-56
	442	0.26	KCl								4.5	"
	355±1[k]	→0		25	8.56	-23.4			→0		4.5	35,54-57
$Fe(CN)_5N_3^{3-/4-}$	240[l]	0.05	KNO_3	$5.0(10^3)$[m]			5.5-7.0		0.05	KNO_3	4.5[n]	58
$Fe(CN)_5NH_3^{2-/3-}$	330[l]	0.05	KNO_3	$1.8(10^5)$[m]			5.5-7.0		0.05	KNO_3	4.5[n]	58
$Fe(CN)_5P\phi_3^{2-/3-}$	540[l]	0.05	KNO_3	$7.0(10^3)$[m]			5.5-7.0		0.05	KNO_3	4.5[n]	58
$Fe(CN)_4bipy^{-/2-}$	550[l]	0.05	KNO_3	$9.5(10^6)$[m]			5.5-7.0		0.05	KNO_3	4.5[n]	58

Table 1 Footnotes

[a] pH 4-6, 20°.

[b] For the cross reaction with $Fe(CyDTA)^-$.

[c] The buffers are A(acetate), T(tris), P(phosphate), G(glycine), C(cacodylate) and L(lutidine).

[d] By optical rotation; 25° value from activation parameters.

[e] Calculated from the cross reaction with $Co(terpy)_2^{3+/2+}$, corrected from 0.5 to 0.1 M NaCl.

[f] Radii calculated from covalent radii and standard bond lengths.

[g] See footnote 48 for a description of the three models.

[h] Calculated from the cross reaction with $Co(phen)_3^{3+}$ at $\mu = 0.05$ M (ref. 49).

[i] Calculated by extrapolation of the equation of ref. 35 and assuming $k_{298} = 4(k_{273})$, approximately pH independent.

[j] Where X is any anion.

[k] Extrapolated to zero ionic strength. $\Delta H^\circ = -26.7 \pm 0.3$ kcal/mole, $\Delta S^\circ = -62 \pm 1$ eu (ref. 57).

[l] pH 5.5 to 7.0.

[m] Recalculated, including electrostatic corrections, from the data of ref. 58 for the cross reaction with $Fe(CN)_6^{3-/4-}$, assuming a potential of 409 mV and an exchange rate of $7.3(10^3)$ $M^{-1}s^{-1}$ for $Fe(CN)_6^{3-/4-}$.

[n] Assumed equal to $Fe(CN)_6^{3-/4-}$.

[o] Assumed equal to $Co(phen)_3^{3+}$.

$$2SO_2^- \rightleftharpoons S_2O_4^{2-} \qquad (55)$$

Hydroquinone goes to the semiquinone after a one electron transfer and two moles of semiquinone disproportionate to give benzoquinone and hydroquinone. A further important property of hydroquinone is that it has a pK of 9.85 (0.65 M, 25°).[60] A value of 10 at 0.04 M has also been given.[61]

The properties of those reagents that are required to be outer sphere, or at least usually observed to be so, are treated next. A water molecule is probably coordinated to $Fe(EDTA)^-$ in aqueous solution; the pK of this coordinated water is 7.58.[62] It is possible that the pK of 9.1 found[63] for $Fe(EDTA)^{2-}$ also refers to a coordinated water. The $Fe(EDTA)^-$ complex forms an oxobridged dimer; a value of 340 M^{-1} (26°, 1.0 M $NaClO_4$, 0.05 M EDTA buffer, pH 9) has been reported[64] for the equilibrium

$$K = \frac{[Fe(EDTA)_2O^{4-}]}{[Fe(EDTA)OH^{2-}]^2}. \qquad (56)$$

The estimates available for the electron exchange rate are from cross reactions of the iron complexes of EDTA and CyDTA. As well as water or hydroxide, $Fe(EDTA)^-$ can bind anions in the seventh coordination position; however, this binding is expected to be considerably weaker for the Fe(II) complex than for Fe(III). Because of this labile position, inner sphere pathways must be considered a possibility. If inner sphere mechanisms seem likely, it may be preferable to use $Fe(HEDTA)^-$ as a test, as there are two

open coordination sites (the seventh and the one left when one acetate of EDTA is replaced by the alcohol of HEDTA) and binding constants for exogenous ligands are somewhat higher.

The tris complexes of cobalt(III) with phenanthroline and its derivatives are an informative series of reagents. The original study of the $Co(phen)_3^{3+/2+}$ exchange was rather imprecise but did highlight the problem of anion catalysis.[36] Later studies with an optically active Co(III) complex[45] have provided more precise rate constants and good activation parameters. The potentials of the derivatives are given in Table 1. Their self-exchange rate constants have been calculated from cross reaction data with $Co(terpy)_2^{3+}$, and these values are also set out in Table 1.

One of the most common reagents used in electron transfer studies of metalloproteins is $Fe(CN)_6^{3-/4-}$. This is the result of the commercial availability of the reagent, its stability, convenient potential, and large extinction change on changing oxidation state. The properties of the reagent itself have also been studied extensively, probably for the same reasons that biochemists have used it; this is fortunate because this system appears to have more significant complications from medium dependences than any other reagent under consideration. The highest pK of $Fe(CN)_6^{3-/4-}$ is about 4.[65] As shown in Table 1, the potential is quite dependent on ionic strength and the type of ion, as is the self-exchange rate; these and other problems of binding of the reagent to proteins probably originate in the solvation properties of such a small,

negative ion. Some care is given in the Marcus calculations to choosing the proper potential and exchange rate for a given medium, but because the media of interest are seldom exactly like those used in the physical measurements, some extrapolation is usually necessary and thus the errors in the parameters chosen, especially the self-exchange rate, are larger than might be preferred. Derivatives of the iron hexacyanides where one cyanide is replaced by another ligand have also been studied and some exchange rates are available.[58]

The last outer sphere reagent to be discussed in $Ru(NH_3)_6^{2+}$. This reagent is less stable than any of the others discussed except chromous; it is light sensitive and is not stable at neutral pH; furthermore, there are often acid dependences of the rates of ruthenium complexes.

B. Proteins

The various properties[1,66-83] of the proteins are collected in Table 2. The errors given in the table are those claimed by the authors and are smaller than those settled on in an earlier section. The radii were calculated from Eq. 26, the charges were calculated from the amino acid sequences as described in Section II-C, the isoelectric points are experimental except in those cases where only an upper limit is given; in those cases the behavior of the protein on ion exchange resins is used. Some comments are in order for the charge calculation; the metal site charge calculation has already been discussed, and the assumption that both propionates of the heme

Table 2. Protein Properties

	E(mV,25°)	pH	Buffer[a]	μ(M)	Salt	MW(10^{-3})	R(A)[b]	Lysines	Arginines	Histidines[c]	Glutamates[d]	Aspartates[d]	Metal Site[e]	Other	Charge[f]	pI	Ref.
cytochrome c (Horse heart)	261[g]	7	T,P,C	0.01-0.23		12.5	16.6	19	2	1(3)	9	3	1/0[h]	-3[i]	7.5/6.5	10.5	1, 66
cytochrome c_{551} (Pseudomonas aeruginosa)	260[j]	7	P	0.2	KCl	8.1	14.4	8	1	0(1)	5	5	1/0[h]	-2[i]	-2/-3	4.7	1, 67
cytochrome f (Parsley)	340	7	P	0.1	NaCl	34.0	23.2	24	11	1(3)	(35)	(37)	1/0[h]	-2[i]		4.7	1, 68
cytochrome c_{552} (Euglena)	370	6-8	TAGP	0.1		10.7	15.8	4	1	0(1)	7	5	1/0[h]	-2[i]	-8/-9	5.5	1, 69, 70
cytochrome c (Candida Krusei)	264[k]	7		0.01		12.0	16.4	11	4	2(4)	7	4	1/0[h]	-2[i]	4/3	>7	1, 66
cytochrome c_2 (Rhodospirillum rubium)	320	7	TAGP	0.1	NaCl	12.8	16.6	17	0	(2)	9	6	1/0[h]	-2[i]	1/0	6.2	71, 72
HiPIP (Chromatium vinosum)	350	7				10.1	15.5	5	2	1	4	5	-1/-2[l]		-2.5/-3.5	3.7	73
Rubridoxin (Clustridium)	-57	7	T	0.1		6.0	13.0	4	0	0	(11)	(6)	-1/-2[m]			<7.3	74
Azurin (Pseudomonas aeruginosa)	328 304	6.4 7	P	0.05		13.9	17.2	11	1	2(4)[n]	4	11	0/-1[o]		-1/-2	5.2	75, 76, 77
Plastocyanin (Bean Phaseolus vulgaris)	350 360[p] 370[q]	6.6	P	0.1		10.7	15.8	5	0	0(2)[n]	9	5	0/-1[o]		-9/-10	<6[r]	68, 78-80
Stellacyanin (Rhus vernicifera)	184	7.1	P	0.3		20	19.5	11	4	2(4)[n]	2(4)	5(21)	0/-1[o]	1[s]	11/10	9.9	81-83

Table 2 Footnotes

[a] The buffers are as given in Table 1.

[b] Calculated from Eq. 28.

[c] The total is in parentheses, the actual number used (outside parentheses) differs if same pK's are known to be shifted.

[d] If the number is in parentheses, only the total of glutamines and glutamates or asparagines and aspartates is known.

[e] Oxidized/reduced.

[f] Calculated as described in the text; oxidized/reduced.

[g] $\Delta H^\circ = -16.8 \pm 0.5$ kcal/mole, $\Delta S^\circ = -36 \pm 1.5$ eu.

[h] Deprotonated heme nitrogens contribute -2.

[i] The two propionate side chains of the heme contribute -2, and for horse heart cytochrome c the N terminus is acetylated; thus there is an additional -1 contribution from the C terminal carboxylate for this protein.

[j] From K = 1 with horse heart cytochrome c (ref. 67).

[k] $\Delta H^\circ = -17.8$ kcal/mole, $\Delta S^\circ = -39$ eu.

[l] Includes a contribution of -4 from thiolates, -8 for four sulfides and +11 for the four irons in the oxidized form.

[m] Four thiolates are coordinated to the single iron.

[n] Assuming two histidines are coordinated.

[o] Assuming a deprotonated amide and a thiolate as ligands.

Table 2 Footnotes (cont'd)

[p] Parsley plastocyanin.

[q] Spinach plastocyanin.

[r] Less than 4.2 of the spinach protein (ref. 78).

[s] See text.

of a cytochrome are charged is from the result for cytochrome c (horse heart). There are not adequate data to make a safe estimate of the charge of stellacyanin, but as there are a great many data available on this protein, an effort was made to make an educated guess in this case, and the assumptions made deserve some comment. The main problem involves the fact that stellacyanin is 20% carbohydrate by weight and the number and type of sugar residues, the number of sugar chains, and the linkage of the sugars to the peptide are unknowns. The problem is further aggravated because the amino acid data available do not distinguish between glutamine and glutamate, or between asparagine and aspartate, and there is the added complication that sugars could be bound to these residues. In charge counting, the linkage of sugars to hydroxyl moieties has no effect, but the more typical asparagine linkages need to be considered. An important distinction that must be made for the amino sugars is whether they have free amines and are charged at neutral pH or are acetylated and thus neutral. The following guesses are made:

(1) Ten of the asparagine/aspartates are covalently linked to sugars (this makes the average chain about four sugar residues long, assuming 40 sugar residues of molecular weight 200 make up the 8,000 dalton sugar contribution); (2) of the remaining 15 aspartate, asparagine, glutamate, and glutamine residues, about half, or 7, or in the acid form; (3) assuming that all but one of the amino sugars are acetylated, and that they compose a total of

4,000 daltons (half of the sugar contribution has been determined to be hexoseamine), there are 17 acetylated positions. This still leaves a charge of 11 on the oxidized protein and clearly more information would be helpful.

Protein electron self-exchange rate constants have been left out of Table 2 because so few are known. The only measured numbers are for cytochrome c (both horse heart and Candida krusei), done by NMR line broadening.[84] The measured rate constants for the horse heart protein are $1(10^3)$ M^{-1} s^{-1} (pH 7, tris, 0.1 M, 40°), with an Arrhenius activation energy of 13 ± 1 kcal/mole, and $1(10^4)$ M^{-1} s^{-1}, with an activation energy of 7 ± 1 kcal/mole under the same conditions except at 1.0 M ionic strength. For the Candida krusei protein under the same pair of conditions the rate constants are $1(10^2)$ and $1(10^3)$ M^{-1} s^{-1}. The rate has also been measured at pH 10 for horse heart cytochrome c and the rate constant is $2(10^4)$ M^{-1} s^{-1}, independent of ionic strength. Similar measurements have been attempted for bean plastocyanin, but the only conclusion that could be reached was that the rate constant was much less than $2(10^4)$ M^{-1} s^{-1} (pH 7, phosphate, 0.1 M, 50°).[85]

V. Inner Sphere Protein-Small Molecule Reactions

There are few well supported examples of inner sphere mechanisms, but those that are available are deserving of comment because of the information they give concerning the protein activation required to take advantage of such a pathway. For the case of the

Cr(II) reduction of cytochrome c,[86] the data have been interpreted as involving crevice opening and adjacent attack at the iron at low pH in the presence of a high concentration of chloride (1 M). The saturation rate at high Cr(II) concentrations is about 60 s^{-1}. Even in this system, however, at high pH or in the presence of good π bridging ions (such as azide or thiocyanate), another mechanism is favored that most likely involves remote attack at the heme edge. The data for the reduction of cytochrome c by dithionite (pH 6.5, 1.0 M) have also been interpreted as involving remote and adjacent pathways,[59] with the latter pathway again being indicated by saturation of the rate constant to a value (30 s^{-1}) near that for the crevice opening process. This issue is not entirely settled, however, as another possible interpretation involves reduction by dithionite and the free radical SO_2^- by parallel paths.[87,88] Inner sphere penetration of a metal center in a protein by a reductant has also been proposed as a pathway in the hydroquinone reduction of tree laccase.[89] In this case the type 2 copper was suggested as the site of attack by the hydroquinone monoanion. Unfortunately, the oxidation state of the type 2 copper cannot be monitored by optical absorption methods, and the reduction of the separate type 3 and type 1 sites must be followed. The results show that these two sites are not reduced at quite the same rate or with quite the same activation parameters. Possible mechanisms include prior reduction of the type 2 center followed by electron transfer from

a coordinated hydroquinone directly to one of the sites. For the fungal form of the enzyme, fast quench EPR analysis has shown that the type 2 copper is transiently reduced and reoxidized during the reduction of the other two sites,[90] but caution must be exercised in comparing the two systems, as their redox mechanisms may well be different.[2]

VI. Outer Sphere Protein-Small Molecule Reactions

The cross reaction equations of Marcus theory will be employed in many of the calculations to be discussed in this section. Some general justification for the use of these equations, besides the argument that the reactions must be outer sphere, can be given. The prediction of a uniform k_{11} value, from given k_{12}, k_{22}, and K values, is not expected because of the presumed mechanistic options for each protein. However, the general pattern of large differences in driving force being paralleled by a difference in rate in the same direction, and large differences in k_{22} leading to a faster cross reaction rate constant corresponding to the reagent with the much larger k_{22}, may be expected. A dramatic difference between the $Co(phen)_3^{3+}$ and the analogous $Co(EDTA)^-$ oxidations of ferrocytochrome c may be cited, where the latter reagent has a self-exchange rate about 10^8 lower[91] than that[45] of the former. The k_{12} for the $Co(EDTA)^-$ oxidation of ferrocytochrome c is at least 10^6 smaller than that for the corresponding $Co(phen)_3^{3+}$ reaction.[92]

The available data for electron transfer reactions between metalloproteins and inorganic complexes are collected in Table 3,[93-110] and the calculated self-exchange rate constants using the parameters from Tables 1, 2, and 3 are given in the k_{11} columns of Table 4.

Electrostatic effects are reflected in the ionic strength dependences of the cross reaction rate constants. As there are several ionic strength dependence studies available, it is of interest to fit the available data to the three equations (Eqs. 5, 6, 28) given in the Theory section. The results of the fits are set out in Table 5,[111] along with the isoelectric points, and the charges taken from the sequences (Table 2). Eq. 6, which predicts a linear dependence of log(k) on $\mu^{\frac{1}{2}}$, is included because of its common use, but it should not be considered as an alternative, as Eq. 5 gives the ionic strength dependence predicted from the standard activity coefficient theory. In these calculations, only the protein charge has been considered as a variable, and the rest of the parameters have been assumed to have the values given in Tables 1 and 2. This is justified as the charge and radius of each of the reagents are well known, and the radius of the protein may reasonably be estimated from Eq. 26, as shown by the comparison to the dimensions of cytochrome c (25 × 30 × 35 Å,[1] compared to a predicted diameter for the equivalent sphere of 33.2 Å). Another approach that has been considered involves the "active site" concept. In this model, there is a small region of the protein that is assumed to have a certain charge and radius and to contribute to the electrostatic interactions in an independent way. If the rest of the protein is considered also, the

Table 3. Protein-Small Molecule Cross Reaction Rate Data

Protein	Reagent	$k(M^{-1}s^{-1})$	T	$\Delta H^{\ddagger}$ (kcal/mole)	$\Delta S^{\ddagger}$ (eu)	pH	Buffer[a]	μ(M)	Salt	Ref.
Cytochrome c (horse heart)	$Fe(EDTA)^{2-}$	$2.57(10^4)$	25	6.0	-18	7.0	P[b]	0.10	NaCl	93
	$Ru(NH_3)_6^{2+}$	$3.8(10^4)$[c]	25	2.9[c]	-28[c]	3.3-7.0	T	0.10	HCl	94
	$Co(phen)_3^{3+}$	$1.50(10^3)$	25	11.3	-6.2	7.0	P	0.10	NaCl	95
	$Co(5\text{-Cl-phen})_3^{3+}$	$1.26(10^2)$	25	11.3	-6	7.0	P	0.10	NaCl	47
	$Co(5,6\text{-(Me)}_2\text{-phen})_3^{3+}$	$2.66(10^2)$	25	9.6	-16	7.0	P	0.10	NaCl	47
	$Co(4,7\text{-(Me)}_2\text{-phen})_3^{3+}$	$2.76(10^1)$	25	14.6	-3	7.0	P	0.10	NaCl	47
	$Co(4,7\text{-}(\phi\text{-}SO_3)_2\text{-phen})_3^{3-}$	$2.87(10^4)$	25	12.8	0	7.0	P	0.10	NaCl	47
	$Fe(CN)_6^{4-}$[d]	$2.4(10^4)$	25			7.0	P, T, C	0.10		96
	$Fe(CN)_6^{4-}$	$2.6(10^4)$	22			7.0	P, EDTA	0.18	Na_2SO_4	97
	$Fe(CN)_6^{3-}$	$8.1(10^6)$	22			7.0	P, EDTA	0.18	Na_2SO_4	97
		$1.2(10^7)$	25			7.2	P, EDTA	0.10	NaCl	59
		$6.5(10^6)$[e]	25			7.0	P	0.10		96
		$6.7(10^5)$	25	0	-27	7.0	P	0.18[f]	KCl	67
		$8.0(10^5)$	25	1.1	-23	7.0	P	0.10	KCl	98
	$Fe(CN)_4bipy^{-}$	$1.6(10^8)$	25			7.0	P	0.10	KCl	98
	$Fe(CN)_5P\phi_3^{2-}$	$3.0(10^7)$	25	1.2	-20	7.0	P	0.10	KCl	98
	$Fe(CN)_5NH_3^{2-}$	$2.5(10^6)$	25	2.4	-21	7.0	P	0.10	KCl	98
	$Fe(CN)_5N_3^{3-}$	$9.0(10^5)$	25	2.9	-21	7.0	P	0.10	KCl	98

Table 3. Protein-Small Molecule Cross Reaction Rate Data

Protein	Reagent	$k(M^{-1}s^{-1})$	T	$\Delta H^{\ddagger}$ (kcal/mole)	$\Delta S^{\ddagger}$ (eu)	pH	Buffer[a]	μ(M)	Salt	Ref.
Cytochrome c_{551} (Pseudomonas aeruginosa)	$Fe(EDTA)^{2-}$	$4.2(10^3)$	25	3.2	-30	7.0	P	0.10		99
	$Co(phen)_3^{3+}$	$5.3(10^4)$	25	12.3	4	7.0	P	0.10	NaCl	100
	$Co(5\text{-Cl-phen})_3^{3+}$	$4.42(10^3)$	25	9.4	-10	7.0	P	0.10	NaCl	47
	$Co(5,6\text{-(Me)}_2\text{-phen})_3^{3+}$	$2.70(10^3)$	25	13.6	7	7.0	P	0.10	NaCl	47
	$Co(4,7\text{-(Me)}_2\text{-phen})_3^{3+}$	$3.17(10^3)$	25	10.9	-6	7.0	P	0.10	NaCl	47
	$Co(4,7\text{-}(\phi\text{-SO}_3)_2\text{-phen})_3^{3-}$	$2.75(10^4)$	25	13.8	8	7.0	P	0.10	NaCl	47
	$Fe(CN)_6^{3-}$	$8(10^4)$	20			7.0	P,EDTA	0.10		101
Cytochrome c (Candida krusei)	$Co(phen)_3^{3+}$	$2.7(10^3)$	25			7.2	P	0.10	NaCl	95
	$Fe(CN)_6^{3-}$	$2.1(10^7)$	25			7.2	P	0.10	NaCl	59
Cytochrome c (Euglena gracilis)	$Fe(CN)_6^{4-}$	$7.8(10^3)$[g]	23	5.2	-21	7.0	TAGP			102
	$Fe(CN)_6^{3-}$	$4.0(10^4)$	23	0	-37	7.0	TAGP			102
Cytochrome f (Parsley)	$Fe(CN)_6^{3-}$	$8.0(10^4)$	25			7.0	P	0.10	NaCl	68
Cytochrome c_2 (Rhodospirillum rubrum)	$Fe(CN)_6^{4-}$	$6.6(10^4)$[h]	20	11.4	1.8	7.0	P	0.10	NaCl	104
	$Fe(CN)_6^{3-}$	$2.2(10^6)$	20	5.2	-10.2	7.0	P	0.10	NaCl	104
HiPIP (Chromatium vinosum)	$Fe(EDTA)^{2-}$	$1.7(10^3)$	25	0.4	-41	7.0	P	0.1	NaCl	105
	$Co(phen)_3^{3+}$	$2.8(10^3)$	26	14	4	7.0	P	0.1	NaCl	105

Table 3. Protein-Small Molecule Cross Reaction Rate Data

Protein	Reagent	$k(M^{-1}s^{-1})$	T	$\Delta H^{\ddagger}$ (kcal/mole)	$\Delta S^{\ddagger}$ (eu)	pH	Buffer[a]	μ(M)	Salt	Ref.
HiPIP (Chromatium vinosum)	$Fe(CN)_6^{4-}$	$1.8(10^2)$	25			7.0	T	0.10		3
	$Fe(CN)_6^{4-}$	$1.49(10^2)$	20	4.2	-35	7.3	T	0.008		102
	$Fe(CN)_6^{3-}$	$2.4(10^3)$	25	-0.2	-44	7.0	P	0.10	NaCl	105
	$Fe(CN)_6^{3-}$	$4.2(10^3)$	25			7.0	T	0.10		3
	$Fe(CN)_6^{3-}$	$1.15(10^3)$	20	0	-45	7.3	T	0.008		102
	$Ru(NH_3)_6^{2+}$	$3.1(10^5)$	25			7.0	T	0.10		3
	$Co(bipy)_3^{3+}$	$4.5(10^2)$	25			7.0	T	0.10		107
Rubridoxin (Clostridium)	$Ru(NH_3)_6^{2+}$	$9.5(10^4)$	25	~1.4	~ -31	6.3-7.0	T	0.10	HCl	108
Azurin (Pseudomonas aeruginosa)	$Fe(EDTA)^{2-}$	$1.3(10^3)$	25	2.0	-37	7.0[e]	P	0.20	$(NH_4)_2SO_4$	109
	$Co(phen)_3^{3+}$	$3.2(10^3)$	25	14.3	7	7.0	P	0.20	NaCl	100
	$Co(5\text{-Cl-phen})_3^{3+}$	$4.21(10^2)$	25	8.0	-17	7.0	P	0.20	NaCl	100
	$Co(5,6\text{-}(Me)_2\text{-phen})_3^{3+}$	$1.54(10^3)$	25	11.6	-5	7.0	P	0.20	NaCl	100
	$Co(4,7\text{-}(Me)_2\text{-phen})_3^{3+}$	$6.41(10^1)$	25	9.9	-17	7.0	P	0.20	NaCl	100
	$Fe(CN)_6^{3-}$	$1.2(10^4)$	20			7.0	P	0.10		101
	$Fe(CN)_6^{3-}$	$2.7(10^4)$	25	-4.1	-52	7.0	P,EDTA	0.22		106
	$Fe(CN)_6^{4-}$	$3.4(10^2)$	25	5.9	-27	7.0	P,EDTA	0.22		106

Table 3. Protein-Small Molecule Cross Reaction Rate Data

Protein	Reagent	$k(M^{-1}s^{-1})$	T	$\Delta H^{\ddagger}$ (kcal/mole)	$\Delta S^{\ddagger}$ (eu)	pH	Buffer[a]	μ(M)	Salt	Ref.
Plastocyanin (Bean)	$Fe(EDTA)^{2-}$	$8.2(10^4)$	25	2.1	-29	7.0[e]	P	0.20	$(NH_4)_2SO_4$	109
	$Co(phen)_3^{3+}$	$4.9(10^3)$	25	14.0	5	7.0	P	0.10	$(NH_4)_2SO_4$	100
	$Co(5\text{-}Cl\text{-}phen)_3^{3+}$	$6.96(10^2)$	25	11.5	-6	7.0	P	0.10	$(NH_4)_2SO_4$	100
	$Co(5,6\text{-}(Me)_2\text{-}phen)_3^{3+}$	$7.97(10^2)$	25	13.6	1	7.0	P	0.10	$(NH_4)_2SO_4$	100
	$Co(4,7\text{-}(\phi\text{-}SO_3)_2\text{-}phen)_3^{3-}$	$2.59(10^1)$	25	7.8	-26	7.0	P	0.10	$(NH_4)_2SO_4$	100
	$Fe(CN)_6^{4-}$	$1.9(10^4)$	25	8.4	-11	6.0	A	0.20		110
Spinach	$Fe(CN)_6^{4-}$	$2.0(10^4)$	20	8.8	-9.1	6.0	A	0.20		110
(Parsley)	$Fe(CN)_6^{3-}$	$7(10^4)$	25			7.0	P	0.10	NaCl	68
Stellacyanin (Rhus vernicifera)	$Fe(EDTA)^{2-}$	$4.3(10^5)$	25	3.0	-21	7.0[e]	P	0.50	$(NH_4)_2SO_4$	109
	$Co(phen)_3^{3+}$	$1.8(10^5)$	25	6	-13	7.0	P	0.10	$(NH_4)_2SO_4$	110
	$Co(5,6\text{-}(Me)_2\text{-}phen)_3^{3+}$	$1.85(10^4)$	25	9.5	-7	7.0	P	0.10	$(NH_4)_2SO_4$	110
	$Co(4,7\text{-}(\phi\text{-}SO_3)_2\text{-}phen)_3^{3-}$	$2.31(10^6)$	25	5.9	-10	7.0	P	0.10	$(NH_4)_2SO_4$	110

Table 3 Footnotes

[a] Buffer abbreviations are as given in Table 1.

[b] Other media have also been studied.

[c] An acid dependent path has also been observed, but these values are acid independent.

[d] Binding of ferricyanide and ferrocyanide to cytochrome c is now well established (see refs. 34 and 87); the rate constants here are the limiting second order rate constants at low reagent concentrations.

[e] pH dependence determined.

[f] Ionic strength dependence determined and found to be large.

[g] Ionic strength and pH dependences have also been performed, and the pH dependence of the potential is available.

[h] Ionic strength and pH dependences and anion inhibition (except by cacodylate) have been determined.

Table 4. Calculated Protein Self-Exchange Rate Constants, Including Electrostatic Corrections

Protein	Reagent	w_{12}[a,b]	w_{21}[a,b]	w_{11}[a,c]	w_{22}[a,d]	ΔG_{11}^{*}[a,e]	$k_{11}(M^{-1}s^{-1})$[e]	ΔG_{11}^{*corr}[a,f]	$k_{11}^{corr}(M^{-1}s^{-1})$[f]
Cytochrome c (Horse heart)	$Fe(EDTA)^{2-}$	-0.567	-0.246	0.406	0.493	14.63	$1.2(10^{2})$	16.36	6.2
	$Ru(NH_3)_6^{2+}$	0.655	0.851	0.406	3.401	13.51	$7.6(10^{2})$	15.82	$1.6(10^{1})$
	$Co(phen)_3^{3+}$	0.490	0.377	0.406	0.507	13.51	$7.6(10^{2})$	13.55	$7.1(10^{2})$
	$Co(5\text{-Cl-phen})_3^{3+}$	0.404	0.311	0.406	0.328	12.94	$2.0(10^{3})$	12.95	$2.0(10^{3})$
	$Co(5,6\text{-}(Me)_2\text{-phen})_3^{3+}$	0.431	0.331	0.406	0.377	12.63	$3.4(10^{3})$	12.65	$3.3(10^{3})$
	$Co(4,7\text{-}(Me)_2\text{-phen})_3^{3+}$	0.490	0.377	0.406	0.507	15.17	$4.6(10^{1})$	15.22	$4.3(10^{1})$
	$Co(4,7\text{-}(\phi\text{-}SO_3)_2\text{phen})_3^{3-}$[g]	-0.282	-0.434	0.406	0.304	12.11	$8.1(10^{3})$	13.53	$7.4(10^{2})$
		-0.490	-0.754	0.406	1.014	11.78	$1.4(10^{4})$	14.44	$1.6(10^{2})$
		-0.731	-1.031	0.406	0.956	10.34	$1.6(10^{5})$	13.45	$8.4(10^{2})$
	$Fe(CN)_6^{4-}$[h]	-1.056	-0.686	0.406	2.408	7.19	$3.3(10^{7})$	11.73	$1.6(10^{4})$
	$Fe(CN)_6^{3-}$[h,i]	-0.686	-1.056	0.406	2.408	8.18	$6.2(10^{6})$	12.71	$2.9(10^{3})$
	$Fe(CN)_6^{3-}$[j,k]	-0.433	-0.667	0.406	1.752	8.634	$2.9(10^{6})$	11.88	$1.2(10^{4})$
	$Fe(CN)_5N_3^{3-}$	-0.686	-1.056	0.406	2.408	5.78	$3.6(10^{8})$	10.34	$1.6(10^{5})$
	$Fe(CN)_5NH_3^{2-}$	-0.458	-0.792	0.406	1.204	8.74	$2.4(10^{6})$	11.58	$2.0(10^{4})$
	$Fe(CN)_5P\phi_3^{2-}$	-0.458	-0.792	0.406	1.204	8.24	$5.6(10^{6})$	11.08	$4.7(10^{4})$
	$Fe(CN)_4bipy^{-}$	-0.229	-0.528	0.406	0.401	10.67	$9.3(10^{4})$	12.20	$7.0(10^{3})$
Cytochrome c_{551} (Pseudomonas aeruginosa)	$Fe(EDTA)^{2-}$	0.194	0.146	0.079	0.493	16.80	3.0	17.03	2.0
	$Co(phen)_3^{3+}$	-0.287	-0.128	0.079	0.507	9.28	$9.7(10^{5})$	10.29	$1.8(10^{5})$
	$Co(5\text{-Cl-phen})_3^{3+}$	-0.236	-0.105	0.079	0.328	8.71	$2.5(10^{6})$	9.47	$7.0(10^{5})$

Table 4. Calculated Protein Self-Exchange Rate Constants, Including Electrostatic Corrections

Protein	Reagent	w_{12}[a,b]	w_{21}[a,b]	w_{11}[a,c]	w_{22}[a,d]	ΔG_{11}^{*}[a,e]	$k_{11}(M^{-1}s^{-1})$[e]	ΔG_{11}^{*corr}[a,f]	$k_{11}^{corr}(M^{-1}s^{-1})$[f]
Cytochrome c_{551}									
	$Co(5,6\text{-}(Me)_2\text{-}phen)_3^{3+}$	-0.252	-0.112	0.079	0.377	9.88	$2.5(10^5)$	10.71	$8.7(10^4)$
	$Co(4,7\text{-}(Me)_2\text{-}phen)_3^{3+}$	-0.287	-0.128	0.079	0.507	9.55	$6.1(10^5)$	10.56	$1.1(10^5)$
	$Co(4,7\text{-}(\phi\text{-}SO_3)_2\text{-}phen)_3^{3-}$	0.164	0.146	0.079	0.304	12.16	$7.4(10^3)$	12.24	$6.6(10^3)$
		0.287	0.255	0.079	1.014	11.21	$3.7(10^4)$	11.76	$1.5(10^4)$
		0.434	0.353	0.079	0.956	10.40	$1.5(10^5)$	10.64	$9.7(10^4)$
	$Fe(CN)_6^{3-i}$	0.406	0.361	0.079	2.408	13.42	$8.9(10^2)$	15.14	$4.9(10^1)$
Cytochrome c (Candida krusei)	$Co(phen)_3^{3+}$	0.231	0.205	0.104	0.507	12.73	$2.9(10^3)$	12.90	$2.2(10^3)$
	$Fe(CN)_6^{3-i}$	-0.324	-0.576	0.104	2.408	6.78	$6.7(10^7)$	10.17	$2.2(10^5)$
Cytochrome c_{552} (Euglena gracilis)	$Fe(CN)_6^{4-i}$	1.230	1.038	0.705	2.408	11.00	$5.4(10^4)$	11.85	$1.3(10^4)$
	$Fe(CN)_6^{3-i}$	1.038	1.230	0.705	2.408	12.06	$8.9(10^3)$	12.91	$2.1(10^3)$
Cytochrome c_2 (Rhodospirillum rubrum)	$Fe(CN)_6^{4-i}$	-0.141	0	0	2.408	7.49	$2.0(10^7)$	10.03	$2.7(10^5)$
	$Fe(CN)_6^{3-i}$	0	-0.141	0	2.408	8.19	$6.2(10^6)$	10.73	$8.4(10^4)$
HiPIP (Chromatum vinosum)	$Fe(EDTA)^{2-}$	0.213	0.149	0.091	0.493	19.81	$1.9(10^{-2})$	20.02	$1.3(10^{-2})$
	$Co(phen)_3^{3+}$	-0.296	-0.141	0.091	0.507	10.75	$8.1(10^4)$	11.79	$1.4(10^4)$
	$Fe(CN)_6^{4-i}$	0.398	0.417	0.091	2.408	15.22	$4.2(10^1)$	16.91	2.5
	$Fe(CN)_6^{3-i}$	0.417	0.397	0.091	2.408	15.62	$2.2(10^1)$	17.30	1.3
	$Ru(NH_3)_6^{2+}$	-0.247	-0.519	0.019	3.401	12.72	$2.9(10^3)$	16.96	2.3
	$Co(bipy)_3^{3+}$	-0.056	-0.170	0.021	0.507	12.94	$2.0(10^3)$	13.70	$5.6(10^2)$

Table 4. Calculated Protein Self-Exchange Rate Constants, Including Electrostatic Corrections

Protein	Reagent	w_{12}[a,b]	w_{21}[a,b]	w_{11}[a,c]	w_{22}[a,d]	ΔG_{11}^{*}[a,e]	$k_{11}(M^{-1}s^{-1})$[e]	ΔG_{11}^{*corr}[a,f]	$k_{11}^{corr}(M^{-1}s^{-1})$[f]
Azurin[1] (Pseudomonas aeruginosa)	$Fe(EDTA)^{2-}$	0.041	0.041	0.015	0.493	19.66	$2.4(10^{-2})$	20.09	$1.9(10^{-2})$
	$Co(phen)_3^{3+}$	-0.074	-0.025	0.015	0.507	11.09	$4.5(10^{4})$	11.71	$1.6(10^{4})$
	$Co(5\text{-}Cl\text{-}phen)_3^{3+}$	-0.058	-0.019	0.015	0.328	10.02	$2.8(10^{5})$	10.44	$1.4(10^{5})$
	$Co(5,6\text{-}(Me)_2\text{-}phen)_3^{3+}$	-0.062	-0.021	0.015	0.377	9.06	$1.4(10^{6})$	9.53	$6.3(10^{5})$
	$Co(4,7\text{-}(Me)_2\text{-}phen)_3^{3+}$	-0.074	-0.025	0.015	0.507	12.31	$5.8(10^{3})$	12.93	$2.0(10^{3})$
	$Fe(CN)_6^{3-}$	0.198	0.132	0.015	2.408	14.15	$2.6(10^{2})$	16.24	7.6
	$Fe(CN)_6^{3-}$ m	0.104	0.070	0.015	1.752	14.07	$3.0(10^{2})$	15.66	$2.0(10^{1})$
	$Fe(CN)_6^{4-}$ m	0.070	0.104	0.015	1.752	13.71	$5.5(10^{2})$	15.30	$3.7(10^{1})$
Plastocyanin (Bean)	$Fe(EDTA)^{2-}$	0.743	0.413	0.882	0.493	15.18	$4.6(10^{1})$	15.35	$3.4(10^{1})$
	$Co(phen)_3^{3+}$	-0.820	-0.492	0.882	0.507	10.09	$2.5(10^{5})$	12.79	$2.6(10^{3})$
	$Co(5\text{-}Cl\text{-}phen)_3^{3+}$	-0.677	-0.406	0.882	0.328	8.93	$1.7(10^{6})$	11.23	$3.6(10^{4})$
	$Co(5,6\text{-}(Me)_2\text{-}phen)_3^{3+}$	-0.721	-0.432	0.882	0.377	9.34	$8.7(10^{5})$	11.76	$1.5(10^{4})$
	$Co(4,7\text{-}(\phi\text{-}SO_3)_2\text{-}phen)_3^{3-}$	0.471	0.565	0.882	0.304	18.36	$2.1(10^{-1})$	18.51	$1.6(10^{-1})$
		0.820	0.984	0.882	1.014	17.41	1.1	17.50	$9.1(10^{-1})$
		1.229	1.352	0.882	0.956	16.59	4.2	15.84	$1.5(10^{1})$
	$Fe(CN)_6^{4-}$ k	0.804	0.670	0.882	1.752	9.83	$3.8(10^{5})$	11.00	$5.3(10^{4})$
Plastocyanin (Spinach)	$Fe(CN)_6^{4-}$ n	0.804	0.670	0.882	1.752	10.25	$1.9(10^{5})$	11.42	$2.6(10^{4})$
Plastocyanin (Parsley)	$Fe(CN)_6^{3-}$	1.153	1.384	0.882	2.408	11.40	$2.7(10^{4})$	12.15	$7.6(10^{3})$
Stellacyanin (Rhus vernicifera)	$Fe(EDTA)^{2-}$	0	0	0	0.493	9.63	$5.4(10^{5})$	10.12	$2.3(10^{5})$

Table 4. Calculated Protein Self-Exchange Rate Constants, Including Electrostatic Corrections

Protein	Reagent	w_{12}[a,b]	w_{21}[a,b]	w_{11}[a,c]	w_{22}[a,d]	ΔG_{11}^{*}[a,e]	$k_{11}(M^{-1}s^{-1})$[e]	ΔG_{11}^{*corr}[a,f]	$k_{11}^{corr}(M^{-1}s^{-1})$[f]
Stellacyanin[o] (Rhus vernicifera)	$Co(phen)_3^{3+}$	0	0	0	0.507	9.46	$7.1(10^5)$	9.97	$3.0(10^5)$
	$Co(5,6\text{-}(Me)_2\text{-}phen)_3^{3+}$	0	0	0	0.377	9.21	$1.1(10^6)$	9.59	$5.8(10^5)$
		0	0	0	0.304	8.56	$3.3(10^6)$	8.86	$2.0(10^6)$
	$Co(4,7\text{-}Ø\text{-}SO_3)_2\text{-}phen)_3^{3-}$	0	0	0	1.014	7.61	$1.6(10^7)$	8.62	$3.0(10^6)$
		0	0	0	0.965	6.73	$6.6(10^7)$	7.74	$1.3(10^7)$

Table 4 Footnotes

[a] All energies are in kcal/mole.

[b] Work terms are calculated using the conditions given in Table 3 and assuming protein charges calculated from the sequences (Table 2).

[c] Work term calculated for 0.1 M ionic strength, pH 7, and assuming protein charges calculated from the sequences (Table 2).

[d] Work term calculated for the condition of the measured self-exchange rate constant given in Table 1.

[e] Calculated without consideration of electrostatic interaction.

[f] Calculated for 0.1 M ionic strength, pH 7, including compensation for electrostatic interactions assuming protein charges calculated from the sequences (Table 2).

[g] The three different values are for three models for the electrostatic interaction; see footnote 48.

[h] From the data of ref. 96.

[i] Using k_{22} ($Fe(CN)_6^{3-/4-}$) of $1.5(10^4)$ $M^{-1}s^{-1}$ and a potential of 425 mV from the 0.1 M ionic strength (KCl) data.

[j] From the data of ref. 67.

[k] Using $k_{22}(Fe(CN)_6^{3-/4-})$ of $2.6(10^4)$ $M^{-1}s^{-1}$ and a potential of 433 mV from the 0.2 M ionic strength data.

[l] A potential of 330 mV is used for azurin, as given in ref. 75.

Table 4 Footnotes (cont'd)

[m] A potential difference of 120 mV is used (ref. 106) and a $Fe(CN)_6^{3-/4-}$ exchange rate of $2.6(10^4)$ $\underline{M}^{-1}$ s^{-1} for 0.2 $\underline{M}$ ionic strength.

[n] Using k_{22} ($Fe(CN)_6^{3-/4-}$) of $2.6(10^4)$ $\underline{M}^{-1}$ s^{-1} and a potential of 435 mV.

[o] Assuming Z = 0 from the ionic strength dependence with $Co(phen)_3^{3+}$; see Table 5.

Table 5. Ionic Strength Dependence Fits[a]

Protein	Reagent	Equation 6 Z_1	Equation 6 k_0	Equation 6 S.E.[b]	Equation 5 Z_1	Equation 5 k_0	Equation 5 S.E.[b]	Equation 28 Z_1	Equation 28 k_0	Equation 28 S.E.[b]	Ref.
Cytochrome c (7.5/6.5, 10.5)[c] (Horse heart)	$Fe(EDTA)^{2-}$	1.69	$2.68(10^5)$	$7.8(10^2)$	5.49	$7.96(10^5)$	$1.2(10^3)$	8.10	$8.58(10^3)$	$1.9(10^3)$	93
	$Co(phen)_3^{3+}$	0.42	$6.00(10^2)$	$1.2(10^1)$	5.73	$3.08(10^1)$	$1.8(10^1)$	4.71	$2.89(10^3)$	$2.0(10^1)$	95
	$Fe(CN)_6^{3-}$	0.64	$6.94(10^7)$	$1.2(10^6)$	2.01	$2.25(10^8)$	$5.1(10^5)$	6.61	$3.81(10^6)$	$5.8(10^5)$	67
	$Fe(CN)_6^{4-}$	0.49	$2.93(10^5)$	$1.1(10^6)$	1.01	$1.90(10^6)$	$9.1(10^2)$	14.6	$5.74(10^3)$	$7.6(10^2)$	67
	Cytochrome c[d] (Horse heart)	1.55	$2.84(10^2)$	$4.8(10^4)$	5.75	$1.9(10^{-1})$	$5.4(10^2)$	10.3	$9.51(10^3)$	$1.1(10^3)$	84
Cytochrome c_{551} (-2/-3, 4.7) (Pseudomonas aeruginosa)	$Co(phen)_3^{3+}$	0.55	$2.32(10^5)$	$8.5(10^3)$	-2.0	$6.52(10^5)$	$7.3(10^3)$	-4.33	$3.47(10^4)$	$7.2(10^3)$	100
Cytochrome c_{552} (-8/-9, 5.5) (Euglena gracilis)	$Fe(CN)_6^{4-}$	-0.18	$1.73(10^3)$	$1.90(10^2)$	-5.9	$5.63(10^1)$	$5.6(10^2)$	-1.30	$4.78(10^3)$	$2.5(10^3)$	69
	$Fe(CN)_6^{3-}$	-0.42	$8.60(10^3)$	$3.1(10^3)$	-7.0	$3.73(10^2)$	$2.6(10^3)$	-2.98	$4.94(10^4)$	$2.5(10^3)$	69
Cytochrome c_2 (1/0, 6.2) Rhodospirillum rubrum)	$Fe(CN)_6^{4-}$[e]	0.73	$1.06(10^6)$	$6.8(10^4)$	4.46	$9.10(10^7)$	$3.9(10^3)$	13.96	$2.54(10^3)$	$7.3(10^4)$	104
	$Fe(CN)_6^{3-}$[f]	0.39	$7.61(10^6)$	$3.1(10^3)$	0.90	$1.90(10^7)$	$2.6(10^3)$	7.26	$6.96(10^5)$	$2.9(10^5)$	104
	$Fe(CN)_6^{4-}$[g]	0.08	$4.80(10^2)$	9.4	-4.8	$1.72(10^1)$	9.6	1.54	$2.47(10^2)$	9.0	104
Azurin (-1/-2, 5.2) (Pseudomonas aeruginosa)	$Fe(EDTA)^{2-}$	-0.15	$1.12(10^3)$	$1.0(10^1)$	-3.55	$3.96(10^2)$	$3.4(10^1)$	-1.10	$1.68(10^3)$	$1.4(10^1)$	111
	$Co(phen)_3^{3+}$	-0.16	$3.18(10^3)$	$3.1(10^1)$	1.04	$2.01(10^3)$	$3.1(10^1)$	-1.89	$1.72(10^3)$	$2.6(10^1)$	100

Table 5. Ionic Strength Dependence

Protein[a]	Reagent	Equation 6 Z_1	Equation 6 k_0	Equation 6 S.E.[b]	Equation 5 Z_1	Equation 5 k_0	Equation 5 S.E.[b]	Equation 28 Z_1	Equation 28 k_0	Equation 28 S.E.[b]	Ref.
Plastocyanin (-9/-10, <6) (Eean)	$Fe(EDTA)^{2-}$	-0.55	$2.05(10^4)$	$3.9(10^3)$	-8.88	$5.62(10^2)$	$7.9(10^2)$	-7.20	$1.39(10^5)$	$1.2(10^3)$	111
Stellacyanin (10, 9.9) (Rhus vernicifera)	$Co(phen)_3^{3+}$	0.00	$1.92(10^5)$	$1.4(10^3)$	3.49	$3.51(10^4)$	$2.2(10^3)$	0.00	$1.89(10^5)$	$1.4(10^3)$	100
HiPIP (2.5/-3.5, 3.7) (Chromatium vinosum)	$Fe(CN)_6^{3-}$	-0.46	$8.52(10^2)$	$2.6(10^1)$	-5.2	$9.3(10^1)$	$1.5(10^2)$	-2.25	$4.1(10^3)$	$1.3(10^2)$	102
	$Fe(CN)_6^{4-}$	0.00	$1.51(10^2)$	5.0	-3.2	$2.6(10^1)$	9.8	-0.01	$1.50(10^2)$	5.0	102

Table 5 Footnotes

[a] Least squares procedure.

[b] The standard error, defined as $(\Sigma (k_{obs}-k_{fit})^2)/N$.

[c] These numbers are the charges calculated from the sequence (oxidized/reduced) and the isoelectric point.

[d] Solving for the charge assuming both oxidation states have the same charge.

[e] This is k_{12} of ref. 104.

[f] This is k_{43} of ref. 104.

[g] This is k_{21} of ref. 104.

problem becomes one of considering two spheres, one within the other, which are tangential at the point of attack by the reagent. The charge and radius of the small "site" are set and the radius of the protein is used for the larger sphere. The charge on the larger sphere is the difference between the total charge (as determined from the sequence) and that assigned to the site. Reasonable guesses for the site can only be made for proteins for which X-ray data are available; therefore, the example calculation given in Table 6 is for cytochrome c. In principle, this approach could also be used for fitting the ionic strength data, but the number of parameters is larger and the results would be difficult to interpret; therefore, the site model will only be used in some example calculations of work terms (vide infra).

Using the work term theory presented in Section II-C, the calculated protein self-exchange rate constants may be corrected for electrostatic (coulombic) effects. In order to make these corrections, a charge and radius are needed for the protein; for this purpose the charges calculated from the sequences and the radii given in Table 2 will be used. The resulting k_{11}^{corr} values are presented in Table 4. The Marcus theory fit to the ionic strength dependences could be used for estimating the charge in order to maintain internal consistency. As the charges calculated in this way (except for $Fe(CN)_6^{3-/4-}$) are close to the sequence charges, and, as ionic strength dependence data are not available for many reactions, these calculations are not presented.

Table 6. Site Model for Cytochrome c Self-Exchange Rate Constant Calculation

Reagent	Model	w_{12}[a]	w_{21}[a]	w_{11}[a]	w_{22}[a]	ΔG_{12}^{*corr}[a]	k_{11}^{corr} ($M^{-1}s^{-1}$)
$Fe(EDTA)^{2-}$	1[b]	-0.567	-0.246	0.406	0.493	16.36	6.2
	2[c,d]	-0.471	-0.236	0.251	0.493	16.10	9.7
	3[e]	-0.790	-0.395	0.712	0.493	17.05	1.9
$Co(phen)_3^{3+}$	1	0.490	0.377	0.406	0.507	13.55	$7.1(10^2)$
	2	0.436	0.291	0.251	0.507	18.64	$6.2(10^2)$
	3	0.614	0.409	0.712	0.507	13.70	$5.6(10^2)$
$Ru(NH_3)_6^{2+}$	1	0.655	0.851	0.406	3.402	15.82	$1.6(10^1)$
	2	0.563	0.844	0.251	3.402	15.77	$1.7(10^1)$
	3	1.037	1.556	0.712	3.402	15.06	$5.6(10^1)$
$Fe(CN)_6^{3-}$[f]	1	-0.433	-0.667	0.406	1.752	11.88	$1.2(10^4)$
	2	-0.461	-0.614	0.251	1.752	11.71	$1.6(10^4)$
	3	-0.862	-1.149	0.712	1.752	13.10	$1.5(10^3)$

Table 6 Footnotes

[a] All energies in kcal/mole; see footnotes b, c, d, and f of Table 4 for a description of the conditions for which the calculations are made.

[b] The same as Table 4 (a radius of 16.6 Å and charges of 7.5 and 6.5).

[c] The site parameters are derived from measurement of a model of oxidized tuna cytochrome c and the assumption that the attack site is near the point the heme edge comes nearest the surface of the protein; model 3 is considered as a single lysine; model 2 is a larger site including several charged groups.

[d] A radius of 8Å and a charge of 2.

[e] A radius of 2Å and a charge of 1.

[f] Ref. 67.

Another approach to treating the problem of electrostatic interaction is to do the calculations with the formula that includes the equilibrium constants for the formation of the precursor and successor complexes (Eq. 29). This is the preferred method when pre-equilibrium binding is shown by saturation behavior in the plot of k_{obsd} *vs.* reagent concentration. There is, however, a problem. Although some of the binding constants may be estimated from the kinetics, others are not so available (this is generally true for the exchange reactions, where both oxidation states are usually positive or negative, and therefore not expected to show discernible binding based on electrostatics), and must be estimated using Eq. 3. An important pair of protein cross reactions which may be treated in this manner involve the iron hexacyanides with horse heart cytochrome *c*, where saturation behavior is observed (as are exceptionally high rates). The cytochrome *c* self-exchange has been calculated using the equilibrium constant approach (Table 7). The result may be compared to predictions based on treatment of the same data with work terms (Table 4).

Shown in Figure 6 is a plot of the log of the ratio between the calculated protein self-exchange rate constant with a variety of reagents and with $Fe(EDTA)^{2-}$ *vs.* log k_{11}^{corr} based on $Fe(EDTA)^{2-}$ alone. The exchange rate constants used in making up the figure are the best

Table 7. Cytochrome c Self Exchange Rate Constant Calculation with Complex Formation $(Fe(CN)_6^{3-/4-}$

P_{21}	$Fe(CN)_6^{4-}$ - cytochrome c(III)	
	Experimental	400 M^{-1}
	Calculated [a]	370 M^{-1}
P_{12}	$Fe(CN)_6^{3-}$ - cytochrome c(II)	
	Experimental	400 M^{-1}
	Calculated [a]	260 M^{-1}
P_{11}	cytochrome c(II) - cytochrome c(III)	
	Calculated [a]	8.7 M^{-1}
P_{22}	$Fe(CN)_6^{4-}$ - $Fe(CN)_6^{3-}$	
	Calculated [a]	0.013 M^{-1}

K = 618 (oxidation) [b]

k_{12} [c] ($M^{-1} s^{-1}$) 6.5(10^5) (oxidation), 2.5 (10^4) (reduction)

k_{22} [d] 1.5(10^4) $M^{-1} s^{-1}$

k_{11} [e] ($M^{-1} s^{-1}$) 3.2 (oxidation) 6.5 (reduction) (1.7 times higher if calculated values are used for P_{12} and P_{21})

Table 7 Footnotes

[a] Using Eqs. 31 and 32, and taking the radius of $Fe(CN)_6^{3-/4-}$ as 4.5 Å, the radius of cytochrome c (6.5/7.5) as 16.6 Å, and 0.1 M ionic strength.

[b] Using potentials of 425 mV ($Fe(CN)_6^{3-/4-}$) and 260 mV (cytochrome c).

[c] Ref. 96.

[d] Table 1.

[e] Eq. 34.

Figure 6. Accessibility of protein redox centers to small molecule reagents based on a plot of log k_{11}^{corr} [reagent] / k_{11}^{corr} [$Fe(EDTA)^{2-}$] vs. log k_{11}^{corr} [$Fe(EDTA)^{2-}$].

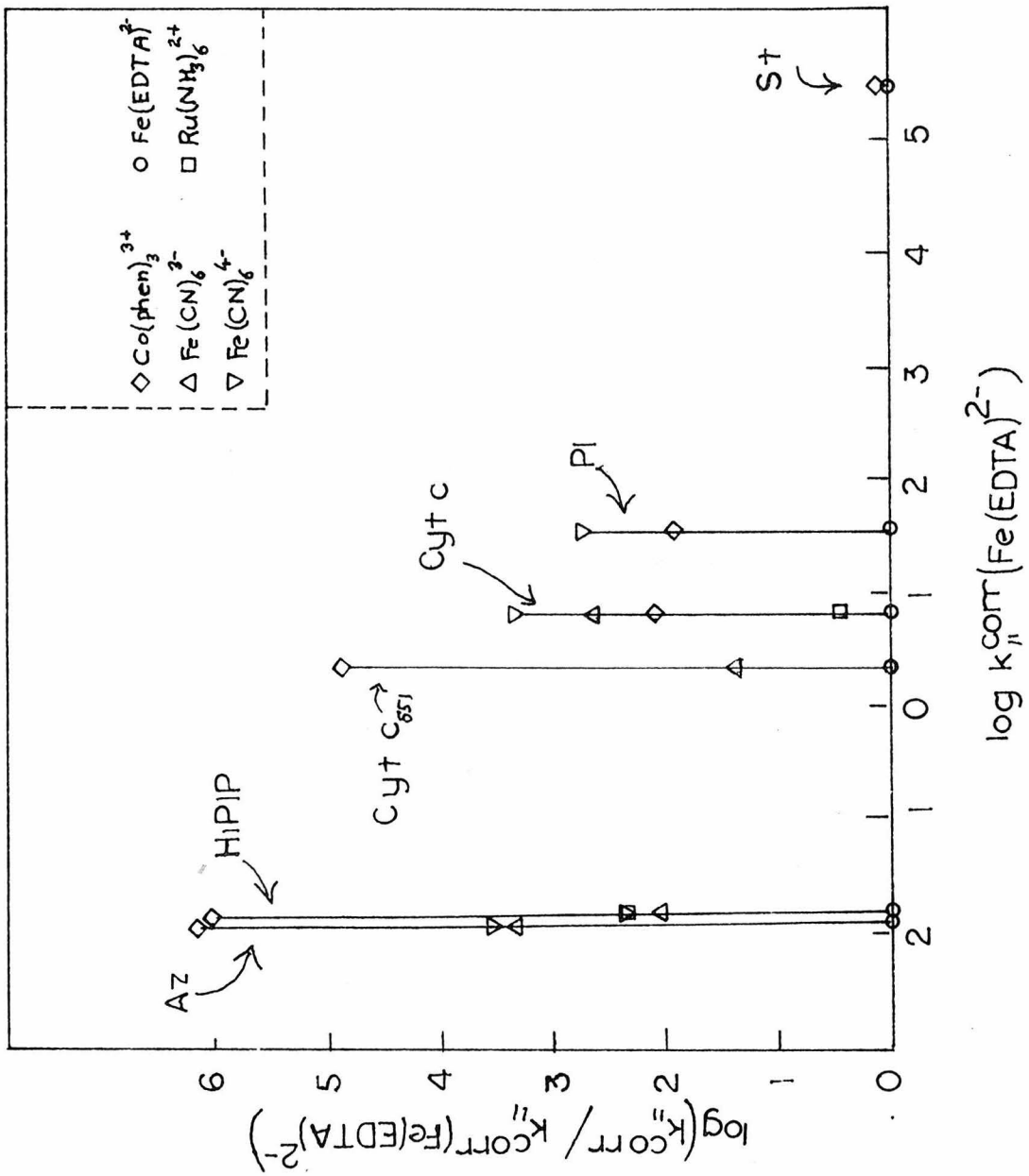
◇ Co(phen)$_3^{3+}$
△ Fe(CN)$_6^{3-}$
▽ Fe(CN)$_6^{4-}$
○ Fe(EDTA)$^{2-}$
□ Ru(NH$_3$)$_6^{2+}$
Az
HiPIP
Cyt c$_{551}$
Cyt c
Pl
S+
$\log\left(k_{II}^{corr}/\ k_{II}^{corr}(Fe(EDTA)^{2-})\right)$
$\log\ k_{II}^{corr}(Fe(EDTA)^{2-})$

calculated values, using the work and f terms. Ignoring, for now, the abscissa, the range of ordinate values can be considered. If a protein acts like a simple inorganic reagent, then the self-exchange rate constant should be independent of the cross reaction it is calculated from, and the calculated k_{11}^{corr} values should cluster about a single point for each protein. If, on the other hand, the k_{11}^{corr} values calculated from the different reagents do not agree, as is usually the case, there can be several reasons. The contributions to ΔG_{11}^{**} include: (1) the inherent activation of the protein metal center, which should to a good approximation be invariant, (2) the nonelectrostatic (i.e., noncoulombic) interactions between the protein and reagent involved in attaining the activated complex configuration, (3) breakdown of the assumption that the adiabaticity factors may be ignored, and (4) deviations from the model used for making the electrostatic calculations (these include contributions to the M terms in Figure 5: non-uniform charge distribution, induced changes in charge distribution, deviations from Debye-Hückel behavior, and any specific medium effects). Several of these factors are related; for example, contributions (2) and (3) are linked because orbital overlap will usually be improved if the reagent can more closely approach the protein metal center; but, as the metal center is at least to some extent protected by the peptide chain, approach by the reagent will involve interactions that are likely to include

noncoulombic ones. Whatever the precise origin of the variation, the wider the range of calculated k_{11}^{corr} values for a single protein from a given set of reagents, the greater is the variety of mechanistic pathways employed by it. These are lowest free energy routes adopted in response to the varying demands (steric, charge, hydrophobicity, and orbital overlap) of the reagent (Figure 7). The calculated k_{11}^{corr} values clearly show that some proteins exhibit a greater reactivity spread than others, ranging from more than six orders of magnitude for azurin to much less than one for stellacyanin. The proteins on the left side of Figure 6 are interpreted as having more available mechanisms (a greater sensitivity to the differences between the reagents), whereas stellacyanin, at the extreme right, apparently employs a single mechanism in its electron transfer reactions. It is of interest to consider what protein properties might parallel the variation in the k_{11}^{corr} spread observed; the most obvious general property is the degree to which the metal site (or the periphery of its conjugated ligand systems) is buried within the peptide. HiPIP is the best available example of a buried site, with the distance of closest approach of the iron-sulfur cluster to the surface estimated[6] as at least 3.5 Å; azurin is another example, as its copper center has been estimated from solution studies to be similarly isolated from the solvent.[15-17] One heme edge of cytochrome c is known from crystal structure studies[1] to be positioned near (2 Å or less) the surface of the protein at one point, and thus is more available for electron transfer than the azurin and HiPIP centers. Less solution data are

Figure 7. Free energy profiles. Three illustrations of the compromise between oribtal overlap (shown as log p, the adiabaticity term) and the interaction energy between the protein and reagent (ΔG_{int}^{**}) to give the rate constant (energy surface), all as a function of the distance between the reactants. Case 1 shows a situation where good overlap is attained at a modest price in interaction energy, thereby leading to a high rate constant. Case 2 illustrates a similar interaction energy as in Case 1, but favorable overlap is only attained at an extremely small r; thus the rate constant is much lower and there is not a single major peak in the log k plot (equivalent to a deep valley in the energy surface). For Case 2 there is a range of protein-reagent distances over which electron transfer could occur with about equal probability. Case 3 illustrates preferential binding of the protein and reagent at a specific radius, thereby leading to a strongly preferred pathway (prominent peak in log k).

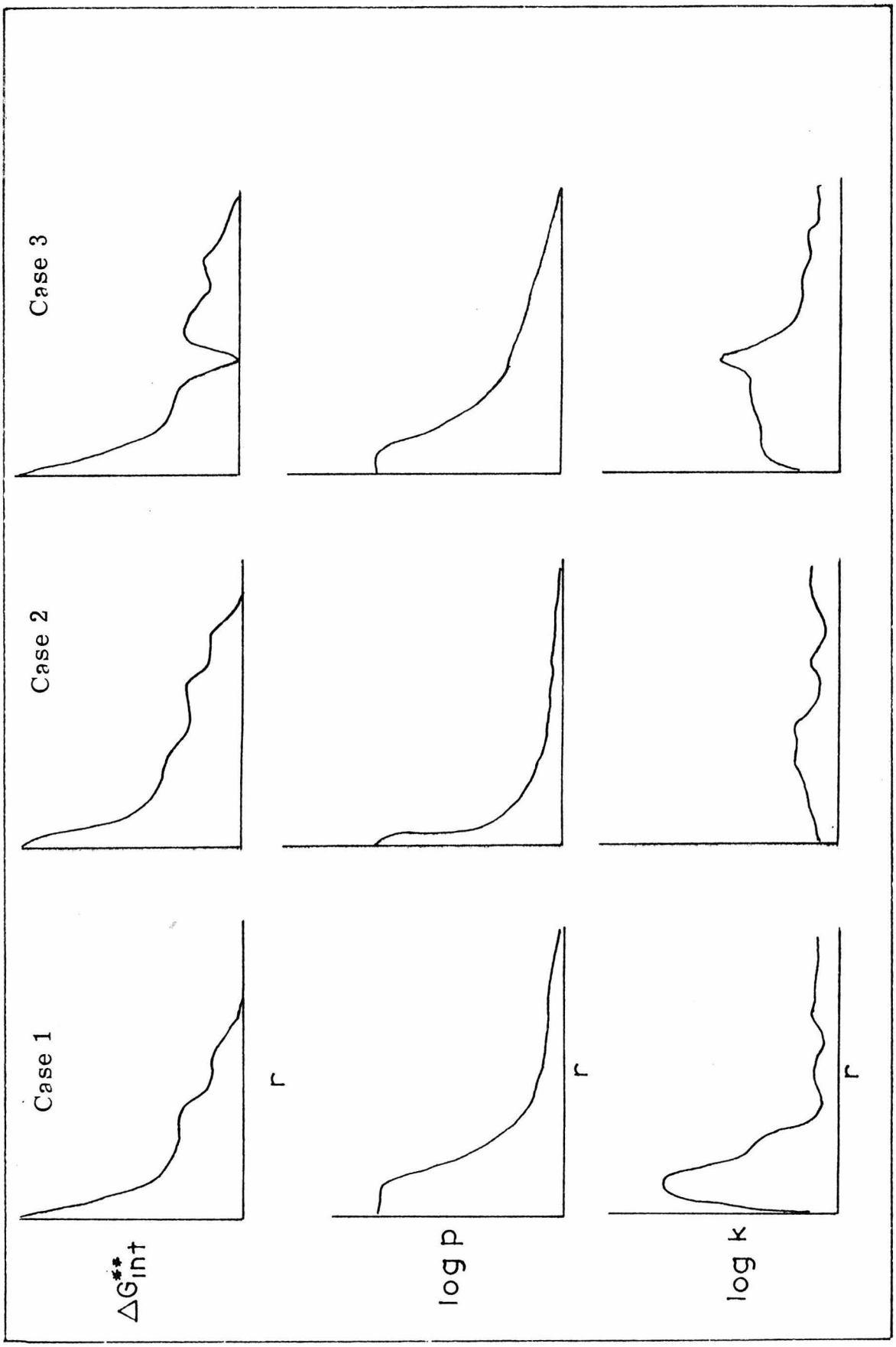
Case 1
Case 2
Case 3
ΔG^{**}_{int}
log p
log k
r
r
r

available for plastocyanin and stellacyanin, but based on the aforementioned reactivity correlations, their copper sites, which are assumed similar in coordination environment to that of azurin, must be more available to reagents in solution than any of the other proteins considered. The property that leads to the range of calculated k_{11}^{corr} values can be called the kinetic availability or accessibility of the metal center. This property is not expected to correlate precisely with X-ray structural evidence, as the availability of a site to external reagents intimately involves protein-reagent interactions as well as the dynamics of conformational changes of the protein molecule in solution. It is comforting, however, that in most cases the static physical picture of buried vs. exposed sites does relate to the kinetic patterns observed.

We shall now consider why $Fe(EDTA)^{2-}$ cross reactions give such a large range of calculated k_{11}^{corr} values, why this range seems to parallel the kinetic availability of the protein metal center, and why the other reagents cause the protein to react so differently from the mechanism with $Fe(EDTA)^{2-}$ in most cases. First, $Fe(EDTA)^{2-}$ is far from spherically symmetrical, with one face that is hydrophobic, being mostly methylene hydrogens, and the opposite face being hydrophilic, owing to the carbonyl oxygens and a coordinated water. Only the hydrophilic side has any π symmetry ligand orbitals, but only the other side is likely to be able to penetrate the hydrophobic residues protecting the metal centers of most proteins. Thus, $Fe(EDTA)^{2-}$ would have to pay a high enthalpic cost to force its π orbitals in close enough to overlap significantly with the orbitals at the redox center of the protein. The alternative of penetration with the

hydrophobic side leading is not attractive, as this side is insulating with respect to π electron transfer. Thus, $Fe(EDTA)^{2-}$ is expected to be quite sensitive to the kinetic accessibility of the protein metal site, as seems to be borne out by the data. For this reason the k_{11}^{corr} values based on $Fe(EDTA)^{2-}$ were selected for the abscissa of Figure 6.

The reagent that usually predicts the highest k_{11}^{corr} is $Co(phen)_3^{3+}$. In this case binding due to electrostatic interactions should not be significant and the work term calculations should make up for the general coulombic interactions; however, the hydrophobic nature of the phenanthroline ligands may be expected to encourage penetration of the protein surface. The blade-like nature of the phenanthroline rings should also encourage penetration as compared to a complex that is more nearly spherical and has the same radius as $Co(phen)_3^{3+}$ (about 7 Å). The matching of the π symmetry of the phenanthroline oribtals with the π symmetry of conjugated ligand systems and the redox orbital of the protein metal center should make the cobalt system more reactive than $Fe(EDTA)^{2-}$. One problem that remains in the $Co(phen)_3^{3+}$ system is that the planar, bidentate phen groups are held in rigid geometric position with respect to each other; thus the two phenanthrolines not involved in the π overlap will still affect the orientation of the pseudo-bridging ligand to the extent that they have preferred interactions with the peptide.

The reactions of $Fe(CN)_6^{3-/4-}$ are often quite fast, beating out $Co(phen)_3^{3+}$ in predicted k_{11}^{corr} in several cases. The main problem

in interpreting the cross reactions of the iron hexacyanides is the possibility (and sometimes the observation) of binding. The work term treatment used to obtain the k_{11}^{corr} values shown in Fig. 6 is applicable in the extreme of no precursor complex formation. The precursor complex formulas should be used when such complexation is observed. One problem, as has been discussed before, is that the estimation of precursor complex formation constants is difficult and usually still necessary for the exchange reactions (and this method apparently does not work well in the $Fe(CN)_6^{3-/4-}$ case (see Table 7) or at least predicts a rather small k_{11}). On symmetry grounds, $Fe(CN)_6^{3-/4-}$ should be quite reactive with proteins, because the electron transfer path is through ligands that have a cylindrically symmetrical π orbital set and that will not have such precise requirements for orientation as does phenanthroline; however, the cyanide ligands do not have as great an advantage in promoting hydrophobic interactions as do the phen groups in the $Co(phen)_3^{3+}$ reactions.

The two reactions given for $Ru(NH_3)_6^{2+}$ are insufficient information for much discussion of this reagent, but in both cases the reactivity shown is between that of $Fe(EDTA)^{2-}$ and $Co(phen)_3^{3+}$. As the ammine ligands are hydrophilic, the ruthenium complex is expected to behave more like $Fe(EDTA)^{2-}$ in this regard, and the ligands do not have π orbitals to facilitate electron transfer into and out of the ruthenium center. However, the t_{2g} orbitals of the second row transition elements extend much farther from the nucleus than those of the first transition series, and in this sense the overall small size of $Ru(NH_3)_6^{2+}$ could be

an advantage for effective π electron transfer.

The second large set of related data involves the oxidation of several of the proteins by tris complexes of various phenanthroline derivatives with Co(III). These data are presented in Figure 8. For convenience, the five derivatives will be given numbers, as follows: $\underset{\sim}{1}$ is the parent complex, $Co(phen)_3^{3+}$; $\underset{\sim}{2}$ is the complex with 5-Cl-phen; $\underset{\sim}{3}$ is 5,6-Me_2 substituted; $\underset{\sim}{4}$ is 4,7-Me_2 substituted; and $\underset{\sim}{5}$ has phenylsulfonates in the four and seven positions of the ring, 4,7-(ϕ-SO_3)$_2$-phen. Complex $\underset{\sim}{2}$ differs from the parent compound primarily because of the inductive effect of the electron-withdrawing chlorine; the perturbation such an effect might have on the potential is compensated for in the Marcus calculation, but the result of different binding capabilities of the Cl compared to an H will show up in the k_{11}^{corr} value. The chlorine substitutent also blocks the 5 position. The self-exchange rate predicted for $\underset{\sim}{2}$ from the cross reaction with $Co(terpy)_2^{2+}$ (see Table 1) is $1.3(10^{-2})\underline{M}^{-1}s^{-1}$, or about 3,000-fold below that for $\underset{\sim}{1}$ and similar to that for $\underset{\sim}{3}$, which is also blocked in the 5 position. The inductive effect and any interaction such as a hydrogen bond to the Cl are not expected to be influential in the reaction with $Co(terpy)_2^{2+}$, so this result is quite reasonable given the previous discussion. Complex $\underset{\sim}{3}$ has the distal edge of each of the phenanthroline rings blocked, but the 4 and 7 positions are left unhindered; this last point is best seen in space filling models of the complex. The methyl substituents are electron donating with respect to hydrogen, and, as with $\underset{\sim}{2}$, the redox potential of $\underset{\sim}{3}$ is higher than that of the parent ion. Substitution at the 4 and 7 positions also produces electronic effects

Figure 8. Comparison of the k_{11}^{corr} values based on reactions involving the ring-substituted $Co(phen)_3^{3+}$ reagents.

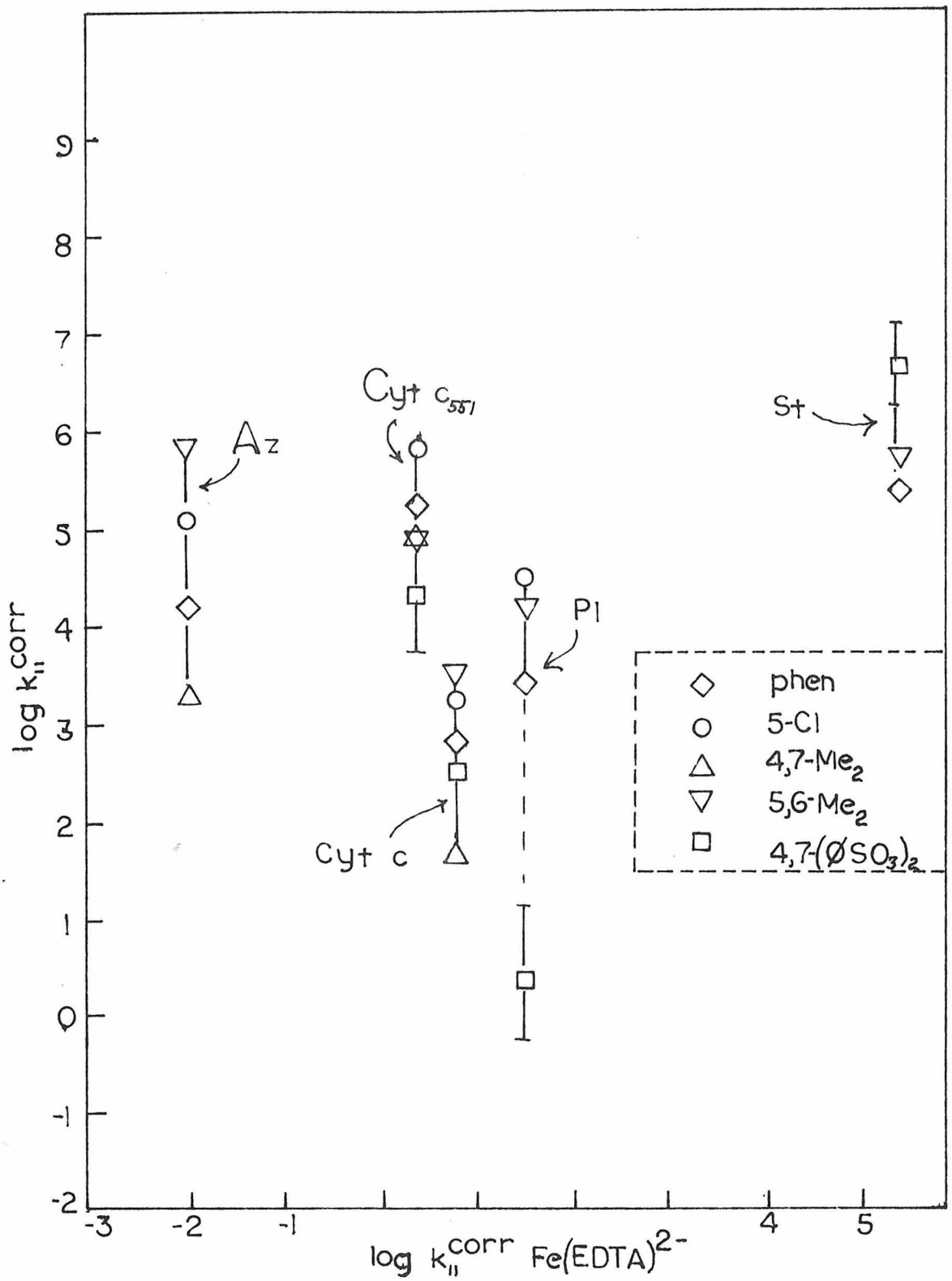
Az
Cyt c_{551}
Cyt c
Pl
St
phen
5-Cl
4,7-Me_2
5,6-Me_2
4,7-$(\phi SO_3)_2$
log k_{11}^{corr}
log k_{11}^{corr} $Fe(EDTA)^{2-}$
9
8
7
6
5
4
3
2
1
0
-1
-2
-3
-2
-1
4
5

on Co(III), as complexes $\underset{\sim}{4}$ and $\underset{\sim}{5}$ have potentials that are 30 and 40 mV, respectively, below that of the parent complex (and roughly 90 mV below $\underset{\sim}{2}$ and $\underset{\sim}{3}$). Sterically, substitution in the 4 and 7 positions blocks both approaches to the phenanthroline rings in the complex (again, this is best seen by examining space filling models); thus, steric effects are expected to be more pronounced in $\underset{\sim}{4}$ than in $\underset{\sim}{3}$. Little difference is observed between the rate constants for the cross reactions of $Co(terpy)_2^{2+}$ with $\underset{\sim}{3}$ and $\underset{\sim}{4}$, but, because of the potential difference, the calculated k_{22} value for $\underset{\sim}{4}$ is 0.77 $\underline{M}^{-1}$ s^{-1}, or about 50-fold less than $\underset{\sim}{1}$. The fact that the calculated k_{11}^{corr} for $\underset{\sim}{4}$ is greater than that for $\underset{\sim}{3}$ or $\underset{\sim}{2}$ is puzzling, and could mean that hydrophobic interactions are more important than steric hindrance in this case. Reagent $\underset{\sim}{5}$ is the only negatively-charged member of the set and is also by far the largest in size, if the radius is taken to include the sulfonate group (various estimates are given in Table 1). The phenyl group may or may not extend the conjugation of the system out to the sulfonate, depending on whether its ring can become coplanar (or approximately coplanar) with the phenanthroline; examination of space filling models makes it clear that the interaction between the phenyl hydrogens alpha to the point of attachment to the phenanthroline and the 3, 5 or 4, 6 hydrogens should strongly encourage the phenyl rings to be well out of the ligand plane. However, attaining approximate coplanarity in a transition state cannot be ruled out, and it should be noted further that in $\underset{\sim}{5}$ there are large hydrophobic channels between the phenyls of each ligand that lead to a

phenanthroline edge. The cross reaction with $Co(terpy)_2^{2+}$ predicts a k_{11}^{corr} of $3.5(10^2)$ to $7(10^3)$ $\underline{M}^{-1}s^{-1}$, depending on the way the work terms are calculated. Anywhere in this range the rate constant is much greater than that for any of the other derivatives; although something special about the interaction between $\underset{\sim}{5}$ and $Co(terpy)_2^{2+}$ is a possibility, it is not likely because the estimate of the k_{11}^{corr} for $\underset{\sim}{5}$ from the cross reaction with $Ru(NH_3)_5py^{2+}$ is also relatively high. Despite the general agreement between the ruthenium and cobalt reagent cross reactions with $\underset{\sim}{5}$, erratic or at least different behavior may be expected for the proteins whose redox centers cannot penetrate to the phenanthroline edge as easily as smaller reactants.

Based on the discussion of the previous paragraph and the model of kinetic accessibility developed earlier, the results for the derivatives of $Co(phen)_3^{3+}$ shown in Figure 8 may now be considered. Complexes $\underset{\sim}{1}$, $\underset{\sim}{2}$, and $\underset{\sim}{3}$ predict larger k_{11}^{corr} values than complexes $\underset{\sim}{4}$ and $\underset{\sim}{5}$, except with stellacyanin, where $\underset{\sim}{5}$ predicts a k_{11}^{corr} about an order of magnitude larger than the value predicted from $\underset{\sim}{1}$ and $\underset{\sim}{3}$. The differences among reagents $\underset{\sim}{1}$, $\underset{\sim}{2}$, and $\underset{\sim}{3}$ are probably too small to interpret, but it is interesting that $\underset{\sim}{2}$ or $\underset{\sim}{3}$ (or both) always does better than $\underset{\sim}{1}$. Thus one of these derivatives always leads to some advantage in protein-reagent interaction.

The observation that stellacyanin is generally less sensitive than the other proteins to the differences among the cobalt complexes is

consistent with the previous conclusion that its copper site is kinetically accessible and thus behaves more like a simple reagent. Considering the other four proteins, $\underset{\sim}{4}$ or $\underset{\sim}{5}$ always predicts a k_{11}^{corr} at least an order of magnitude smaller than the others. The result is consistent with the general steric arguments given in the preceding section, as substitution at the 4,7 positions gives more overall steric hindrance than substitution at the 5,6 positions; thus the proteins (except stellacyanin) are uniformly more sensitive to steric hindrance than is $Co(terpy)_2^{2+}$. The most extreme difference in reactivity involves plastocyanin with $\underset{\sim}{5}$ as compared with all of the other reagents. If the plastocyanin result is accepted,[112] then this response to the difference between $\underset{\sim}{5}$ and $\underset{\sim}{1}$, $\underset{\sim}{2}$, or $\underset{\sim}{3}$ is totally out of character with the differences seen with the other proteins (in no other case is the gap between the k_{11}^{corr} from one to the next nearest reagent greater than an order of magnitude). Apparently the redox centers in plastocyanin and $\underset{\sim}{5}$ cannot easily come together, either because of unfavorable interactions of the protein with the charged sulfonates or an inability to penetrate the hydrophobic channels.

Cytochrome $\underline{c}$ is uniformly about 2 orders of magnitude less reactive with the Co(III) reagents than is cytochrome $\underline{c}_{551}$. The results indicate that the electron transfer mechanism of cytochrome $\underline{c}_{551}$ involves a site that can accept a hydrophobic reagent such as a phenanthroline complex in such a way as to give it good kinetic accessibility to the porphyrin (or the iron). Similarly, plastocyanin is about one order

of magnitude less reactive than azurin. Overall, therefore, the protein reactivity order that may be inferred from cobalt phenanthroline derivatives is much different from that indicated by the cross reactions with $Fe(EDTA)^{2-}$. Although azurin is quite inaccessible to solvent and reagents such as $Fe(EDTA)^{2-}$, the hydrophobic cobalt phenanthroline complexes have little difficulty in gaining access to its blue copper center. The high reactivity of stellacyanin is still consistent, as its site is exposed to all reagents.

Owing to their stability and commercial availability, the iron hexacyanides are the reagents that have been used most widely to study the electron transfer reactivity of metalloproteins. In retrospect, the choice was a poor one, as these small, highly-charged ions often show complicated kinetic behavior because of electrostatic binding, and both the exchange rate and the redox potential of $Fe(CN)_6^{3-/4-}$ are strongly medium dependent. Some discussion of the available data can reasonably be made, provided that we keep in mind the problems associated with binding, even in those cases where it has not been proven. Table 4 and Figure 9 present the available data for the reactions of ferri- or ferrocyanide with ten proteins. Because correction for driving force is made in the Marcus calculation, the calculated value of the protein self-exchange rate should be independent of the direction in which (reduction or oxidation of the protein) the reaction is run.

Figure 9. Relative protein electron transfer reactivities with various inorganic reagents. The cytochromes are (1) horse heart, (2) Pseudomonas aeruginosa, (3) Candida krusei, (4) Euglena gracilis, and (5) Rhodospirillum rubrum. The plastocyanins are (1) bean, (2) spinach, and (3) parsley.

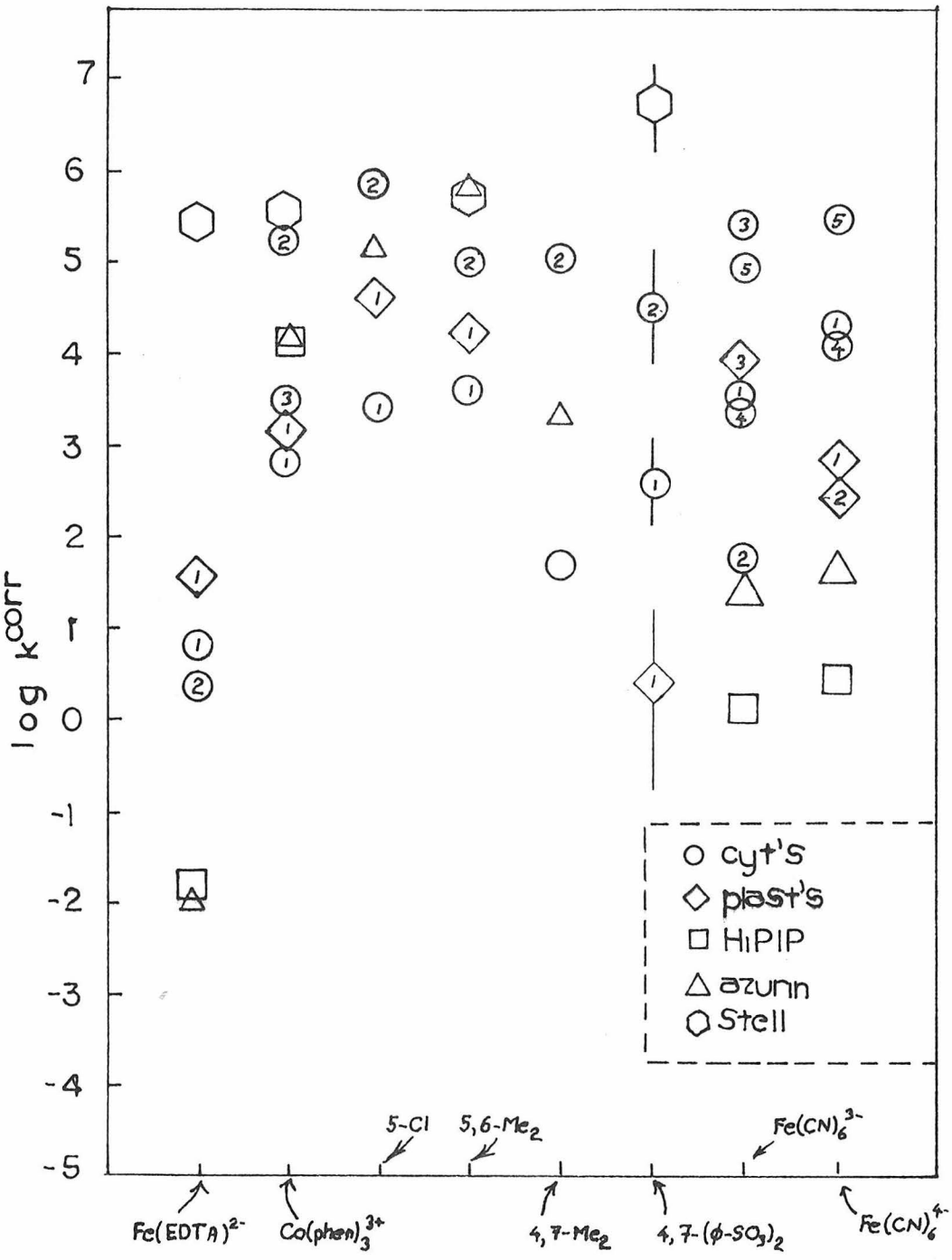
log k^{corr}
7
6
5
4
3
2
1
0
-1
-2
-3
-4
-5
cyt's
plast's
HiPIP
azurin
Stell
5-Cl
5,6-Me$_2$
Fe(CN)$_6^{3-}$
Fe(EDTA)$^{2-}$
Co(phen)$_3^{3+}$
4,7-Me$_2$
4,7-(ϕ-SO$_3$)$_2$
Fe(CN)$_6^{4-}$

For those proteins for which data are available for both ferricyanide oxidation and ferrocyanide reduction, the k_{11}^{corr} values are in sizable disagreement when the ionic strength dependence charges are used. When the sequence charges are used, there is reasonable agreement between the ferri- and ferrocyanide results (except for the Euglena gracilis cytochrome c data) and the proteins may be ranked according to their k_{11}^{corr} values, as was previously done for $Fe(EDTA)^{2-}$ as reagent. The order with $Fe(CN)_6^{3-}$ ($Fe(CN)_6^{4-}$ gives a similar order) is Candida cytochrome c > R. rubrum cytochrome c_2 > plastocyanin > horse heart cytochrome c ≅ Euglena cytochrome c > cytochrome c_{551} > azurin > HiPIP. This order is similar to that based on $Fe(EDTA)^{2-}$ except that azurin and HiPIP have switched places. The ordering from $Fe(EDTA)^{2-}$ is probably more to be trusted because of the binding problem, but the $Fe(CN)_6^{3-/4-}$ results do place the first three cytochromes in the high reactivity category, and suggest some interesting future experiments involving the more trustworthy reagents.

The use of the Marcus theory equations including binding constants might make more sense of the $Fe(CN)_6^{3-/4-}$ data, but the binding constants are not well enough defined and the one example treated (see Table 7) gives such an unexpectedly low k_{11}^{corr} that the method must be considered suspect. This may well be the result of the binding involved not conforming to the equation (Eq. 29) used for estimating the unmeasured precursor and successor binding constants,

because of the ionic strength used or because nonelectrostatic influences are important.

Related to the analysis of the $Fe(CN)_6^{3-/4-}$ reactions is a study of the oxidation of horse heart cytochrome c with various derivatives of ferricyanide as listed in Table 4. The comparison of the k_{11}^{corr} values shows that cytochrome c is most reactive with $Fe(CN)_5N_3^{3-}$, followed by $Fe(CN)_5P\phi_3^{2-}$, then $Fe(CN)_5NH_3^{2-}$ and $Fe(CN)_6^{3-}$ itself, with $Fe(CN)_4bipy^-$ the poorest reagent. The ordering would indicate that the azide must make a better bridge than cyanide. Triphenylphosphine is second best at facilitating the reaction; it could act as a bridge, or it could assist the reaction through favorable protein-$P\phi_3$ hydrophobic interactions, or both. The next two reagents do about as well and are quite similar in shape and ligand composition; they differ mainly in charge (which should have been compensated for anyway). Thus the ammonia does not help the reaction, but the loss of one cyanide does not hurt either. The fact that the bipyridine complex is significantly less reactive is hard to understand and no explanation will be offered. The range of kinetic effects is smaller than would be preferred for solid conclusions, especially as there are large differences in potentials and self-exchange rates for the various reagents. It does seem clear, however, that small complexes containing linear ligands possessing π systems are especially reactive, and hydrophobic interactions are likely to be important.

The analysis of ionic strength (general salt) dependences will now be discussed. Table 5 gives the results of fitting the available ionic strength dependence data to the three equations from Section II-C. Equation 6 will be ignored for the reasons discussed before. First, comparing the fits to the Marcus theory equation (Eq. 27) with the charges derived from the sequence data, it can be seen that the values of Z_1 are consistently similar to the calculated charge except in a few cases. The most general exception to the success of the Marcus theory fits is from the $Fe(CN)_6^{3-/4-}$ data, which give some large values of the protein charge (e.g., a value of 14.6 for the cross reaction between $Fe(CN)_6^{4-}$ and horse heart cytochrome c and the charges derived from the data for the cytochrome c_2 reactions). The other major inconsistency is the zero charge calculated for stellacyanin from the cross reaction with $Co(phen)_3^{3+}$. The result that stellacyanin appears uncharged to $Co(phen)_3^{3+}$ is surprising based on the isoelectric point of the protein, but, as the sequence data are so sketchy and the carbohydrate contributions are not defined, it is not clear that there is a contradiction.

The inconsistencies based on the iron hexacyanide data probably have their origin in the previously-mentioned problems of the medium dependence of many of the properties of this reagent. Foremost among these problems in the present case is the medium dependence of the exchange rate and the ion pairing between ferri or ferrocyanide and most cations. Because of ion association, the effective $Fe(CN)_6^{3-/4-}$ self-exchange rate varies with the concentration of potassium ion, for example, and this dependence is quite large; at 0.1°, the self-exchange

rate varies from 1.75 (10^2) $\underline{M}^{-1}s^{-1}$ at 0.01 $\underline{M}$ to 1.5(10^4) $\underline{M}^{-1}s^{-1}$ at 0.1 $\underline{M}$ K^+ (extrapolated value). As this variation is attributable to a high degree of ion association, the ionic strength dependence equations that are used are invalid and the actual reagents in solution in many cases would be better considered as the K^+-$Fe(CN)_6^{3-/4-}$ pairs. In this regard, it should be emphasized that in the excellent experimental study of the $Fe(CN)_6^{3-/4-}$ exchange rate, electrostatic interaction theory was not used to predict the nature of the dependences on various cations; instead, a rate law was presented that included reaction paths for $Fe(CN)_6^{3-/4-}$ with one or two cations, and different rate constants and the binding constants (or functions thereof) were assigned for each path. In the previous calculations with ferri- or ferrocyanide, the reactants have been assumed to be the free ions (without bound cations), and the work terms have been calculated for these species, but the exchange rates have been chosen to reflect the presence of the cations in the reaction medium. The result of this treatment is to attribute to the medium some of the dependence that is actually electrostatic and belongs in a work term. This trade-off is not as much a problem for the terms that describe the $Fe(CN)_6^{3-/4-}$ exchange as it is for the work terms of the cross reaction. Thus, a better approach would be to include all of the different paths that might be involved, but such an approach could quickly get out of hand and would require a complete re-analysis of the $Fe(CN)_6^{3-/4-}$ exchange rate data, as well as accurate ion pair binding constants under all conditions of interest, which are not available. In some of the cases, the ferricyanide data give quite a reasonable value for Z_1,

whereas ferrocyanide leads to a much different value; this difference is probably attributable to the difference in ion association constants between ferrocyanide (K^+ binding constant about 31 $\underline{M}^{-1}$ at 0.1 $\underline{M}$ ionic strength)[113,114] and ferricyanide (K^+ binding constant 7 $\underline{M}^{-1}$ under the same conditions).[113,114]

The equation (Eq. 5) from transition state theory is somewhat more erratic in its predictions of ionic strength dependences than is the Marcus theory equation, as many of the fits produce a change of sign of the slope in the k $\underline{vs}$. μ plot. Furthermore, in the case of azurin, Eq. 5 leads to a protein charge that is opposite in sign to that predicted from the Marcus theory equation and the sequence calculation. One apparent improvement in the parameters from Eq. 5 is that the ferrocyanide data do not give the large values for Z_1 derived from the Marcus treatment.

The fits from any of these equations are not so successful that they should be considered really accurate models for the electrostatic interactions between proteins and small molecules, as can be seen from the plots of the theoretical curves and experimental points in Figures 2 and 3 in Rosenberg $\underline{et\ al.}$[111] A more dramatic example is the difference observed in changing from acetate to phosphate buffer in the ionic strength dependence of the reaction between cytochrome $\underline{c}$ (horse heart) and $Ru(NH_3)_5py^{3+}$;[44] although only a slightly higher charge is expected on cytochrome $\underline{c}$ at the lower pH, the plots show a much larger effect than would be predicted from such a small change. Clearly, binding of the buffer ions to the protein is involved and only further

careful study of these effects can unravel all of the contributions to this complex problem.

The dependence on pH will next be discussed. Because of all the possible ways that changing hydrogen ion concentration can lead to variation in rate constants, the origin of pH dependences can be quite difficult to establish. The approach to be taken in this analysis is to try first to factor out all of the contributions that have previously been considered, and see if a significant pH dependence is left. The preferred method, then, is to do the full Marcus calculation with potentials and work terms calculated for each pH, thereby accounting for all proton binding to the reagent ($Fe(CN)_6^{4-}$ with a pK of 3.17 at 0.1 M or 3.85 at 0.01 M ionic strength is again the greatest problem)[65] and the protein. Unfortunately, the information necessary for the full calculation is not often available. The pH dependence of redox potentials is seldom determined, and titration data for determining the charge on the protein are also rare.

An example of a set of pH dependences that are considered too small to warrant detailed analysis involves the reduction of several blue proteins by $Fe(EDTA)^{2-}$.[111] The small differences observed in this case could well involve such elusive factors as the influence of changes in the form of the buffer or in ion association. Some of the more complex and interesting pH dependences that have been measured are for the $Fe(CN)_6^{3-/4-}$ reactions with cytochrome c from Euglena gracilis[69] and HiPIP from Chromatium vinosum.[102] In these two studies from Cusanovich's laboratory, the pH dependences both of the ferricyanide and ferrocyanide reactions and of the potentials of the proteins

were determined. The two systems show an intriguingly similar pattern in the pH dependences, and the HiPIP results will be discussed in some detail. Figure 10 shows the measured pH dependences for oxidation and reduction of HiPIP by iron hexacyanides. The filled-in symbols represent the same data corrected for the change in driving force, calculated from the pH dependence of the potential of HiPIP, and assuming the ferri-ferrocyanide potential is 425 mV (there are data[65] that support the contention that the potential should be constant down to pH 6). The corrections are made, therefore, by dividing the observed rate constant by the square root of the equilibrium constant for the reaction in the direction measured. This correction accounts for most of the difference between the ferricyanide and ferrocyanide reactions, but there is still a variance below pH 6. Although the pH dependence of the $Fe(CN)_6^{3-/4-}$ couple is not known in higher ionic strength media, if the potential increases with pH in the medium used for this experiment, as it does in dilute solution, then ferrocyanide and ferricyanide $k_{12}/K^{\frac{1}{2}}$ values could be brought into agreement.

The general increase in $k_{12}/K^{\frac{1}{2}}$ below pH 7 must still be explained (Figure 10). For a negative protein that becomes protonated and thus less negative as the pH is taken below 7, the electrostatic work terms w_{12} and w_{21} will become less positive (since the reagent is negative), and the rate will increase. The same result may be predicted from the protonation of $Fe(CN)_6^{4-}$. The self-exchange work terms, w_{11} and w_{22}, will become less positive, and, as they are subtracted, the rate will increase owing to this contribution. The w_{11} terms

Figure 10. HiPIP-$Fe(CN)_6^{3-/4-}$ pH analyses (data taken from ref. 102).

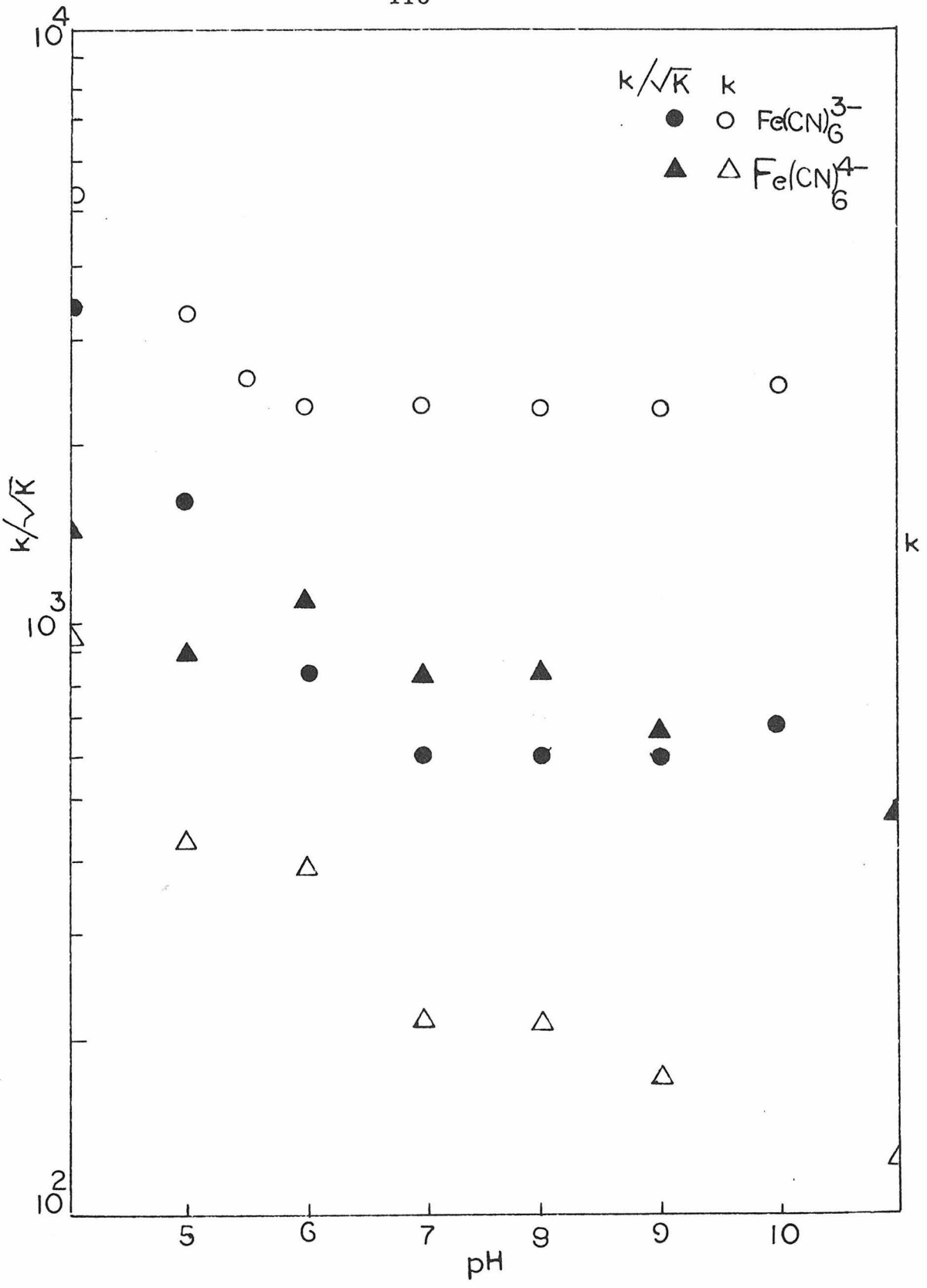
10^4
10^3
10^2
$k/\sqrt{K}$
k
$k/\sqrt{K}$ k
$Fe(CN)_6^{3-}$
$Fe(CN)_6^{4-}$
5
6
7
8
9
10
pH

are usually small because of the large radius of the protein, so they are not very important, especially for a protein with as low a charge as HiPIP. Although the w_{22} term could be rather large and would change by 25% in the extreme case of complete protonation of $Fe(CN)_6^{3-/4-}$, not even half-protonation is expected at the pH values considered in the HiPIP study. Thus the cross reaction work terms can be expected to dominate. A similar general trend of increasing rate with decreasing pH is to be expected if the protein ever becomes positive, as then the magnitude of the work terms will increase with decreasing pH.

The pH dependences for the reactions of the iron hexacyanides with cytochrome $\underline{c_{552}}$ from Euglena gracilis show similar patterns to the one just discussed (Figure 11); when corrections are made for the equilibrium constant, there is general agreement between data for reduction and oxidation except below pH 6, where there is divergence (the $Fe(CN)_6^{3-}$ results again predict a higher value of $k_{12}/K^{\frac{1}{2}}$). Also, there is a general increase in rate for the whole pH range measured, and the dependence becomes steeper in the lower pH region, where protonation of the reagent is expected to contribute.

We shall now comment briefly on the interpretation of the activation parameters for the reactions of small molecules with proteins. The most informative interpretation of the measured activation parameters requires their conversion to $\Delta H_{11}^{\ddagger}$ and $\Delta S_{11}^{\ddagger}$, as was discussed in Section II-H. Unfortunately, the lack of free energy data for the equilibria between the reagents and the proteins (or, the equivalent, the enthalpy and entropy of reduction from the temperature dependence of the potentials)

Figure 11. Cytochrome c (Euglena gracilis)-$Fe(CN)_6^{3-/4-}$ pH analyses (data taken from ref. 69).

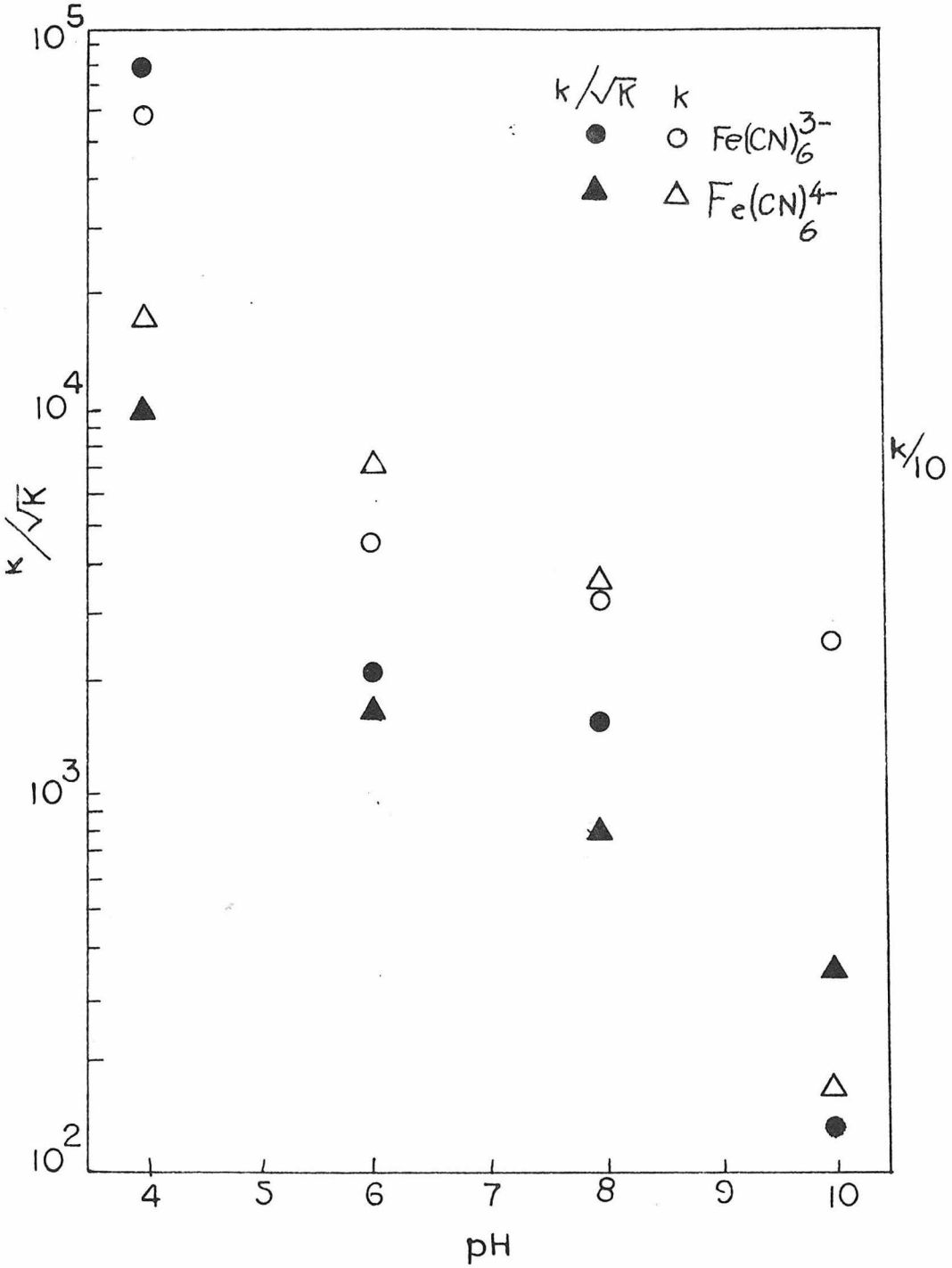
10^5
10^4
10^3
10^2
$k/\sqrt{K}$
$k/\sqrt{K}$ k
$Fe(CN)_6^{3-}$
$Fe(CN)_6^{4-}$
k/10
4
5
6
7
8
9
10
pH

makes these calculations impossible at this time. The existence of some activation parameters that show near zero $\Delta H_{12}^{\ddagger}$ and very negative $\Delta S_{12}^{\ddagger}$ (see especially the reactions of HiPIP) is intriguing, and could mean that the involved reactions employ long-distance electron transfer mechanisms that are highly "forbidden". The clear involvement of the standard free energy terms can be seen in the uniformly high $\Delta H_{12}^{\ddagger}$ for $Co(phen)_3^{3+}$ reactions, whereas the $Fe(CN)_6^{3-}$ reactions often show low $\Delta H_{12}^{\ddagger}$ and negative $\Delta S_{12}^{\ddagger}$ values. This latter trend correlates with the quite negative ΔH° and ΔS° for the $Fe(CN)_6^{3-/4-}$ couple itself (see Table 1). Further analysis of the activation parameters with the aid of the equilibrium thermodynamic parameters should prove enlightening, but with the data presently available generalizations are difficult to make and any interpretation is hazardous.

VII. Protein-Protein Reactions

The available data on protein-protein electron transfer reactions are set out in Table 8. In Table 9 calculated and observed protein-protein k_{12} values are compared; the calculated rate constants are based on the largest predicted k_{11}^{corr} value for each protein. This approach has been taken as any deviation from "predicted" behavior is as likely to be a function of complementary interactions between the two proteins as it is to be a difference in the activation process of only one of them. The first clear observation is that most of the reactions (all except three with cytochrome c (horse heart)) are faster than predicted (even with the bias that a large predicted k_{11}^{corr} is used), and the ratio $k_{12}^{obsd}/k_{12}^{corr}$ varies greatly. The former observation would seem to indicate that most proteins share some properties that allow them to interact better

Table 8. Protein-Protein Reaction Data

Oxidant	Reductant	$k(M^{-1}s^{-1})$	T	$\Delta H^{\ddagger}$(kcal/mole)	$\Delta S^{\ddagger}$(eu)	pH	Buffer[a]	μ(M)	Salt	Ref
Plastocyanin[b]	Cytochrome c[c]	$1.0(10^6)$	25			7.0	P	0.1	NaCl	68
Plastocyanin	Cytochrome c_{551}[d]	$7.5(10^5)$	25			7.0	P	0.1	NaCl	68
Plastocyanin	Cytochrome f[e]	$3.6(10^7)$	25			7.0	P	0.1	NaCl	68
Azurin	Cytochrome f	$1.0(10^6)$	25			7.0	P	0.1	NaCl	68
Cytochrome c	Azurin	$1.1(10^3)$	20	13	0	7.0	P,EDTA	0.1	NaCl	103
Azurin	Cytochrome c	$\sim 1(10^3)$	20			7.0	P,EDTA	0.1		101
Cytochrome c_{551}	Azurin	$6.1(10^5)$[f]	25	13.5	-10.7	7.0	P	0.05		77
Azurin	Cytochrome c_{551}	$8.1(10^6)$	25	10.6	8.6	7.0	P	0.05		77
Cytochrome c_{551}	Azurin	$3(10^5)$	20	16	26	7.0	P	0.1		101
Azurin	Cytochrome c_{551}	$1.4(10^6)$	20	9	25	7.0	P	0.1		101
Cytochrome c	Cytochrome c_{551}	$8(10^4)$[g]	25	12	4	7.2	P,EDTA	0.1	NaCl	103
Cytochrome c	Cytochrome c_{551}	$1.6(10^4)$[h]	4.5	11	1	7.0	P	0.2	KCl	67
Cytochrome c_{551}	Cytochrome c	$1.6(10^4)$	4.5			7.0	P	0.2	KCl	67
Cytochrome c_{552}	HiPIP[i]	$5.8(10^6)$[j]	24			7.0	P	0.12	NaCl	69
HiPIP	Cytochrome c_{552}	$3.0(10^6)$	24			7.0	P	0.12	NaCl	69
Cytochrome c_2	HiPIP	$3.1(10^4)$[k]	20			7.0	P	0.12	NaCl	102
HiPIP	Cytochrome c_2	$1.5(10^5)$[k]	20			7.0	P	0.12	NaCl	102

Table 8 Footnotes

[a] Buffer abbreviations are as given in Table 1.

[b] Plastocyanin is from parsley.

[c] Cytochrome c from horse heart unless otherwise indicated.

[d] Azurin and cytochrome c_{551} are from Pseudomonas (whether from Pseudomonas aeruginosa or fluorescens is not clear).

[e] Cytochrome f is from parsley.

[f] Two forms of azurin, one not kinetically active with cytochrome c_{551}, are indicated.

[g] Ionic strength dependence has been performed.

[h] Ionic strength independent 0.03 to 0.3 M; $k = 4(10^4)\ M^{-1}s^{-1}$ at 25° from $E_A = 12$ kcal/mole.

[i] HiPIP is from Chromatium vinosum.

[j] Temperature jump data indicate that this reaction is not simply bimolecular.

[k] Ionic strength independent.

Table 8. Calculated Protein-Protein Rate Constants, Including Electrostatic Corrections

Oxidant	Reductant	w_{12}[a,b,c]	w_m[a,b,c]	w_{11}[a,b,d]	w_{22}[a,b,d]	$\Delta G^*_{12\,corr}$[b,e]	k^{corr}_{12} ($M^{-1}s^{-1}$)[e]	k^{obsd}_{12} ($M^{-1}s^{-1}$)	$k^{obsd}_{12}/k^{corr}_{12}$
Plastocyanin[g,h]	Cytochrome c[i]	-0.528	-0.677	0.882	0.406	10.48	$1.3(10^5)$	$1.0(10^6)$	7.7
	Cytochrome c_{551}[i]	0.307	0.227	0.882	0.079	9.89	$3.5(10^5)$	$7.5(10^5)$	2.1
Cytochrome c[i]	Azurin[i]	-0.118	-0.051	0.406	0.015	13.13	$1.5(10^3)$	$1.1(10^3)$	0.73
Cytochrome c_{551}[i]	Azurin[i,j]	0.078	0.058	0.079	0.015	11.52	$2.2(10^4)$	$6.1(10^6)$[j]	$2.8(10^2)$
Azurin[i,j]	Cytochrome c_{551}[i]	0.058	0.078	0.015	0.079	10.51	$1.2(10^5)$	$8.1(10^5)$[j]	$6.8(10^1)$
Cytochrome c_{551}[i]	Azurin[i,k]	0.040	0.030	0.079	0.015	11.78	$1.4(10^4)$	$3(10^5)$[k]	$2.1(10^2)$
Azurin[i]	Cytochrome c_{551}[i]	0.030	0.040	0.015	0.079	10.21	$2.0(10^5)$	$1.4(10^5)$[k]	7.0
Cytochrome c[i]	Cytochrome c_{551}[i]	-0.235	-0.136	0.406	0.079	11.48	$2.3(10^4)$	$8.0(10^4)$[l]	3.5
Cytochrome c[i]	Cytochrome c_{551}[i]	-0.096	-0.056	0.406	0.079	11.59	$2.0(10^4)$	$1.6(10^4)$[m]	0.80
Cytochrome c_{551}[i]	Cytochrome c[i]	-0.056	-0.096	0.079	0.406	11.59	$2.0(10^4)$	$1.6(10^4)$[m]	0.80
Cytochrome c_{552}[n]	HiPIP[i]	0.229	0.184	0.705	0.091	11.54	$2.1(10^4)$	$5.8(10^6)$	$2.8(10^2)$
HiPIP[i]	Cytochrome c_{552}[n]	0.184	0.229	0.091	0.705	12.01	$9.7(10^3)$	$3.0(10^6)$	$3.1(10^2)$

Table 9 Footnotes

[a] The subscript 1 refers to the oxidant and 2 to the reductant.

[b] All energies in kcal/mole.

[c] Work terms are calculated using the conditions given in Table 4 and assuming protein charges calculated from the sequences (Table 2).

[d] Work terms are calculated for the conditions appropriate to the calculated self-exchange rate constant (μ 0.1 M, pH 7).

[e] Calculated for the cross reaction condition of Table 8.

[f] From Table 8.

[g] Conventions for protein names are as given in footnotes b to e to Table 8.

[h] The self-exchange rate constant is calculated from the cross reaction with $Fe(CN)_6^{3-}$.

[i] The self-exchange rate constant is calculated from the cross reaction with $Co(phen)_3^{3+}$.

[j] From the cross reaction and potential (azurin = 304 mV) data of ref. 77.

[k] From the cross reaction data of ref. 101 and using E (azurin) of 330 mV.

[l] From the cross reaction data of ref. 103.

[m] From the cross reaction data of ref. 67

[n] The self-exchange rate constant is calculated from the cross reactions with $Fe(CN)_6^{3-/4-}$.

with each other than with small molecules; such interactions may well be hydrophobic in nature and on the average outweigh specific coulombic contacts. Unfortunately, most of the reactions between physiological partners cannot be compared to calculated values as the information for making the calculation is not available. One possible exception is the reaction between cytochrome $\underline{c}_{551}$ and azurin. Taking the data of Rosen and Pecht,[77] which is considered to be the most reliable, the ratios are 210 for the oxidation of azurin and 68 for the reduction. A similar pattern of disagreement between oxidation and reduction is found in the results of another study,[101] but in this case the ratios are smaller. The fact that the ratios do not agree tends to indicate that the potential differences being used are improper (however, the potentials used in the first case give the equilibrium constant as measured by Rosen and Pecht). Although it is tempting to suggest that the large value of the ratio indicates that specific interaction between physiological partners is involved, such a conclusion is shaky at best. In this regard, it should be noted that the ratio for cytochrome $\underline{c}_{552}$ and HiPIP is similar to that for azurin-cytochrome $\underline{c}_{551}$, and the former two proteins are clearly not physiological partners.

VIII. Summary and Conclusions

In this chapter a method has been presented for sorting out several of the contributions to the energetics of protein-small molecule electron transfer reactions. This method involves the formalism of the Marcus theory of outer sphere electron transfer, which allows isolation of the following components of the activation energy: (1) the activation of the

reagent metal center; (2) the contribution to the activation energy from the free energy change for the reaction; and (3) the electrostatic (coulombic) contributions to the reagent self-exchange, the protein self-exchange, and the cross reaction, assuming a model of uniformly-charged hard spheres. The calculated activation energy that results from this treatment refers to the protein self-exchange reaction were the protein to react with itself in the same manner it reacts with the reagent. Important contributions to this activation energy are: (1) the nonelectrostatic (i.e., noncoulombic) interaction between the protein and reagent required to position the reagent for most favorable electron transfer; (2) the contributions from the varying adiabaticity (overlap between reagent and protein redox orbitals) of the reactions; (3) the inherent activation of the metal center, resulting from the need to attain, for example, bond lengths between the protein metal center and its ligands that are intermediate between those of the oxidized and reduced state; and (4) electrostatic interactions, both those covered by the model used for making the work term calculations, and those not considered, including induced changes in charge distribution and shape of the protein and reagent.

The result of treating protein-small molecule electron transfer data in the manner outlined above is a collection of calculated protein self-exchange rate constants. Large variations in the k_{11}^{corr} values are observed for most proteins considered. It is concluded that the two most important contributions to this large variation are the extent of

orbital overlap in the transition state and the nonelectrostatic interaction between the protein and reagent, and together these influences define the kinetic accessibility of the protein redox center to a given reagent. The contributions from orbital overlap and nonelectrostatic interaction are closely related and coupled in their influence. As most protein metal sites are, to some extent at least, protected from reactants in the medium by the peptide, any near-approach to the metal center will require interaction with the blocking residues; as electron transfer will be much more efficient if there is good orbital overlap between the redox orbitals of the protein and reagent, close approach is expected to greatly increase the rate of electron transfer. A compromise thus must be reached (see Figure 7) between the benefit gained from the reagent penetrating close to the protein metal site, and the thermodynamic cost of such penetration. Analysis of the data indicates that hydrophobic reagents penetrate more easily and ligands with π symmetry orbitals available facilitate overlap with the redox centers of the proteins. The kinetic accessibility based on $Fe(EDTA)^{2-}$ increases according to azurin $\cong$ HiPIP $<$ cytochrome $\underline{c}_{551}$ $<$ cytochrome $\underline{c}$ (horse heart) $<$ plastocyanin $<$ stellacyanin (see Figure 6), which parallels the extent to which the metal center is buried in the peptide for those cases where structural data are available.

Protein-protein reactions are in general more difficult to treat. However, most measured protein-protein rate constants are larger than would be expected based on even the largest k_{11}^{corr} values. Interestingly, we have found no clear cut evidence for specificity between

natural partners from the limited amount of evidence available. The protein-protein reactions apparently benefit from numerous interactions that are individually small but as a whole can be much more significant than those between a small molecule and a protein. Clearly, this area needs much more careful experimentation and analysis.

IX. References and Footnotes

1. R. E. Dickerson and R. Timkovich, The Enzymes, P. D. Boyer, ed., Academic Press, New York, 3rd Edition, Vol. 11, Chapter 7, 1976.
2. J. A. Fee, Structure and Bonding, 23, 1 (1975).
3. L. E. Bennett, Prog. Inorg. Chem., 18, 1 (1973).
4. C. W. Carter, Jr., J. Kraut, S. T. Freer, N. H. Xuong, R. A. Alden, and R. G. Bartsch, J. Biol. Chem., 249, 4212 (1974).
5. C. W. Carter, Jr., J. Kraut, S. T. Freer, and R. A. Alden, J. Biol. Chem., 249, 6339 (1974).
6. L. E. Bennett, personal communication.
7. R. H. Holm, B. A. Averill, T. Herskovitz, R. B. Frankel, H. B. Gray, O. Siiman, and F. J. Grunthaner, J. Amer. Chem. Soc., 96, 2644 (1974).
8. D. R. McMillin, R. A. Holwerda, and H. B. Gray, Proc. Nat. Acad. Sci. (USA), 71, 1339 (1974).
9. D. R. McMillin, R. C. Rosenberg, and H. B. Gray, Proc. Nat. Acad. Sci. (USA), 71, 4760 (1974).
10. E. I. Solomon, J. W. Hare, and H. B. Gray, Proc. Nat. Acad. Sci. (USA), 73, 1389 (1976).
11. E. I. Solomon, P. J. Clendening, H. B. Gray, and F. J. Grunthaner, J. Amer. Chem. Soc., 97, 3878 (1975).
12. J. K. Markley, E. L. Ulrich, S.P. Berg, and D. W. Krogmann, Biochemistry, 14, 4428 (1975).

13. J. W. Hare, E.I. Solomon, and H. B. Gray, J. Amer. Chem. Soc., 98, 3205 (1976).

14. J. W. Hare, Ph.D. Thesis, California Institute of Technology, 1976.

15. N. Boden, M. C. Holmes, and P. F. Knowles, Biochem. Biophys. Res. Comm., 57, 845 (1974).

16. S. H. Koenig and R. D. Brown, Ann. NY Acad. Sci., 222, 752 (1973).

17. G. H. Rist, J. S. Hyde, and T. Vänngård, Proc. Nat. Acad. Sci. (USA), 67, 79 (1970).

18. F. Basolo and R. G. Pearson, Mechanisms of Inorganic Reactions, 2nd Ed., John Wiley, New York, 1967.

19. R. G. Wilkins, The Study of Kinetics and Mechanism of Reactions of Transition Metal Complexes, Allyn and Bacon, Boston, 1974.

20. R. A. Marcus and N. Sutin, Inorg. Chem., 14, 213 (1975).

21. The equation is $Z = pr^2(8\pi kT/\mu)^{\frac{1}{2}}$ where p is the probability of reaction during an encounter (including "cage" effects), r is the sum of reactant radii, k is the Boltzmann constant and μ is the reduced mass $(m_1 m_2/(m_1+m_2))$; Z is insensitive to changes in radius and mass since the mass is proportional to about $4\pi r^3/3$ and thus Z is proportional to $r^{\frac{1}{2}}$. Z is about twice as large for two proteins of molecular weight 10,000 and radius 15 Å as it is for two small molecules of molecular weight 200 and radius 4 Å. In a Marcus treatment, electrostatic influences are relegated to the activation energy term. R. M. Noyes, Prog. React. Kinetics, 1, 129 (1961).

22. N. Sutin, Inorganic Biochemistry, G. L. Eichhorn, ed., Elsevier, New York, Vol. 2, p. 611.

23. S. Glasstone, K. J. Laidler, and H. Eyring, Theory of Rate Processes, McGraw Hill, New York, 1940.

24. A. Haim and N. Sutin, Inorg. Chem., 15, 476 (1976).

25. J. G. Kirkwood and J. B. Shumaker, Proc. Nat. Acad. Sci. (USA), 38, 855, 863 (1952).

26. C. Tanford, Physical Chemistry of Macromolecules, John Wiley, New York, 1961, p. 466.

27. R. A. Alberty and G. G. Hammes, J. Chem. Phys., 62, 154 (1958).

28. Ref. 26, p. 467.

29. A. D. Pethybridge and J. E. Prus, Prog. Inorg. Chem., 17, 327 (1972).

30. R. A. Holwerda, S. Wherland, and H. B. Gray, Ann. Rev. Bioph. Bioeng., 5, 363 (1976).

31. A. Shejter, I. Aviram, R. Margalit, and T. Goldkorn, Ann. New York Acad. Sci., 244, 51 (1975).

32. T. J. Przystas and N. Sutin, J. Amer. Chem. Soc., 95, 5545 (1973).

33. R. Margalit and A. Shejter, Eur. J. Biochem., 32, 500 (1973).

34. E. Stellwagen and R. D. Cass, J. Biol. Chem., 250, 2095 (1975).

35. R. J. Campion, C. F. Deck, Jr., and A. C. Wahl, Inorg. Chem., 6, 672 (1967).

36. B. R. Baker, F. Basolo, and H. M. Neumann, J. Phys. Chem., 63, 371 (1959).

37. J. J. Hopfield, Proc. Nat. Acad. Sci. (USA), 71, 3640 (1974).

38. J. E. Leffler and E. Grunwald, Rates and Equilibria of Organic Reactions, Wiley, New York, 1963, Chapter 9.

39. R. Lumry and S. Rajender, Biopolymers, 9, 1125 (1970).

40. G. Schwarzenbach and J. Heller, Helv. Chim. Acta, 34, 576 (1951).

41. O. K. Borggaard, Acta Chem. Scand., 26, 393 (1972).

42. R. G. Wilkins and R. E. Yelin, Inorg. Chem., 7, 2667 (1968).

43. M. D. Lind and J. L. Hoard, Inorg. Chem., 3, 34 (1964).

44. D. Cummins, unpublished results.

45. H. M. Neumann, quoted in R. Farina and R. G. Wilkins, Inorg. Chem., 7, 514 (1968).

46. G. P. Khare and R. Eisenberg, Inorg. Chem., 9, 2211 (1970).

47. J. V. McArdle, Ph.D. Thesis, California Institute of Technology, 1976.

48. The treatment of the reagents as spheres with the charge centered on the metal ion is least likely to be correct for $Co(4,7\text{-}(\phi\text{-}SO_3)_2\text{-phen})_3^{3-}$, as in this case two-thirds of the charge is on the sulfonate groups at the periphery of the ligands. Furthermore, estimation of the radius of this complex is complicated by the large, open channels that exist between the ligands. Because of this latter problem, two of the three cases considered in all calculations differ in the radius chosen, using

two extremes of 11.5 (estimated distance from the cobalt to the sulfonate oxygens) and 7 Å (the radius used for the unsubstituted parent complex). The third model is designed to compensate for the location of the charged groups; in this approach the cobalt(III) center and all but two of the sulfonates are taken as a unit of radius 7 Å and charge -1 (-2 for Co(II)); the remaining two sulfonates are treated as individual centers of radius 3 Å and -1 charge. This is designed to over estimate the charge contributions, as two of the sulfonates are given heavy weight through their small radii, and the "trailing" sulfonates are grouped with the nearer cobalt and this composite center is given a small radius.

49. R. Farina and R. G. Wilkins, Inorg. Chem., 7, 514 (1968).
50. D. Cummins and H. B. Gray, to be submitted for publication.
51. H. S. Lim, D. J. Barclay, and F. C. Anson, Inorg. Chem., 11, 1460 (1972).
52. T. J. Meyer and H. Taube, Inorg. Chem., 7, 2369 (1968).
53. H. C. Stynes and J. A. Ibers, Inorg. Chem., 10, 2304 (1971).
54. I. M. Kolthoff and W. J. Tomsicek, J. Phys. Chem., 39, 945 (1935).
55. B. I. Swanson and R. R. Ryan, Inorg. Chem., 13, 283 (1973).
56. D. B. Brown and D. F. Shriver, Inorg. Chem., 8, 37 (1969).
57. G. I. Hanania, D. H. Irvine, and P. George, J. Phys. Chem., 71, 2022 (1967).

58. R. Stasiw and R. G. Wilkins, Inorg. Chem., 8, 156 (1969).

59. C. Creutz and N. Sutin, Proc. Nat. Acad. Sci. (USA), 70, 1701 (1973).

60. J. Baxendale and H. R. Hardy, Trans. Faraday Soc., 49, 1140 (1953).

61. J. Baxendale, H. R. Hardy, and C. H. Sutcliffe, Trans. Faraday Soc., 47, 963 (1951).

62. R. Skochdople and S. Chaberek, J. Inorg. Nucl. Chem., 11, 222 (1959).

63. R. L. Gustafson and A. E. Martell, J. Phys. Chem., 67, 576 (1963).

64. H. J. Schugar, A. T. Hubbard, F. C. Anson, and H. B. Gray, J. Amer. Chem. Soc., 91, 71 (1969).

65. J. Jordan and G. J. Ewing, Inorg. Chem., 1, 587 (1962).

66. R. Margalit and A. Shejter, Eur. J. Biochem., 32, 492 (1973).

67. R. A. Morton, J. Overnell, and H. A. Harbury, J. Biol. Chem., 245, 4653 (1970).

68. P. M. Wood, Biochim. Biophys. Acta, 357, 370 (1974).

69. F. E. Wood and M. A. Cusanovich, Arch. Bioch. Bioph., 168, 333 (1975).

70. G. W. Pettigrew, Biochem. J., 139, 449 (1974).

71. K. Sletten, K. Dus, H. DeKlerk, and M. D. Kamen, J. Biol. Chem., 243, 5492 (1968).

72. K. Dus, K. Sletten, and M. D. Kamen, J. Biol. Chem., 243, 5507 (1968).

73. K. Dus, H. DeKlerk, K. Sletten, and R. G. Bartsch, Biochim. Biophys. Acta, 140, 291 (1967).

74. W. Lovenberg and B. E. Sobel, Proc. Nat. Acad. Sci. (USA), 54, 193 (1967).

75. T. Yamanaka, Biochemistry of Copper, J. Peisach, P. Aisen, and W. E. Blumberg, eds., Academic Press, New York, 1966, pp. 275-92.

76. R. P. Ambler and L. H. Brown, Biochem. J., 104, 784 (1967).

77. P. Rosen and I. Pecht, Biochemistry, 15, 775 (1976).

78. J. A. M. Ramshaw, R. H. Brown, M. D. Scawen, and D. Boulter, Biochim. Biophys. Acta, 303, 269 (1973).

79. N. Sailasuta, F. C. Anson, and H. B. Gray, to be submitted for publication.

80. P. R. Milne, J. R. E. Wells, and R. P. Ambler, Biochem. J., 143, 691 (1974).

81. B. Reinhammar, Biochim. Biophys. Acta, 153, 299 (1968).

82. B. Reinhammar, Biochim. Biophys. Acta, 205, 35 (1970).

83. J. Peisach, W. G. Levine, and W. E. Blumberg, J. Biol. Chem., 242, 2847 (1967).

84. (a) R. K. Gupta, Biochim. Biophys. Acta, 292, 291 (1973); (b) R. K. Gupta, S. H. Koenig, and A. G. Redfield, J. Magn. Res., 7, 66 (1972).

85. J. K. Beattie, D. J. Fensom, H. C. Freeman, E. Woodcock, H. A. O. Hill, and A. M. Stokes, Biochim. Biophys. Acta, 405, 109 (1975).

86. J. K. Yandell, D. P. Fay, and N. Sutin, J. Amer. Chem. Soc., 95, 1131 (1973).

87. W. G. Miller and M. A. Cusanovich, Bioph. Struc. Mech., 1, 97 (1975).

88. D. O. Lambeth and G. Palmer, J. Biol. Chem., 248, 6095 (1973).

89. R. A. Holwerda and H. B. Gray, J. Amer. Chem. Soc., 96, 6008 (1974).

90. R. Aasa, R. Branden, J. Deinum, B. G. Malmstrom, B. Reinhammar, and T. Vänngård, FEBS Lett., 61, 115 (1976).

91. Y. A. Im and D.H. Busch, J. Amer. Chem. Soc., 83, 3357 (1961).

92. C. L. Coyle, unpublished results.

93. H. L. Hodges, R. A. Holwerda, and H. B. Gray, J. Amer. Chem. Soc., 96, 3132 (1974).

94. R. X. Ewall and L. E. Bennett, J. Amer. Chem. Soc., 96, 940 (1974).

95. J. V. McArdle, H. B. Gray, C. Creutz, and N. Sutin, J. Amer. Chem. Soc., 96, 5737 (1974).

96. R. M. Zabinski, K. Tatti, and G. H. Czerlinski, J. Biol. Chem., 249, 6125 (1974).

97. K. G. Brandt, P. C. Parks, G. H. Czerlinski, and G. P. Hess, J. Biol. Chem., 241, 4180 (1966).

98. J. C. Cassatt and C. P. Marini, Biochemistry, 13, 5323 (1974).

99. C. L. Coyle and H. B. Gray, to be submitted for publication.

100. (a) J. V. McArdle, C. L. Coyle, H. B. Gray, G. S. Yoneda, and R. A. Holwerda, to be submitted for publication; (b) J. V. McArdle, K. Yocom, and H. B. Gray, to be submitted for publication.

101. E. Antonini, A. Finazzi-Agro, P. Guerrieri, G. Rotilio, and B. Mondovi, J. Biol. Chem., 245, 4847 (1970).

102. I. A. Mizraki, F. E. Wood, and M. A. Cusanovich, Biochemistry, 15, 343 (1976).

103. C. Greenwood, A. Finazzi-Agro, P. Guerrieri, L. Avigliano, B. Mondovi, and E. Antonini, Eur. J. Biochem., 23, 321 (1971).

104. F. E. Wood and M. Cusanovich, Bioinorg. Chem., 4, 337 (1975).

105. J. Rawlings, S. Wherland, and H. B. Gray, J. Amer. Chem. Soc., 98, 2177 (1976).

106. M. Goldberg and I. Pecht, Biochemistry, submitted for publication.

107. L. E. Bennett, The Iron-Sulfur Proteins, Vol. III, W. Lovenberg, Ed., Academic Press, New York, 1976, Chapter 9.

108. C. A. Jacks, L. E. Bennett, W. N. Raymond, and W. Lovenberg, Proc. Nat. Acad. Sci. (USA), 71, 1118 (1974).

109. S. Wherland, R. A. Holwerda, R. C. Rosenberg, and H. B. Gray, J. Amer. Chem. Soc., 97, 5260 (1975).

110. D. Fensom, quoted in R. A. Holwerda and H. B. Gray, J. Amer. Chem. Soc., 97, 6036 (1975).

111. R. C. Rosenberg, S. Wherland, R. A. Holwerda, and H. B. Gray, J. Amer. Chem. Soc., in press.

112. This reaction might be somewhat suspect, as it was run against the driving force for the reduction (by 20 mV), but the 100- to 1,000-fold excess of oxidant used gives minimum 98 percent completion. Therefore, coupled with the result that the concentration dependence on 5 was found to be linear with a zero intercept, the driving force problem is not expected to be too serious (the same may not be said for the cross reaction run at a 10-fold excess, and the reaction 5 with azurin is apparently complicated by this and other problems).

113. R. W. Chlebek and M. W. Lister, Can. J. Chem., 44, 437 (1966).

114. W. A. Eaton, P. George, and G. I. H. Hanania, J. Phys. Chem., 71, 2016 (1967).

Table 1 (Supplement) Ionic Strength Dependence Data

Protein	Reagent	μ(M)	k($M^{-1}s^{-1}$)[b,c]	Ref.
Cytochrome c[a] (Horse heart)	$Fe(EDTA)^{2-}$[a]	0.02	$8.21(10^4)$	93
		0.04	5.55	
		0.04	5.44	
		0.06	3.88	
		0.06	4.24	
		0.08	2.73	
		0.08	3.03	
		0.10	2.06	
		0.10	2.13	
	$Co(phen)_3^{3+}$[a]	0.06	$1.27(10^3)$	95
		0.06	1.18	
		0.10	1.51	
		0.10	1.53	
		0.14	1.83	
		0.14	1.75	
		0.17	2.05	
		0.17	2.02	
		0.20	2.22	
		0.20	2.15	
	$Fe(CN)_6^{4-}$[a]	0.035	$> 18(10^4)$	67
		0.242	3.2	
		0.321	1.9	
		0.400	1.7	

Protein	Reagent	μ(M)	$k(M^{-1} s^{-1})$	Ref.
HiPIP (Chromatium vinosum)	$Fe(CN)_6^{3-}$ [d]	0.008	$1.15(10^3)$	102
		0.033	1.47	
		0.058	1.95	
		0.108	2.53	
		0.158	3.01	
		0.208	3.82	
Azurin	$Fe(EDTA)^{2-}$ [f]	0.010	$1.16(10^3)$	111
		0.010	1.13	
		0.035	1.31	
		0.035	1.33	
		0.075	1.39	
		0.075	1.40	
		0.130	1.48	
		0.130	1.46	
		0.200	1.51	
		0.200	1.51	
		0.350	1.70	
		0.350	1.69	
	$Co(phen)_3^{3+}$ [a]	0.05	$2.61(10^3)$	100
		0.05	2.43	
		0.08	2.20	
		0.08	2.26	
		0.12	2.11	
		0.12	2.08	
		0.16	2.11	
		0.16	1.83	
		0.20	2.02	
		0.20	1.89	

Protein	Reagent	μ(M)	k(M^{-1} s^{-1})
Cytochrome c (Euglena gracilis)	$Fe(CN)_6^{3-}$	0.027	0.713(10^4)
		0.033	1.32
		0.055	2.03
		0.082	2.59
		0.132	3.31
		0.520	5.75
Cytochrome c_2 (Rhodospirillum rubrum)	$Fe(CN)_6^{4-}$ d, e (k_{12})	0.035	7.0(10^4)
		0.085	13.
		0.135	6.6
		0.235	1.5
		0.535	0.63
		1.035	0.15
	$Fe(CN)_6^{3-}$ d, e (k_{43})	0.035	6.0(10^6)
		0.085	3.6
		0.135	2.2
		0.235	1.5
		0.535	1.1
		1.035	0.5
	$Fe(CN)_6^{3-}$ d, e (k_{21})	0.035	4.5(10^2)
		0.085	4.0
		0.135	3.5
		0.235	3.0
		0.535	2.6
		1.035	2.4
HiPIP (Chromatium vinosum)	$Fe(CN)_6^{4-}$	0.008	1.49(10^2)
		0.033	1.38
		0.058	1.73
		0.108	1.52
		0.158	1.36
		0.208	1.54

Protein	Reagent	μ(M)	$k(M^{-1} s^{-1})$	Ref.
Cytochrome c	$Fe(CN)_6^{3-}$ [a]	0.028	$4.20(10^7)$	67
		0.039	2.89	
		0.090	1.66	
		0.153	1.05	
		0.202	0.660	
		0.280	0.593	
		0.313	0.604	
		0.423	0.482	
	Cytochrome c (Horse heart) [a]	0.068	$1.24(10^3)$	84
		0.148	2.48	
		0.231	4.70	
		0.305	6.11	
		0.384	8.90	
		0.469	14.6	
Cytochrome c_{551}	$Co(phen)_3^{3+}$ [a]	0.02	$2.13(10^5)$	100
		0.02	1.13	
		0.06	7.40	
		0.06	7.60	
		0.10	6.22	
		0.10	6.09	
		0.15	5.28	
		0.15	5.25	
		0.20	4.56	
		0.20	4.46	
Cytochrome c (Euglena gracilis)	$Fe(CN)_6^{4-}$ [d]	0.027	$1.54(10^3)$	69
		0.033	2.22	
		0.055	2.84	
		0.082	3.41	
		0.132	3.63	
		0.520	5.25	

Protein	Reagent	μ(M)	$k(M^{-1}s^{-1})$	Ref.
Plastocyanin (Bean)	$Fe(EDTA)^{2-}$[g]	0.05	$3.11(10^4)$	111
		0.10	4.95	
		0.20	7.59	
		0.30	8.91	
		0.50	11.3	
Stellacyanin	$Co(phen)_3^{3+}$[a]	0.052	$1.89(10^5)$	100
		0.194	1.89	
		0.296	1.93	
		0.390	1.92	
		0.502	1.84	

Supplemental Table 1 Footnotes

[a] pH 7, phosphate, 25°.

[b] When two values are given at an ionic strength, they reflect two reagent concentrations.

[c] For a given protein-reagent pair all rate constants carry the same multiplicative factor.

[d] pH 7, phosphate, 20° (NaCl).

[e] Rate constants are identified as given by the authors for the mechanism involving complex formation.

[f] pH 6.8, phosphate, 25°.

[g] pH 6.9, phosphate, 25°.

CHAPTER 2

MACHINES

This chapter presents descriptions of kinetics instrumentation which the author was primarily responsible for setting up, and which, at the time of this writing, has not evolved away from the original design so far as to be unrecognizable from these descriptions. These descriptions are primarily introductions to the instruments and not user's manuals.

The Caltech Stopped-Flow Rapid Scanning Spectrometer

The stopped-flow rapid scanning spectrometer is based on the Tektronix rapid scanning spectrometer system (RSS) and an Aminco-Morrow stopped-flow mixing system. As presently configured (see the Figure) the system can reliably collect data at a maximum of 50 spectra/sec with up to 512 wavelengths per spectrum. The spectral range is 350 to 1100 nm; a 400 nm wide spectrum may be taken (starting at any even 100 nm from 300 to 700 nm) with 4 nm resolution, or a 200 nm wide spectrum with 2 nm resolution in the range 300 to 500 nm may be selected. A maximum of approximately 4,000 data points may be collected in any one run. The stopped flow syringes and mixing chamber are thermostatted and designed for anaerobic operation. Data are collected as light intensity versus time at each channel of the Vidicon detector after being digitized (to ten bit precision) by the processor of the digital processing oscilloscope (DPO). The following sections treat each subsystem in more detail.

Stopped-Flow Mixing System

The mixing system is a standard Aminco-Morrow unit with the following modifications. First, gas-tight Hamilton valves have been added between the two drive syringes and the mixing jet. These valves were found necessary because of the ease with which mixed solution was forced back into the drive syringes, both when the stop syringe was emptied and when one syringe was being flushed. These valves are connected with the same Teflon tubing as the other valves, and are mounted in the plate which was designed to cover the compartment and hold the fibre optics bundle. The triggering system was converted from the normal system, which provides a 14 volt signal when the stop syringe microswitch is closed, to providing a simple short circuit, as required by the trigger circuitry of the oscilloscope. The last modification was the introduction of a copper-constantan thermocouple, placed in one of the Kel-f drive syringes by drilling a fine hole in the thick wall of the syringe. The thermocouple does not come into contact with the solution in the syringe. The thermocouple has been calibrated between 6 and 36°C and the dependence is well represented by the equation

$$T = 25.53 + 24.74\ X\ (mV) - 2.468\ X\ (mV)^2.$$

A potentiometer is available for precision measurements, and a strip chart recorder for following the temperature continuously, although less precisely. Temperature of the stopped-flow is maintained by a Forma circulating bath. The solution in the bath (usually distilled water) circulates around the drive syringes the cell compartment, and the cell support via ports drilled in the alumi-

num block. The whole stopped-flow is supported on a rigid steel bracket anchored to the table.

Optical System

The standard light source is a 150 watt high pressure xenon arc with an Oriel power supply and lamp housing. The parallel light from the collimating lens system (two quartz lenses) passes through a ten centimeter water filter, an iris, a converging lens, a pinhole, and is finally focused onto the cell by a lens supported on a magnetic base. After passage through a one millimeter diameter, one centimeter path length observation cell, the light enters a quartz fibre optic bundle which is coupled to the spectrometer. The fibre optics have a minimum transmittance of 45% from 550 to 1100nm, and 10% at 250nm. A filter holder for standard two by two centimeter glass filters is situated after the last lens of the lamp housing. The function of the water filter is to absorb the large amount of infrared radiation given off by the lamp, which would otherwise heat the sample. The pinhole blocks the scattered light from the source.

Further filtering, with either glass or solution filters, can help achieve a flatter baseline, or remove additional unwanted radiation. The amethyst filter gives the best results for the 300 to 700nm range, in the former case; while an example of the latter is the removal of ultraviolet light by a one centimeter thick pyrex filter.

A second source available is a 50 watt tungsten-iodine lamp with the same low ripple power supply as is used in the Durrum stopped-flow. This lamp is much weaker than the xenon source in the region below 400nm, but gives a smoother baseline, especially

above 800nm where the xenon spectrum is a forest of spikes. The lamp is typically stuck inelegantly next to the cell, where it causes sample heating. A better arrangement would be to mount the lamp on another magnetic base (which is available) and move it behind the final lens, but this might require a reflector behind the lamp to maintain a reasonable intensity.

Anaerobic Operation

A gas scrubbing system is available for oxygen-free (or at least a good try) operation. The scrubber is a column of MnO dispersed on vermiculite, which is green when active and turns brown as it becomes depleted. The column is easily regenerated by heating it under a constant stream of hydrogen. After passing through the column, that portion of the gas to be used for deoxygenating solutions is passed through two bubblers to equilibrate it with water vapor. A separate, dry portion is passed through the cell compartment to prevent oxygen leakage there. Since the gas flowing through the cell compartment could disturb temperature equilibrium, especially at low temperatures, the gas stream is first passed through a copper coil immersed in the reservoir of the Forma bath.

DPO/RSS

The rest of the hardware, from the fibre optics on through the spectrometer, DPO, computer, terminal, copier, and cassette, is from Tektronix and part of the original package. These units are well documented in the Tektronix literature, so they will be only briefly described here. Light which has passed through the cell

and the fibre optics enters the spectrometer through slits (and filters, if chosen) at the back and then is dispersed by one of two gratings onto the Vidicon detector. This detector is an array of photodiodes with 512 separate channels, each of which is illuminated by a different range of wavelengths from the dispersed output, the specific wavelengths dependent on the position of the grating. This arrangement allows a wide range of the spectrum to be sampled continuously with no moving parts. Another feature of the photodiode detector is that the charge which builds up on any diode (channel) is proportional to the total amount of light which has reached that diode since the last read cycle (when the charge is read, it is neutralized, and the charging process begins again). Thus, signal-to-noise enhancement may be obtained by increasing the signal (light intensity) or by waiting longer between read cycles. One point to realize, however, is that this detector does not respond well to large changes in light level which are much faster than the sweep (read) rate. Thus, if the sweep rate is slow, say one per second, and the shutter is then closed, thus blocking all light from entering the spectrometer, the display on the DPO will show that it takes several scans before the signal is down to the baseline level. This problem is a function of the number of scans not the absolute light level; thus at 20 ms per scan, the response time would still be a few scans. Another problem of the Vidicon detector is that it is more sensitive at the longer wavelengths and less sensitive at higher energy (the opposite of a phototube), thus

the wavelength range available extends further into the near infrared, but sensitivity falls off quickly below 400nm when compared to, say, a Cary. This latter problem might be lessened if the fibre optics were not used, but the alignment difficulties and the problem of access to the valves at the front of the stopped-flow, have discouraged attempting this modification.

The signal passes from the spectrometer, through the double RSS plug-in, is digitized and displayed on the DPO, which can store up to four spectra in its own memory. In optimizing the signal as it appears in the DPO memory, several factors must be considered. First, the signal level must be high enough that one of the lower gain settings may be used, thus cutting down on the noise in the processed signal. The light level reaching the detector is a function of both the lamp intensity (which could be varied, but in practice is left at a maximum), filters, and the slit width. The latter is the most often changed. The compromise is that the larger the slit width, the greater the signal (up to the point of saturating the Vidicon), but the lesser the resolution. Secondly, the baseline has some sharp spikes, such as those above 400nm in the xenon spectrum, the digitizer, in treating the wavelength information, will have a little "jitter" and thus one spectrum will have the spike in a given channel and the next spectrum might have the spike in the adjacent channel. This problem introduces noise both in averaging spectra and in taking a normal sequence of spectra, but it can be minimized if the slit is opened enough that the spike becomes more broad.

A few properties of the digitizer should be known to properly understand the limitations of the data collected. First, the digitizer has 10-bit precision, that is to say, it effectively divides the y axis of the DPO readout (including one large square above and below the graticules shown, for a total vertical scale of 10 large divisions) into 1024 ranges and determines which of these includes the signal level of interest. Thus, each large square is divided into about 100 smaller divisions and a signal level is digitized to a precision of 1% of a large graticule. From this, it is clear that the change in signal level observed during a kinetic run should be at least one large square, and a larger change is certainly preferable. The problem of setting the gain, filters, and other parameters, so that all wavelengths of interest are on scale and show as large a deflection as possible, is one of the more difficult ones in RSS applications, primarily because the baseline (lamp spectrum) is far from flat. The second important property of the digitizer is that it randomly chooses the order in which it will digitize the incoming signal, thus at scan rates higher than 20 ms (or if the horizontal scale expansion is used) some channels may not be digitized. This arrangement is fine if an entire spectrum is being collected, since missed channels will be at different locations in different spectra, but when only selected spectral elements are wanted it becomes quite frustrating and prevents the use of higher scan speeds. Data are also lost, at high scan rates with large data sets, because they cannot be transferred fast enough from the DPO to the computer. The origin of this problem is discussed in the RSS TEK BASIC language manual.

Software

A brief discussion of the philosophy and scope of the program library and the language RSS TEK BASIC is the last subject. A detailed discussion of the various programs available is not presented as the collection is now large and continually being both increased and improved. The language RSS TEK BASIC as supplied by Tektronix has many excellent features, including versatile data acquisition and efficient processing of the type of arrays collected in RSS experiments. The primary disadvantage is array dynamic range. Briefly, this problem arises because the arrays are stored in scientific notation with a single exponent for the entire array. Thus when the values in an array vary by enough that the exponent would change were they written out separately, the mantissa changes instead, and only the largest number in the array retains full precision. This problem is further compounded because even in the best of cases, only enough binary digits are kept to assure 4 decimal places of precision. This procedure was chosen by Tektronix because it matches the precision of the data from the DPO, and saves space in storing arrays, but wreaks havoc in later data processing (for instance when an array is raised to a power). Precision can be partially retained by storing values as their natural logarithms, but this process is slow. To circumvent this problem (which is only important in the processing of acquired data) a version of BASIC which is more precise has been purchased from DEC.

The programs are written as small routines for special applications. This approach is taken to minimize the amount of

storage space taken by programs at any one time so that more room is available for data. At any time several of the programs which are commonly used may be in core and still leave room for the largest data sets. Several programs (DACOL) are used in the collection of data. These prompt the operator when the computer is ready for different parts of the data (shutter closed, reference spectrum, data set, and infinity spectrum) and modifications of the simplest program also calculate offsets, and check for errors in the data. A program which may be used to "rerun" the data is available and quite useful when collecting fast kinetic data. The program (MOVIE) displays the consecutive data sets on the DPO screen, overlaying four at a time. Many programs for data analysis are available, and it is hoped that this collection will grow as users develop programs for their own needs. The general philosophy is based on using weighted least squares fitting of the data to integrated rate laws. The rate laws treated so far (simple first order, parallel first order, etc.) have not required numerical integration methods, and unless the user has a great deal of patience, such approaches might be more efficiently performed on a larger computer. The weighting factors for the least squares analysis are calculated from the standard deviation of the raw data (calculated with the aid of the program EXPSD) and the correct propogation of error formulas derived for each function to be fit. Routines are available for plotting both points and functions, and these allow either automatic scaling or manual scaling. For applications directed more towards

obtaining the spectrum of an intermediate rather than the kinetics of its formation or decay, there are programs which calculate absorbance from collected data and a selected reference spectrum (remember that the instrument uses a single beam) and plot the spectra versus the wavelength or wavenumber. All of these programs are changing and improving, mostly due to the work of Bob Scott. The program library will be changing, especially as DEC BASIC is implemented.

System Tests

Various tests have been run on the system. The most convincing is the simple analysis of the $KMnO_4$ spectrum. When the spectrum as taken on the RSS (calculated from water and $KMnO_4$ spectra) is compared to the spectrum taken on the Cary 17, they are virtually identical from 700 to 350nm, providing that the RSS spectrum is shifted four channels (about 3nm) to higher energy, and the pathlength of the cell is 0.95cm instead of 1.00cm. Both of these corrections are reasonable, since the first is essentially a wavelength calibration and the second is the result of the non-rigid character of the Aminco Morrow stopped-flow cell (it is a sandwich construction with several layers of Teflon components squeezed by a screw clamp).

Figure: Block outline of the Caltech Rapid Scanning Spectrometer System

Rapid Scanning Spectrometer System

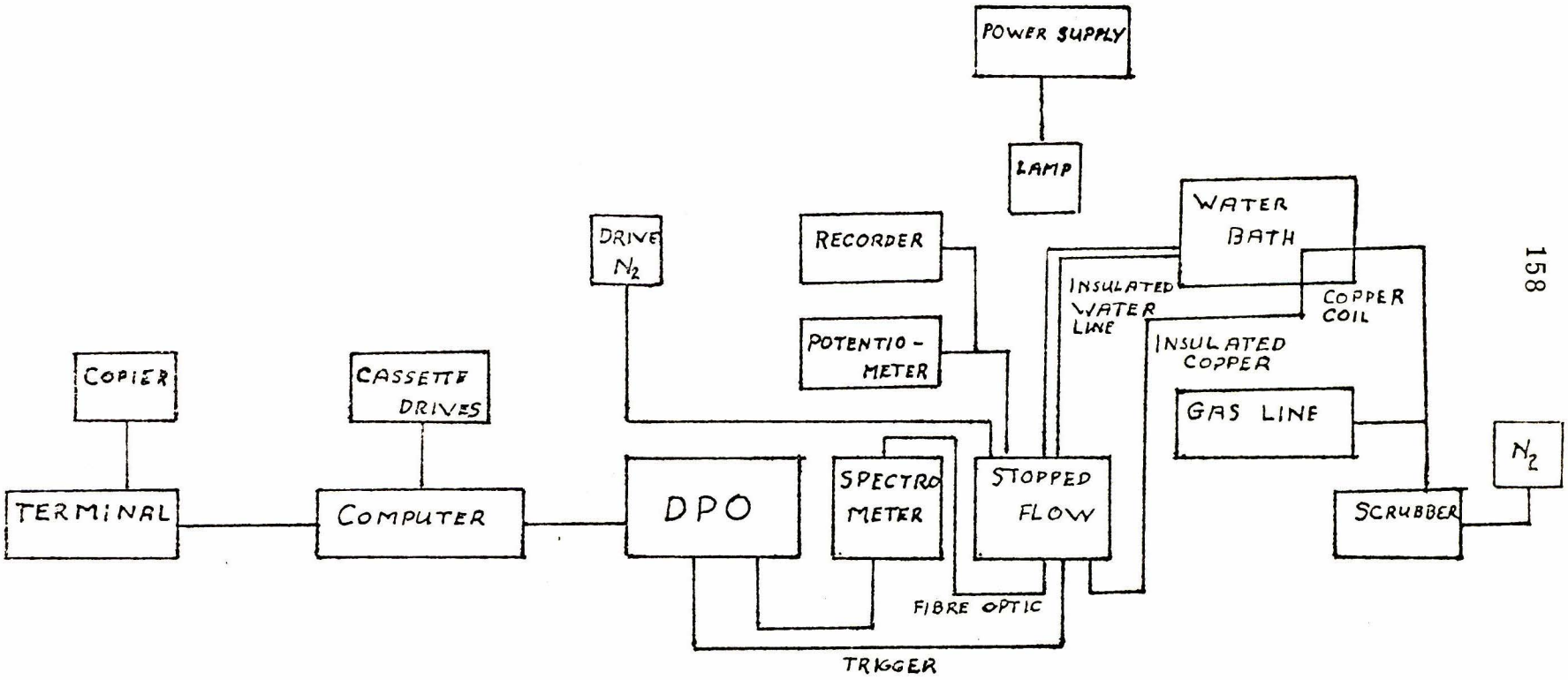

CHAPTER 3

CALCULATION OF SPIN CHANGE ACTIVATION BARRIERS: HAZARDS IN THE APPLICATION OF SIMPLIFIED LIGAND FIELD THEORY

Introduction

In two cases of interest to the inorganic kineticist, attempts have been made to apply simplified ligand field theory, using Racah parameters, to the problem of determining spin change activation energies. These two cases are the water exchange of hexaquocobalt(III) and the electron transfer reaction between cobalt(II) and cobalt(III) hexammines. It is the purpose of this chapter to demonstrate the pitfalls associated with such calculations.

In attempting to use spectroscopic data to estimate the difference in energy between proposed intermediates or activated states in a kinetic scheme, it is important to consider changes in metal-ligand distances which take place in the kinetic experiment and which do not take place in the electronic excitation, which is assumed to be "vertical". A change in the metal-ligand bond length is expected because the population of the antibonding e_g level has been increased in the high-spin state. In the two examples discussed here, an attempt will be made to include this variable in the calculations.

$Co(H_2O)_6^{3+}$: The Kinetic Availability of the High-Spin State

For over twenty years a controversy has festered concerning the energy of the high-spin ($^5T_{2g}$) state of hexaquocobaltic ion. In 1951, Taube et al.[1] proposed that the anomalously fast water exchange of Co(III) could be explained if the high-spin state were within 5 kcal/mole of the ground state. Spectroscopic treatments of the problem were hampered by difficulty in preparing samples of the ion free from contamination by Co(II). In 1966, Johnson and Sharpe[2] interpreted the electronic spectrum of $CsCo(SO_2)_2 \cdot 12H_2O$ in such a way as to indicate that the high-spin state is 15 kcal/mole above the ground state. The Johnson-Sharpe interpretation will be challenged here.

In order to attempt to account for the varying bond lengths in the kinetic process, the following pathway will be considered as a possible route through high spin Co(III). The low-spin form with the low-spin radius expands; at some radius, short of the high-spin radius, the spin change takes place and a metastable intermediate is formed which then undergoes exchange. The process is subsequently reversed to yield the low-spin species with the exchanged ligand. The respective bond lengths cannot be directly treated here. Instead, approximations for the spectral parameters corresponding to the two spin forms will be derived and from these the spin change energy will be estimated. It is assumed that the energy required for expansion of the ion and the activation energy for the exchange of the high-spin form are small.

The tack to be taken in treating the spectral data is the following. The value of the parameters 10Dq and B will be taken from the electronic absorption spectrum of the low-spin form. The parameters for the high-spin form will be assumed† to be those of $Fe(H_2O)_6^{3+}$.[5] The energy of the transition $^5T_{2g} \leftarrow {}^1A_{1g}$ will then be calculated for various values of 10Dq, and C between those for the high- and low-spin states. Some discussion of what constitutes a reasonable value of C/B will be given.

The electronic absorption spectrum of $CsCo(SO_4)_2 \cdot 12H_2O$ at 77 °K as determined in our laboratory[3] is as follows: maxima at 597 and 399 nm with a shoulder at 500 nm. The two major peaks correspond to the two singlet transitions (to T_{2g} and $^1T_{1g}$), yielding a B value of 472 cm^{-1}. The 597 nm peak (17,500 cm^{-1}) corresponds to 10Dq - C. If C is varied from 4B to 9B, 10Dq varies from 19,200 cm^{-1} to 21,550 cm^{-1}. For comparison, Johnson and Sharpe chose 10Dq = 20,800 cm^{-1}, B = 513 cm^{-1}, and C = 4,250 cm^{-1}.

A problem which still must be considered is the value C/B which is reasonable to use for Co(III) in the calculation. Although values of 4 to 5 are commonly assumed,[4] Johnson and Sharpe claim spectral evidence for the transition $^3T_{1g} \leftarrow {}^1A_{1g}$, which leads to a value of C/B of 8.2. Furthermore, recent work[6] on a single crystal of $K_3Co(CN)_6$ has located $^3T_{1g} \leftarrow {}^1A_{1g}$, leading to an assignment of

† The fact that $Fe(H_2O)_6^{3+}$ possesses two e_g electrons in its ground state, just as high-spin $Co(H_2O)_6^{3+}$ would have, is the justification for this assumption.

C/B = 8.75. The weakness of the singlet → triplet bands makes all of these assignments difficult, but the weight of the evidence favors the 8 to 9 range for low-spin $\underline{d}^6$ cases, and a value of 8.5 will be used in the following calculations. The value of 3.13 determined for $Fe(H_2O)_6^{3+}$ will be used for the high-spin form.

The value of the promotion energy is calculated from the strong-field diagonal element E = 2(10Dq) - 5B - 8C.

From Table 1 it is clear that the spin promotion energy could, within the approximation of this treatment, be quite small if the spectral parameters are close to those assumed for the high-spin state. It is reasonable to expect, by the Evans-Polanyi Rule[7] (Hammond Postulate), the form that undergoes spin change to more closely resemble the high-spin state than the low-spin form, since the latter will be of lower energy in any case.

$Co(NH_3)_6^{2+/3+}$: The Spin Activation Barrier to Electron Transfer

The immeasurably slow electron transfer between Co(II) and Co(III) hexammine has received much attention from kineticists[8] and theoretically, in terms of relative Marcus theory, from various "static" measurements of structure and spectra. The most recent such treatment is that of Stynes and Ibers.[9] These authors concluded from spectral data that the minimum spin change activation energy needed, to meet the requirement that both systems be in the high- or low-spin state prior to electron transfer, is of the order of 25 kcal/mole. The high- to low-spin transition of the Co(II) species is determined as being the lowest energy pathway. This interpretation will also be challenged.

Table 1

$Co(H_2O)_6^{3+}$

Promotion Energy

$^3T_{2g} \leftarrow {}^1A_{1}g$

10Dq cm^{-1}	B cm^{-1}	C cm^{-1}	% High Spin Character	E cm^{-1}	E kcal mole
21,500	528	4,490	0	4,440	12.7
19,940	611	4,184	20	3,353	9.6
18,380	695	3,878	40	2,261	6.5
17,600	737	3,725	50	1,715	4.9
16,820	778	3,572	60	1,174	3.4
15,260	862	3,266	80	82	0.2
13,700	945	2,960	100	(-1,005)	(-)

There is not universal acceptance of the spectral parameters for the cobalt hexammines. As with the cobalt(III) hexaquo system, there is the problem of what C/B ratio to use. There is evidence for a C/B ratio near 8 for the Co(III) ion,[10] but none for the Co(II) species. Therefore calculations will be done for C/B values of 4.5 and 8.0. The references given are for the 10Dq and B values.

For each set of spectral parameters, the spin change energy was first calculated assuming ground state geometries. The value 10Dq' is that value of 10Dq which is required to make the spin change energy 1000 cm^{-1}. The strong-field expression for the energy of the Co(III) transition $^5T_{2g} \leftarrow {}^1A_{1g}$ is E = 2(10Dq) - 5B - 8C. For the $^2E_g \leftarrow {}^4T_{1g}$ transition of the Co(II) system E = 4(B+C) - 10Dq was used. Jørgensen has estimated[12] that 10Dq decreases 10% to 20% per electron transferred from a t_{2g} to an e_g orbital. On this basis, the E' values were calculated, using 10Dq - 30% for the Co(III) case and 10Dq + 15% for the Co(II), in place of 10Dq.

The results of this approach, as shown in Table 2, may now be discussed. On the assumption that C/B = 4.5, the Co(II) complex is predicted to have the lower transition energy. This is the same qualitative result as reached by Stynes and Ibers, but the most reasonble estimate for the promotion energy, E', is 13.4 kcal/mole. This estimate for the transition energy is over 10 kcal/mole below that of Stynes and Ibers. For the assumption that C/B = 8.0, the Co(III) transition is predicted to be of lower energy, and in this case the energy could be quite low. In either case, the predicted

Table 2

$Co(NH_3)_6^{2+/3+}$

Spectral Parameters Cm^{-1}

Ion	Data	10Dq	B	C/B	C
$Co(III)^{10}$	A	25,000	531	4.5	2,400
	B	25,000	531	8.0	4,250
$Co(II)^{11}$	C	10,900	780	4.5	3,500
	D	10,900	780	8.0	6,250

Transition Energies

Ion	Data	E cm^{-1}	E' cm^{-1}	10Dq'* cm^{-1}	10Dq'/10Dq
Co(III)	A	28,200	13,200	11,400	0.46
	B	13,361	(-)	18,800	0.76
Co(II)	C	6,300	4,700	18,200	1.67
	D	17,200	15,600	27,100	2.48

*Dq such that E = 1,000 cm^{-1}.

activation energy is considerably lower than that predicted by Stynes and Ibers, therefore the origin of the requisite activation energy barrier to self exchange must be sought elsewhere.

Conclusion

The results of the calculations made here must be considered in terms of the approximate nature of the theory involved. The spectral parameters are imprecisely known, especially C, and the dependence of these parameters on metal-ligand distances can only be estimated. The formulas for the transition energies are greatly simplified. Nevertheless, the conclusion which can be reached is that there is not necessarily a large energy difference between the high- and low-spin states of any of the cobalt complexes considered, and that this energy difference may well be 5 kcal/mole or less.

References

1. H. L. Friedman, J. P. Hunt, R. A. Plane, and H. Taube, J. Amer. Chem. Soc., 73, 4028 (1951).
2. D. A. Johnson and A. G. Sharpe, J. Chem. Soc. (A) 1966, 798.
3. Unpublished results of G. Geoffroy.
4. B. N. Figgis, Introduction to Ligand Fields, Interscience, 1966.
5. H. B. Gray, "Structural Models for Iron and Copper Proteins Based on Spectroscopic and Magnetic Properties," in Adv. in Chem. Series No. 100.
6. Unpublished results of V. Miskowski.
7. M. G. Evans and M. Polanyi, Trans. Faraday Soc., 34, 11 (1938).
8. N. S. Biradar, D. R. Stranks, and M. S. Vaidya, Trans. Faraday Soc., 58, 2421 (1962).
9. H. C. Stynes and J. A. Ibers, Inorg. Chem., 10, 2304 (1971).
10. D. A. Johnson and A. G. Sharpe, J. Chem. Soc. (A), 1966, 798.
11. K. B. Yatsimirskii and I. I. Yolchenskova, Teor. Eksp. Khim., 4, 808 (1968).
12. C. K. Jørgenson, Absorption Spectra and Chemical Bonding in Complexes, p. 128, Oxford, Pergamon Press, New York, 1962.

CHAPTER 4

KINETIC STUDIES OF THE REDUCTION OF *Rhus vernicifera* LACCASE AND ITS AZIDE DERIVATIVES BY $Fe(EDTA)^{2-}$ AND $Fe(HEDTA)^{-}$

Introduction

As presented in the Appendix, the $Fe(EDTA)^{2-}$ reduction of laccase is characterized as requiring about 10 kcal/mole in protein activation energy. The model for attack is a protein conformational change to accept the reductant near the type 2 copper followed by electron transfer to the type 1 site. It has been shown with hydroquinone as the reductant that reduction of type 3 has similar activation parameters and reduces in parallel with the type 1 site, thus it is considered to have the same mechanism for the attack of reductant as the type 1 site. In order to prove any preference in the mechanism for inner or outer sphere attack, the following study was done with $Fe(HEDTA)^{-}$. The HEDTA ligand has a $-CH_2CH_2OH$ in place of one of the acetates of EDTA, and therefore has one open coordination position which EDTA lacks. It is to be expected that $Fe(EDTA)^{2-}$ will be an outer sphere reductant (although it is best considered seven coordinate), whereas $Fe(HEDTA)^{-}$ can more easily go inner sphere if such a path is preferred. By studying the effects of the anionic inhibitor azide, which is thought to bind to the type 2

copper (at least at high azide concentrations when an absorption at 405 nm develops) the effect of a good π bridging ligand is probed, and the effect of the inhibitor can be compared to its effect with hydroquinone as the reductant.

Experimental

Solution Preparation. The experimental techniques are as explained in the appendix, with the following additions. In the experiments with azide ion introduced as an inhibitor, the azide was in the laccase solutions only and therefore underwent dilution in the mixing cell of the stopped flow. Solutions of $Fe(HEDTA)^-$ were prepared in the same manner as described for $Fe(EDTA)^{2-}$ except that mixtures of the triacid and trisodium salt of HEDTA were used to eliminate any contribution to hydrogen ion concentration, instead of the procedure described for the EDTA solutions.

Data Analysis. First order data were analyzed as described in the appendix. Parallel first order data analysis was performed by fitting the data in a least squares sense to the equation

$$A_{tot} = A_1 e^{-k_1 t} + A_2 e^{-k_2 t}$$

where A represents absorbance at 614 nm (in the case of the azide dependence data). The k_{obs} values for the azide dependence of the reduction of the laccase-azide complex by $Fe(EDTA)^{2-}$ and $Fe(HEDTA)^-$ were fit to the equation

$$k_{obs} = \frac{k_1 + k_2 K[N_3^-]}{1 + K[N_3^-]}$$

where $[N_3^-]$ free is assumed equal to total azide and $K = [\text{laccase} \cdot N_3]/[\text{laccase}][N_3^-]$ by a weighted least squares procedure.

Results

Table 1 and Figure 1 show the data for the reduction of laccase by $Fe(HEDTA)^-$ at pH 6.8 and pH 6.0, $\mu = 0.5$ M, 25° C (0.2 M from phosphate buffer). The second order rate constants calculated from these data for reducing agent concentrations less than 0.4 nM are listed with the corresponding second order rate constants with $Fe(EDTA)^{2-}$ as the reductant in Table 2. Table 3 gives the observed rate constants for the reduction of laccase in the presence of varying azide and at 0.1 M NaN_3 with varying $Fe(EDTA)^{2-}$. Figure 2 shows the azide dependence with $Fe(EDTA)^{2-}$ as the reductant, and Figure 4 shows the $Fe(EDTA)^{2-}$ dependence in the presence of 0.1 M NaN_3. The solid lines in the last two figures represent the weighted least squares fit to the one equilibrium constant and two rate constant equation given in the experimental section. The best fit parameters are $k_1 = 0.61\ sec^{-1}$, $k_2 = 0.013\ sec^{-1}$, and $K = 6400$ for $Fe(HEDTA)^-$ (2.5 mM) and $k_1 = 0.87\ sec^{-1}$, $k_2 = 0.00\ sec^{-1}$ and $K = 5500$ for $Fe(EDTA)^{2-}$ (2.5 mM).

Discussion

The concentration dependence of $Fe(HEDTA)^-$ reduction of laccase at both pH 6.8 and 6.0 shows a marked discontinuity at about 4 mM reductant. Along with apparent leveling off, the data becomes much poorer and the scatter extreme for the two highest concentration points at pH 6.8. It is not clear that the data are still

Table 1. Fe(HEDTA)$^-$ Reduction of Laccase

[Fe(HEDTA)$^-$] (mM)	pH	k	Standard Error* (10^3)
0.313	6.8	0.0536	0.376
0.627	6.8	0.326	24.3
1.25	6.8	0.817	6.30
3.13	6.8	1.83	6.75
6.27	6.8	1.86	109.0
12.5	6.8	1.78	115.0
0.25	6.0	0.00598	14.7
0.50	6.0	0.0888	6.05
1.25	6.0	0.293	4.00
2.50	6.0	0.612	3.41
5.00	6.0	1.09	0.220

*This is the standard error of the mean of the multiple determinations performed.

Figure 1. $Fe(HEDTA)^-$ reduction of laccase, concentration dependence on $Fe(HEDTA)^-$, 0.5 M ionic strength, (A) for pH 6.8, (B) for pH 6.0; the lines are drawn for the concentration ranges listed in table 2.

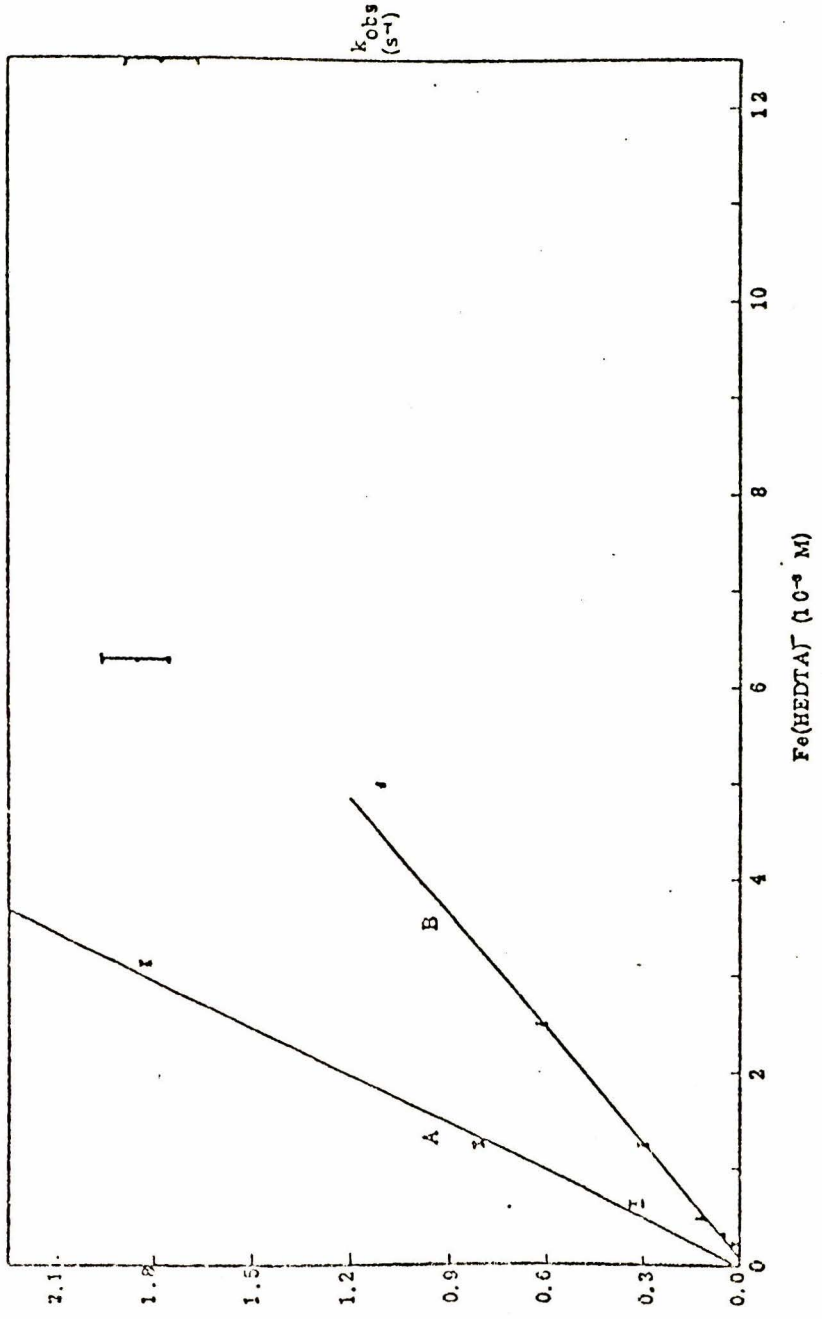
k_{obs} (s^{-1})
2.1
1.8
1.5
1.2
0.9
0.6
0.3
0.0
0
2
4
6
8
10
12
A
B
Fe(HEDTA)$^-$ (10^{-3} M)

Table 2. Second Order Rate Constants $Fe(HEDTA)^-$ and $Fe(EDTA)^{2-}$ Reduction of Laccase

Reductant	pH	k ($M^{-1}sec^{-1}$)	Standard Deviation*	Reducing Agent Range (mM)
$Fe(HEDTA)^-$	6.0	261	0.08	0.25 - 2.5
$Fe(HEDTA)^-$	6.8	647	0.5	0.313 - 3.13
$Fe(EDTA)^{2-}$	6.9	260	0.7	0.5 - 20.0
	5.9	421	5.9	

*This is the standard deviation of the slope from the least squares analysis of the concentration dependence and is included as a measure of goodness of fit, not precision.

Table 3. $Fe(HEDTA)^-$ and $Fe(EDTA)^{2-}$ Reduction of Laccase-Azide Complexes[a]

Reductant	Reductant Concentration mM	$[N_3^-]$ mM	k_1	SE (10^3)	k_2	SE (10^3)
$Fe(EDTA)^{2-}$	2.5	0	0.873	16.8	--	--
		0.5	0.148	4.93	--	--
		2.5	0.116	2.81	--	--
		5.0	0.0749	1.51	--	--
		25.0	--	--	0.0654	0.677
		50.0	0.00594	0.614	0.0509	1.21
		100.0	0.00979	0.616	0.0800	1.37
		150.0	--	--	0.0640	0.210
$Fe(HEDTA)^-$	2.5	0	0.613	6.62	--	--
		0.5	0.151	1.25	--	--
		2.5	0.0858	1.93	--	--
		5.0	0.0657	6.11	--	--
		25.0	0.0125	1.26	0.0925	2.58
		50.0	0.0144	0.192	0.069	0.545

Table 3 (Continued)

Reductant	Reductant Concentration mM	$[N_3^-]$ mM	k_1	SE (10^3)	k_2	SE (10^3)
		100.0	0.0193	1.05	0.121	2.00
		150.0	0.0190	0.270	0.120	2.14
$Fe(EDTA)^{2-}$ [b]	0.5	0.1	0.00205	1.35	0.0164	5.40
	1.0	0.1	0.00542	57.3	0.0401	3.37
	2.5	0.1	0.00693	1.01	0.0749	0.0101
	5.0	0.1	0.0140	37.1	0.122	20.2
	10.0	0.1	0.0343	97.8	0.266	33.7

[a] The conditions are 25.1 °C, μ 0.5 M (0.2 M from buffer) pH 6.0.

[b] The second order rate constants and their standard deviations from the least squares treatment are $k_1 = 2.45\ M^{-1}\ s^{-1}$ $(6.4\ (10^{-5}))$, $k_2 = 2.54\ M^{-1}\ s^{-1}$ $(2.4\ (10^{-3}))$.

Figure 2. $Fe(HEDTA)^-$ reduction of laccase as a function of azide. Azide concentrations are given after mixing. The curve is drawn for $k_1 = 0.61\ s^{-1}$, $k_2 = 0.013\ s^{-1}$ and $K = 6400\ M^{-1}$. The conditions are pH 6.0, ionic strength 0.5 M, 25 °C, and 2.5 mM $Fe(HEDTA)^-$.

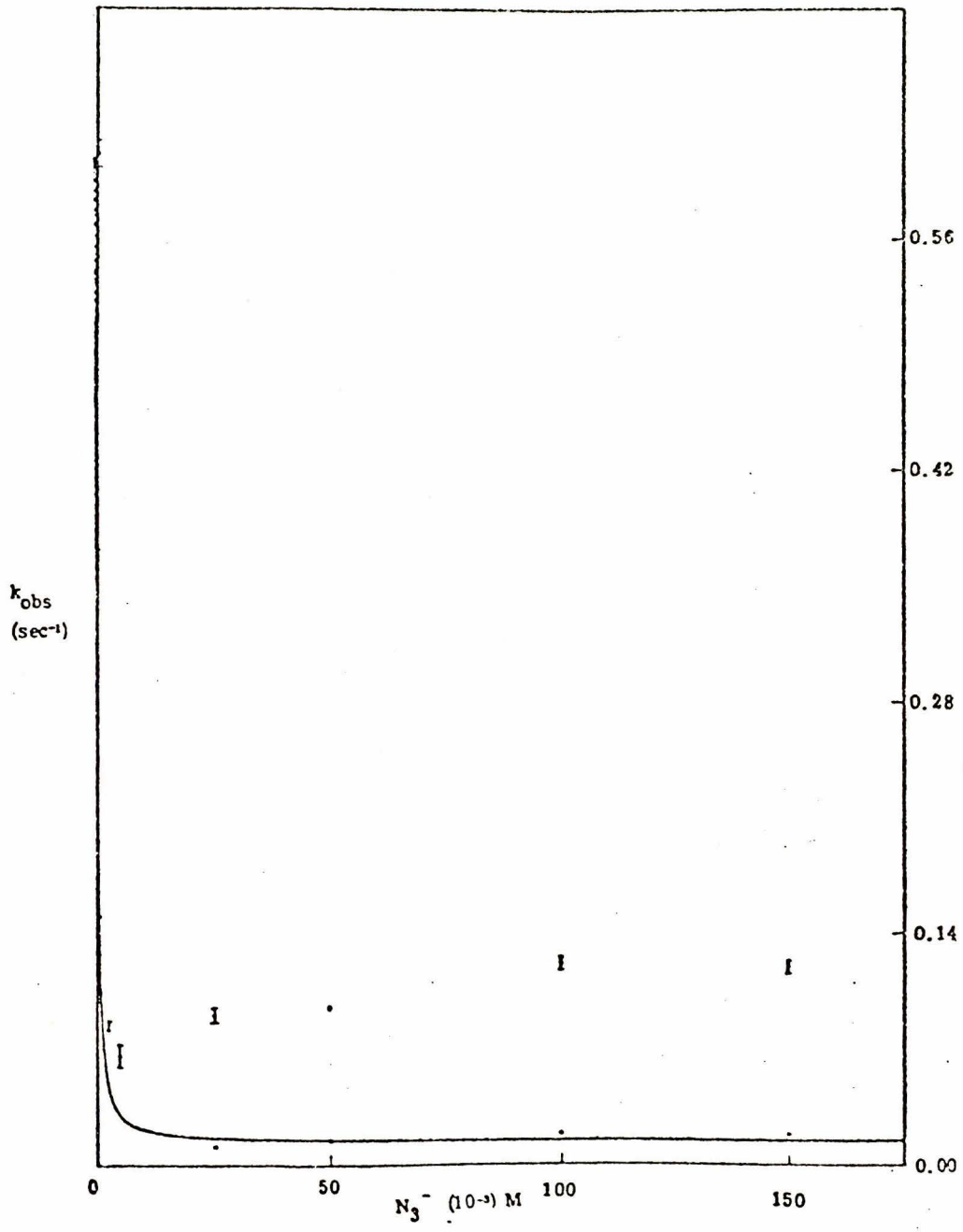
k_{obs}
(sec^{-1})
0.56
0.42
0.28
0.14
0.00
0
50
100
150
N_3^- (10^{-3}) M

Figure 3. $Fe(EDTA)^{2-}$ reduction of laccase as a function of azide. Azide concentrations are given after mixing. The curve is drawn for $k_1 = 0.87\ s^{-1}$, $k_2 = 0.00\ s^{-1}$, and $K = 5500\ M^{-1}$. The conditions are pH 6.0, ionic strength 0.5 M, 25 °C, and 2.5 mM $Fe(EDTA)^{2-}$.

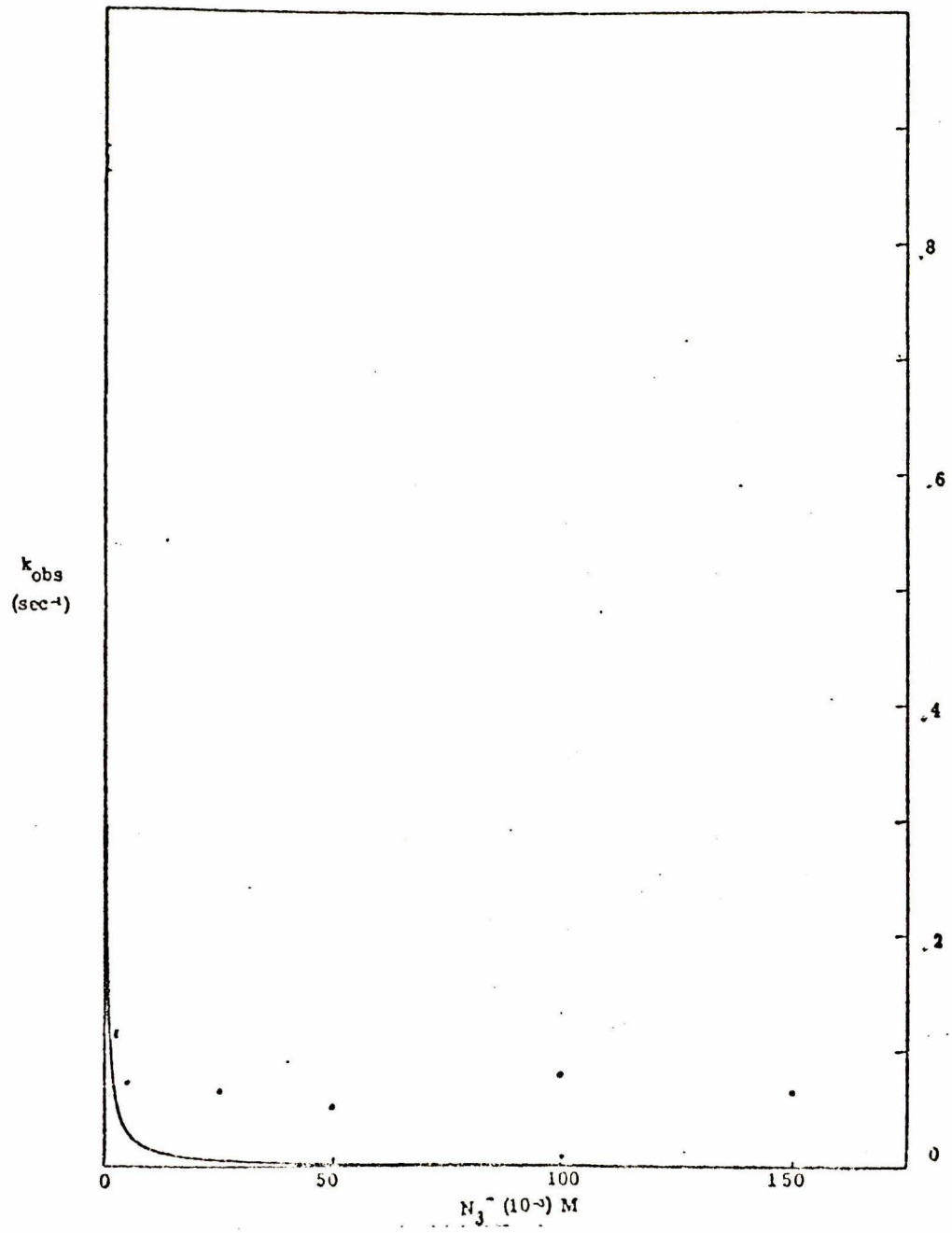
k_{obs}
(sec^{-1})
.8
.6
.4
.2
0
0
50
100
150
N_3^- (10^{-3}) M

Figure 4. Concentration dependence of the $Fe(EDTA)^{2-}$ reduction of the laccase-azide complex. The conditions are 0.1M azide, pH 6.0, 0.5 M ionic strength, and 25°C. The two sets of data are for the two parallel first order paths observed at this azide concentration, the lower line and the x's use the right scale and the upper line and the I's use the left scale.

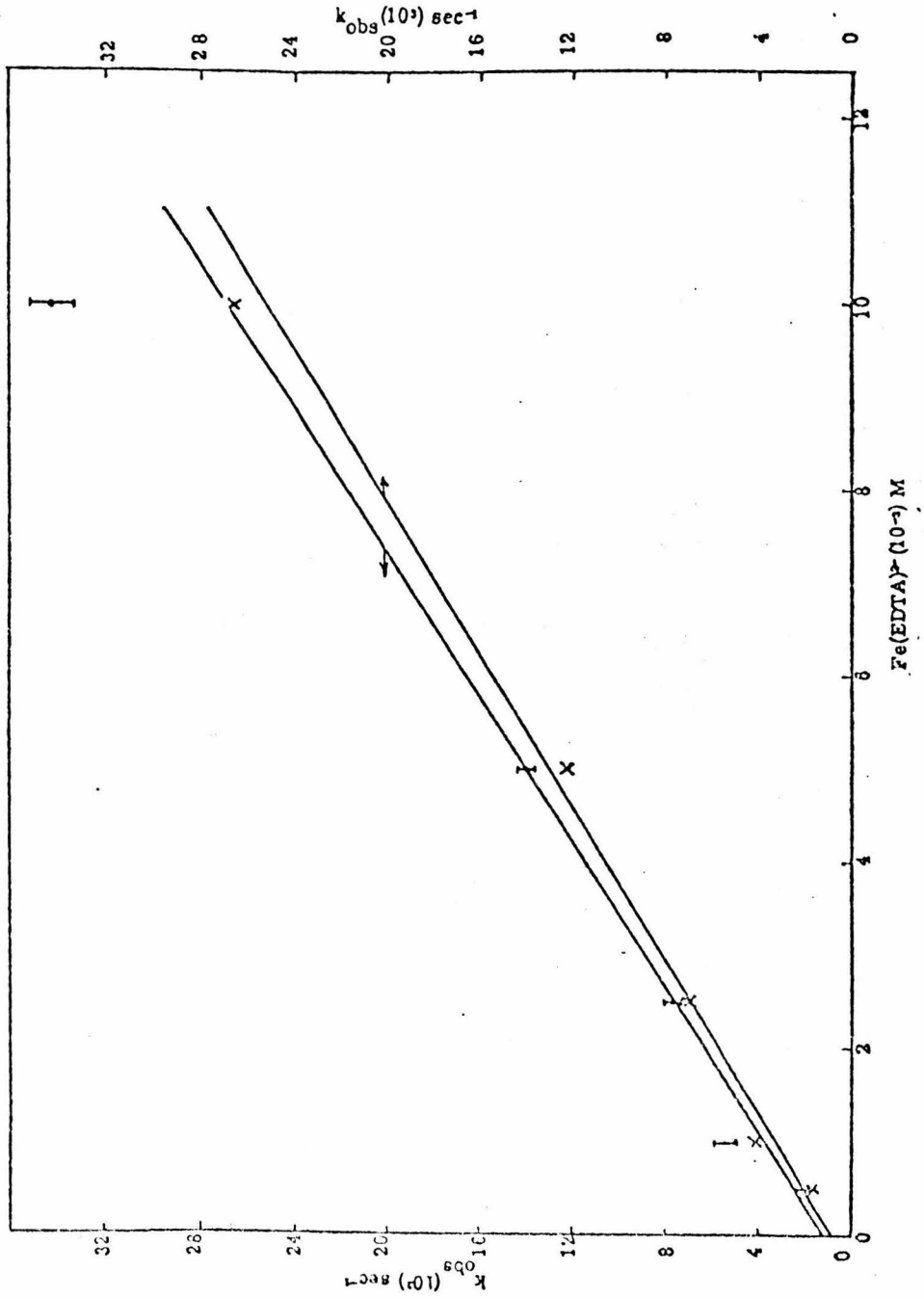
$k_{obs}(10^3)$ sec^{-1}
0
4
8
12
16
20
24
28
32
0
2
4
6
8
10
12
Fe(EDTA)$^-$ (10^{-4}) M

strictly first order, and therefore, further analysis of the concentration dependence above 4 mM is not warranted. A similar trend has been noted with $Fe(EDTA)^{2-}$ as the reductant, but in this case the leveling off of rate does not begin until at least 20 mM reductant. Considering only the linear part of the concentration dependence, it is clear that the pH dependence is contrary to that observed with $Fe(EDTA)^{2-}$ and greater in magnitude (with $Fe(EDTA)^{2-}$ the rate decreased by less than 50% between pH 6 and 7, whereas with Fe(HEDTA) there is a 250% increase over the same pH range).

In the presence of azide there is a strong inhibition of the rate at low azide concentrations and some increase due to one of the two parallel paths observed at higher azide concentrations. The following mechanism is proposed to account for the observed azide dependence

$$L + N_3^- \overset{\text{fast}}{\underset{K_1}{\rightleftharpoons}} L \cdot N_3 \qquad\qquad L \cdot N_3 + N_3^- \overset{\text{slow}}{\underset{K_2}{\rightleftharpoons}} L \cdot 2N_3$$

Under pseudo-first-order conditions for laccase (P is laccase with the type 1 copper reduced)

$$L \overset{k_1}{\rightarrow} P \qquad\qquad L \cdot N_3 \overset{k_2}{\rightarrow} P \qquad\qquad L \cdot 2N_3 \overset{k_3}{\rightarrow} P$$

$$L_{TOT} = (L + L \cdot N_3)_{t=0} e^{-((k_1 + k_2 K_1 (N_3^-))/(1 + K_1 (N_3^-)))} + (L \cdot 2N_3)_{t=0} e^{-k_3 t}$$

where the first equilibrium is rapidly attained, and the second equilibrium is so slow to be attained that the amount of laccase with

two azides bound is constant after it has come to equilibrium in the drive syringe. This mechanism is consistent with the fit of the low azide data to an equilibrium constant and two rate constants, and the azide independence of the faster of the two rates in the parallel first order region (indentified with the two azide form). The mechanism also predicts that there be a linear concentration dependence on reducing agent even in the parallel first order region. This has been shown to be the case with $Fe(EDTA)^{2-}$ as the reductant. The mechanism is also consistent with the previously measured binding constant of 45 M^{-1} for a species which absorbs at 405 nm if this is identified with the two azide form.[1] The parallel first order region of the azide concentration dependence begins at 50 mM azide (before mixing) when there would be about 50% of the laccase in the 405 nm absorbing form. The next lower point, 10 mM azide before mixing, would have about 30% of the 405 nm form, but the observed rate at this concentration is expected to be the same for the two proposed parallel paths, and therefore is not expected to be detected as parallel first order behavior. At 5 mM azide there is predicted to be less than 20% of the 405 nm absorbing species in the protein stock solution, and therefore it may very well not be detected, as is the case.

One way to test whether the species which gives the biphasic kinetics at higher azide is identical with that which gives the binding constant of 45 M^{-1} and the 405 nm absorbance would be to measure the binding constant from the kinetics. This could be done by

analyzing the pre-exponential parameter for the new rate which comes in at higher azide, since this parameter should be proportional to the concentration of the species giving that rate. This was not done because this parameter is evaluated by extrapolating that component of the absorbance versus time curve which gives the rate to zero time, and zero time is not well defined, both inherently because of the mixing time involved in stopped flow kinetics and specifically for this case because of the induction period observed in most laccase kinetics. A particular previous observation which is inconsistent with the kinetics as they have been explained is the study of the rate of anation to give the 405 nm absorbing species.[1] The mechanisms which fit the laccase azide anation studies require some sort of pre-equilibrium, either with an activated form of the protein or with an outer sphere type of complex with the azide, followed by anation. In any case, the rate for the dissociation of azide from the complex, which is a lower limit on the rate of equilibration of the azide bound form after dilution, 0.014 sec^{-1}, is of the same order of magnitude as the slowest processes being observed. The results would have been more consistent with analysis given for the biphasic kinetics if this rate had been an order of magnitude lower.

The analysis of the rate at low azide combined with assigning the slower rate of the biphasic region of the azide dependence to an inhibited form in fast equilibrium with azide free laccase leads to an assignment of the equilibrium constant for the binding of one azide to laccase as about 6000. The two values derived from the $Fe(EDTA)^{2-}$ (5500) and $Fe(HEDTA)^{-}$ (6400) are considered to be in reasonable

agreement considering the precision of the methods involved. This is also reasonably consistent with a value of $\sim 10^3$ estimated from spectrophotometric measurements.[2]

The differences between $Fe(EDTA)^{2-}$ and $Fe(HEDTA)^{-}$ can now be considered. As already noted, the HEDTA complex has a larger pH dependence and it is contrary to that of EDTA. The origin of this is not clear, but assuming that the dependence observed with EDTA is essentially that of the protein (this is reasonable since this is the smallest pH dependence observed with any of the three reductants we have used, and $Fe(EDTA)^{2-/-}$ does not have a pK in the region around pH 6-7) then the observed pH dependence must be attributed to the $Fe(HEDTA)^{-/}$ system. In the case of the HEDTA system, there is a pK which shifts from 9 in the ferrous form to 4 in the ferric form, thus a proton is lost on oxidation near neutral pH.[3] The availability of a group near the active site to accept this proton would stabilize the products of the reduction of the laccase, and this would be expected to stabilize Fe(III) with respect to Fe(II) and thus make the ferrous form more strongly reducing. If the group which is available at pH 7 is not available at pH 6, the rate is expected to decrease at pH 6 based on free energy correlation. The small pH effect in the case of $Fe(EDTA)^{2-}$ may reflect an increased electrostatic binding between the reductant and laccase in the pH 6 form of laccase which would have a charge one higher at the site of protonation. Because of the contrary pH dependencies and the unknown value of the potential for the $Fe(HEDTA)^{-}$ couple, this part of the discussion cannot be taken further.

In the presence of azide at pH 6, although the azide free protein reacts faster with $Fe(EDTA)^{2-}$ than with the HEDTA complex, the two azide form reacts faster with the HEDTA complex than with $Fe(EDTA)^{2-}$. One explanation for this difference is that $Fe(HEDTA)^{-}$ having a charge one unit more positive than $Fe(EDTA)^{2-}$, is less affected by the introduction of negative charge in the region of reduction. Another explanation is that the HEDTA complex can bridge through the azide to type 2 copper (assuming that this is the binding site for the azide) and this π symmetry bridge facilitates the transfer of an electron from the π symmetry t_{2g} orbital of Fe(II) through the π symmetry orbitals of azide to the protein and eventually to the σ symmetry orbitals of the copper center. This latter explanation is weak for several reasons. First, such a pathway is expected to be of low energy only when all orbitals from the reductant through the bridge to the oxidant are of the same symmetry.[14] Furthermore, this explanation assumes that the azide is bound to the site being reduced, and since the type 2 site is assumed to be the position of the bound azide it is required that type 2 be reduced. The results with hydroquinone as the reductant do not require that type 2 be reduced for either type 1 or type 3 reduction (although it could be reduced prior to the reduction of type 3). The potential of type 2 (~ 365 mV)[5], at least in the native state, is also against reduction of this site, but the potential and coordination geometry are expected to change after coordination of azide. Perturbation of the iron center's potential by azide is also a possibility, but the low affinities of even the Fe(III) centers for azide preclude this possibility.

Within the assumption of type 2 binding of anions, which is supported by ESR evidence for the 405 nm absorbing form,[2] some discussion of the different possibilities for the binding of two azides may be given. The first binding constant for azide to Cu^{2+} (aq) is 230 at 0.2 M ionic strength ($NaClO_4$).[6] This is most comparable to the binding constant for the species which absorbs at 405 nm. It is to be expected that the binding constant for azide to type 2 copper will be lower than that to Cu^{2+}(aq), since the protein copper center is probably already coordinated by strong bonds in several positions. A further hint as to the coordination is that anation and azide inhibition kinetics following the 405 nm band are much cleaner at pH 6, and there seems to be a lower affinity at pH 7. This would be consistent with loss of an equatorial type 2 copper ligand and its replacement by azide, or the shift of a ligand such that the apical position on the type 2 copper is available for coordination to the azide. Since the azide with the lower binding constant is an activator it must either promote the reduction through a bridging role, or it must make the preferred reduction site more available than it is with only one azide bound. The high binding constant and strong inhibition of the other azide bound probably reflects binding influenced by groups other than just the type 2 copper; a possibility is type 3 copper which has been suggested as a site for azide binding, especially in ceruloplasmin.[7] The simplest explanation consistent with the results given here for the ferrous reductants is that the high binding constant azide fills the anion binding pocket enough to force the reducing agent to transfer its

electron from a greater distance. This mode of binding need not be directly to type 2 copper, and this is actually argued against since the binding constant is so high. The binding of the 405 nm absorbing species (at pH 6) and the suspected concomitant shift in type 2 copper ligation then opens the binding site slightly and allows closer approach of the reducing agent for more efficient outer sphere electron transfer.

In conclusion, some of the previous results on the reduction of laccase-azide complexes by hydroquinone will be mentioned to demonstrate the complicated nature of the whole issue. With hydroquinone as the reductant, the reduction was shown to be azide independent (0.02-0.15 M azide), as was essentially observed with the iron reductants over the same range, but with hydroquinone the reduction was also reducing agent independent (2.5-50 mM). This result led to the conclusion that a dissociation of the azide or another ligand was required for the reduction of type 1 to take place. Parallel first order kinetics were not observed with hydroquinone, and furthermore there was an initial fast reduction which could not be measured, but was attributed to native laccase. The results given here are not consistent with any laccase being totally free of azide at the concentrations used in the hydroquinone study; on the contrary, there should be some laccase which is free of the 405 nm absorbing azide and therefore more strongly inhibited. However, the requirement that hydroquinone act as an inner sphere reductant may explain the apparent requirement for azide dissociation. Previous studies of the reduction of the 330 nm band in laccase were not possible with the ferrous

reductants because the reductant masked this region, and previous studies of the reduction of the 405 nm band could not be duplicated because of the formation in the iron case of an $Fe-N_3$ species which absorbed at almost exactly the same wavelength.

References

1. R. A. Holwerda and H. B. Gray, J. Amer. Chem. Soc., 96, 6008 (1974).
2. L. Morpurgo, G. Rotilio, A. Finazzi-Agro, and B. Mondovi, Biochim. Biophys. Acta, 336, 324 (1974).
3. R. Skochdople and S. Chaberek, J. Inorg. Nucl. Chem., 11 (1959).
4. R. Przystas and N. Sutin, J. Amer. Chem. Soc., 95, 5545 (1973).
5. B. R. M. Reinhammar, Biochim. Biophys. Acta, 275, 245 (1972).
6. L. G. Sillen and A. E. Martell, Stability Constants of Metal Ion Complexes, The Chemical Society, London, (1964.)
7. W. Byers, G. Curzon, K. Barbett, B. E. Speyer, S. N. Young, and R. J. P. Williams, Biochim. Biophys. Acta, 310, 38 (1973).

CHAPTER 5

THE HETEROPOLY BLUE 18-MOLYBDODIPHOSPHATE AS A REAGENT: PREPARATION, STABILITY, PROBLEMS AND POSSIBILITIES

Introduction

The isopoly and heteropoly acids and salts formed from V, Nb, Ta, Cr, Mo and W are characterized by extensive condensation of the acid anhydrides to form large, oxygen bridged cage structures. The isopoly forms contain only one acid, while the heteropoly compounds are co-condensation products with other acids and metal ions (36 different elements which could form heteropoly ions were listed in 1961).[1] In the heteropoly anions, the guest is completely within the cage structure of the parent complex, but a further variation involves a hybrid structure between heteropoly anions and classical coordination complexes, in this case a central metal ion is coordinated to the oxygens of a heteropoly anion and to conventional ligands (NH_3, H_2O, pyridine, halide, etc.).[2]

The complex chosen for this work was the heteropolymolybdate $P_2Mo_{18}O_{62}^{6-}$. This complex is a dimer, each half contains one tetrahedral phosphorus surrounded by a ring of six molybdates; the phosphorus shares three oxygens with this ring of molybdates, each oxygen bridges two Mo atoms as well as the phosphorus, the remaining three Mo atoms form a cap and all share one oxygen with

the phosphorus and each shares two oxygens with the molybdates making up the ring. The dimer is symmetric about a plane between the two phosphorus atoms and parallel to the two rings of molybdates. This complex was chosen because it is the most stable of the class of heteropoly blues, clusters which accept many electrons and turn intensely blue in the process. The characteristic spectral changes which occur on reduction and the reduction potentials have been investigated; the band maxima and extinction coefficients (M^{-1} cm^{-1}) for the two, four, and six electron reduced species (pH 1.4, sulfuric acid) are 758 nm (11,000), 676 nm (19,400), and 599 nm (23,800), respectively.[3] The potentials for the three two electron steps (one electron reductions were not observed with the heteropolymolybdate, but were observed with the analogous heteropolytungstate) at pH 7 are 600, 180, and 20 mV (vs. hydrogen). The highest potential is pH independent in the range pH 4 to 10, then increases with decreasing pH, the other two potentials increase with pH over the entire range from pH 14 to 0, with a slope of 60 mV per pH unit below pH 6. The reduced species have been isolated and are more stable to alkaline degradation than the parent complex.[4]

Experimental

The complex $(NH_4)_6[P_2Mo_{18}O_{62}]$ $14H_2O$ was made by the method of Tsigidinos.[1] Fifteen milliliters of concentrated phosphoric acid was added to a solution of 100 g $NaMoO_4$ $2H_2O$ in 400 ml of water, followed by 80 ml of concentrated HCl. The yellow solution was refluxed for eight hours, solid NH_4Cl was added until precipitation began, then 100 ml of saturated NH_4Cl was added to give about 40 g of product.

The complex is quite soluble (unlike any Mo_{12} species which might be present) and thus is easily contaminated with NH_4Cl, thus the ammonium salt was converted to the less soluble methylammonium salt which could be recrystallized from warm water to give soft bundles of fibres. This product was dried in a dessicator. The product was characterized by its spectrum and behavior with reducing agents. The extent of hydration was determined by thermogravimetric analysis with a DuPont instrument. Samples of 30 to 40 mg were heated to 150° by which temperature no further weight loss was observed. The weight loss was 1 to 2 mg, and all weights were measured to 0.03 mg. Assuming the final form to be anhydrous, the water loss from the original sample was calculated and four runs gave stoichiometries of 6.00, 6.03, 5.66, and 5.80 molecules of water per cluster, thus six waters were assumed.

Kinetics of decomposition were followed at 315 nm at 25 with a Cary 14 spectrophotometer in a thermostated cell holder. The heteropolymolybdate solution, originally in water acidified to pH 3 with phosphoric acid, was added to an equal volume of the buffer/salt solution to give a final ionic strength of 0.5 M (0.2 from phosphate buffer; 0.3 from ammonium sulfate) and the desired pH (measured at the completion of the experiment).

Results and Discussion

Decomposition of the totally oxidized heteropolymolybdate was first order for 3 to 4 half lives. Rate constants at pH 7.1, 6.6, and 6.2 were 5.5 (10^{-3}) s^{-1}, 4.6 (10^{-3}) s^{-1}, and 2.9 (10^{-3}) s^{-1}. Thus,

with half lives of about 3 minutes, the complex is quite suitable for stopped flow experiments, but the more stable pH 3 solutions should be used and the pH jumped in the stopped flow experiment. The large extinction increase also makes this reagent appealing for use as the reagent in excess.

Oxidation of ferrocytochrome c by the heteropolymolybdate was attempted, but it was found that the protein was precipitated by the reagent on the stopped flow time scale.[6] A similar attempt was made with Rhus vernicifera laccase; in this case oxidation was observed in non-kinetic studies, but technical problems with maintaining an anaerobic environment and the rate of the reaction with the lower potential reagent $Co(phen)_3^{3+}$ discouraged further work.

References

1. G. A. Tsigidinos, Ph.D. Thesis, Boston University, 1961.
2. L. C. W. Baker and J. S. Figgis, J. Amer. Chem. Soc., 93, 3794 (1970).
3. E. Papaconstantinou and M. T. Pope, Inorg. Chem., 9, 667 (1970).
4. E. Papaconstantinou and M. T. Pope, ibid., 6, 1152 (1967).
5. Ref. 1, p 106.
6. D. Cummins and S. Wherland, unpublished observations.

CHAPTER 6

$Mn(CyDTA)^-$ AS A REAGENT: PREPARATION AND STABILITY

Introduction

Manganese(III) has not been commonly studied because of the susceptibility of this oxidation state to disproportionation to manganese(II) and manganese(IV) oxide; this problem is especially severe for the aquo ion, which is also a strong oxidant. The complexes of manganese(III) are significantly more stable with respect to disproportionation and are also weaker oxidants, owing to the high binding constants of the ligands.[1] The complexes of manganese(III) with EDTA and related ligands have been studied, especially its kinetic properties as an oxidant, by R. E. Hamm and coworkers. Systems studied include the oxidation of oxalate,[2] azide,[3] V(VI)-CyDTA,[4] H_2O_2,[5] and nitrite.[6]

From the work of Hamm and Suwyn,[1] the most stable of the complexes was found to be Mn(CyDTA) (CyDTA = trans-1,2-diaminocyclohexanetetraacetate). The spectrum of the complex in the pH range 2 to 7 shows a single broad peak at 510 nm, with an extinction coefficient of 345 M^{-1} cm^{-1}; at higher pH the peak shifts to higher energy, 448 nm with a shoulder on the low energy side, and has an extinction of 329 M^{-1} cm^{-1}. The transition between the two shows the form of a titration curve with a pK of 8.11. In analogy with the $Fe(EDTA)^-$ [7] system, this transition can be explained by the

ionization of a coordinated water molecule, and the subsequent formation of an oxygen bridged dimer. The E^0 value for $Mn(CyDTA)^{-1/-2}$ has been determined[1] at 25 in 0.05 M sodium acetate and a total ionic strength of 0.2 M made up with sodium perchlorate, as 814 mV. Decomposition of the complex to give some oxidized ligand and the manganese(II) complex, has been studied[1] in acetate buffer, pH 3 to 6, and found to be independent of pH and buffer concentration, with a rate constant of $6.5(10^{-6})$ s^{-1} at 25° and activation parameters of 24.3±0.3 kcal/mole and -1.5± 0.4 eu.

Experimental

The complex was synthesized by the method of Hamm and Suwyn, but crystals were not easily obtained by the freezing procedure outlined by these authors, but patience eventually produced dark red crystals which gave the following analysis (Caltech analysis by S. Rothschafer).

$KMn(CyDTA)H_2O$ Theory: C, 37.01; H, 4.44; N, 6.17

Found: C, 36.20; H, 4.28; N, 6.16

This compound was kept in the freezer and is reported to be light sensitive.

Kinetics were run in a Cary 14 spectrophotometer in a thermostatted cell holder. The ionic strength dependence was run with only phosphate buffer present, at pH 6; the temperature dependence was performed at 0.5 M ionic strength, pH 6.0, 0.2 M from buffer and 0.3 M from $(NH_4)_2SO_4$. Data analyzed by optimizing the infinity value, or by the Guggenheim method gave the same rate constants.

Results

The pH 6, 25° rate constants (times 10^5 s^{-1}) at ionic strengths 0.5, 0.2, 0.1, and 0.05 M are 12, 7.4, 8.4, and 8.0, respectively. Under the conditions of 0.5 M ionic strength (0.2 M from buffer, 0.3 M from $(NH_4)_2SO_4$, pH 6 the rate constants were $1.1(10^{-4})$ s^{-1} at 25, and 3.9 (10^{-4}) s^{-1} at 38, which gives activation parameter estimates of 18 kcal/mole and -16 eu.

The stability of $Mn(CyDTA)^-$ is significantly less than observed by Hamm and Suwyn, but this may be because of the higher ionic strengths used in this work, and because these data were taken at the extreme of the pH range they claim. The stability of the complex makes it convenient for even the slowest of stopped-flow experiments, and because of the larger temperature coefficient of the reaction, the Mn(III) solutions could be kept at a pH at least as high as six for several hours without appreciable decomposition. The extinction change on reduction might be useful to follow when using this reagent, but when it is used in excess, the baseline absorbance might be too large, and the extinction change would not be large enough to use in many protein reactions where 10^{-4} M concentrations are usually used.

$Mn(CyDTA)^-$ will oxidize Rhus vernicifera laccase, but the reaction was not studied kinetically.

References

1. R. E. Hamm and M. A. Suwyn, Inorg. Chem., 6, 139 (1967).
2. M. A. Suwyn and R. E. Hamm, Inorg. Chem., 6, 142 (1967).
3. M. A. Suwyn and R. E. Hamm, Inorg. Chem., 6, 2150 (1967).
4. D. J. Boone, R. E. Hunt, and J. P. Hunt, Inorg. Chem., 11, 1060 (1972).
5. T. E. Jones and R. E. Hamm, Inorg. Chem., 13, 1940 (1974).
6. T. E. Jones and R. E. Hamm, Inorg. Chem., 14, 1027 (1975).
7. H. J. Schugar, A. T. Hubbard, F. C. Anson, and H. B. Gray, J. Amer. Chem. Soc., 91, 71 (1969).

APPENDIX

KINETIC STUDIES OF THE REDUCTION OF BLUE COPPER PROTEINS BY $Fe(EDTA)^{2-}$

Introduction

Copper-containing proteins are found in a variety of biological electron-transfer systems. Of the different copper centers tha have been classified, the most distinctive is the type 1, which gives proteins associated with it their characteristic blue color.[1] This work is concerned with the relative reactivity of the type 1 site in four proteins, stellacyanin, plastocyanin, azurin, and *Rhus* laccase. Plastocyanins are common components of chloroplasts, azurins are found in several bacteria, and stellacyanin and laccase may be isolated from the latex of the Japanese lacquer tree.[1] Plastocyanin, azurin, and stellacyanin are one-copper proteins and are thought to have simple electron-transfer functions. Laccase is a four-copper protein and is classed as a *p*-diphenol:O_2 oxidoreductase (E.C. 1.10.3.2).

Detailed kinetic comparisons of the four proteins have not been made previously. One problem that must be overcome is that reactions involving some of the most common reducing agents, including ferrocyanide, give complex kinetic behavior.[2] We have used $Fe(EDTA)^{2-}$ in the present investigation, because it has given simple pseudo-first-order kinetics under anaerobic conditions with horse heart ferricytochrome *c*.[3] Furthermore, this complex cleanly reduces all four blue proteins.

Experimental Section

Laccase and stellacyanin were prepared essentially by the method of Reinhammar.[4] The acetone powder from Japanese Rhus vernicifera lacquer was acquired from Saito and Co., Ltd., Tokyo. Laccase was purified to an A_{280}/A_{614} of 15.2-15.6. Stellacyanin was used with A_{280}/A_{604} of 5.60-5.75.

Plastocyanin from French bean (Phaseolus vulgaris) was purified by the method of Milne and Wells[5] to an A_{280}/A_{597} of 1.1-1.2.

Azurin was extracted and purified from Pseudomonas aeruginosa (ATCC 10145) by a slight modification of procedures given by Ambler.[6] In the present case, the pH of the acetone powder extract was lowered only to 4.0 before the diluted extract was applied to a CM Cellulose column (30 × 4.5 cm Whatman CM 23 equilibrated with 0.05 M NH_4OAc, pH 4.0). Subsequent stepwise elution and further purification were performed as described elsewhere.[6] The purified oxidized azurin had an A_{625}/A_{280} ratio of 0.44 and showed one band on starch gel electrophoresis.[7] A slight hint of a band at 415 nm was observed in the most concentration azurin solutions, indicating only a trace of cytochrome impurity was present. The yield of purified azurin was 280 mg from 180 gm of the acetone powder. Purified azurin was dialyzed into 0.05 M NH_4OAc(pH 4.0) buffer, millipore filtered, and stored at 4°. Before each series of kinetic experiments, the azurin was dialyzed against the requisite buffer solution.

Laccase, stellacyanin, and plastocyanin were shell frozen and stored under liquid nitrogen. Azurin was millipore-filtered and stored

refrigerated in sterile vials in 0.05 M, pH 4.0 ammonium acetate buffer.

Reagent grade chemicals were used without further purification. Sephadex and Whatman ion exchangers and Sephadex gel filtration resins were used. Union Carbide dialysis membrane was boiled extensively to remove sulfur-containing impurities. Rubber serum caps were boiled in concentrated base before using.

The nitrogen gas used for deoxygenation of kinetic solutions was purified of oxidizing impurities by passage through two chromous scrubbing towers.

Kinetic Measurements and Data Analysis. All kinetic experiments were performed on a Durrum Model D-110 stopped-flow spectrometer. Solutions to be mixed were allowed at least 15 min at room temperature and 30 min at other temperatures to come to temperature equilibrium. Bath temperature was maintained ± 0.2° with a Forma Scientific bath. Drive syringes with Viton O rings were used, and the valve block inlets were modified to accept gas-tight fittings for Teflon needles, through which deoxygenated solutions were drawn. Any solution which remained in the Teflon needle transfer lines for more than the time needed to transfer was not used, as these lines are oxygen permeable. Most data were collected on a 128 channel analog input buffer, collecting points at intervals of 1-9999 msec. Absorbance changes of 0.05 were routinely used. These data were then transferred to disk storage on the Caltech PDP-10 time-sharing system. Some data were taken as Polaroid pictures from

a Tektronix 564B oscilloscope or, for slow runs, from Hewlett-Packard Model 700 B-x-y recorder traces.

Laccase and stellacyanin solutions were prepared by first dialyzing against triply distilled water and then diluting to volume with precisely weighed amounts of phosphate buffer and ammonium sulfate to give the desired pH, ionic strength, and protein concentration. Plastocyanin and azurin were made up by dialyzing against the desired protein concentration. Protein solutions were degassed by gentle bubbling with deoxygenated nitrogen, or by evacuation of the serum-capped bottles through a large needle, followed by storage under a stream of deoxygenated nitrogen. Laccase solutions were maintained cold, whereas the other proteins were left at room temperature for the duration of a day of kinetic experiments.

Ferrous EDTA solutions were made up by dissolving ferrous ammonium sulfate hexahydrate in deoxygenated water and then transferring an aliquot of this solution to a deoxygenated solution of disodium dihydrogen EDTA, phosphate buffer, and ammonium sulfate. The protons released from the EDTA were neutralized with sodium hydroxide and the pH of the resulting stock solution was determined with a Brinkmann pH meter using a combination electrode in the bubbler. This stock solution was then diluted into deoxygenated solutions of buffer and ammonium sulfate. All transfers were done with Hamilton gas-tight syringes. The concentration of EDTA was maintained in at least 20% excess over iron.

All data were analyzed as pseudo-first-order in protein with the reducing agent in 100-10,000-fold excess. Standard first-order plots were typically linear over at least 3 half-lives, and rate constants were taken from unweighted least-squares analysis. For the laccase data, an initial induction period had to be ignored. The origin of this induction period and a discussion of the rationale for ignoring it have been discussed at length elsewhere, and will not be repeated here.[8] The wavelengths followed were 626, 614, 597, and 604 nm for azurin, laccase, plastocyanin, and stellacyanin, respectively.

For concentration and temperature dependence data, weighted least-squares analyses were done. Weighting factors for the concentration dependence fits were the square of the inverse of the standard deviation from the mean of the multiple determinations done (usually three) from one filling of the drive syringes. For the temperature dependence data, the Eyring plots had the ln (k/T) values weighted as one over their standard deviations, with the standard deviations determined in the same way.[9]

Results

Plots of k_{obsd} vs. $Fe(EDTA)^{2-}$ for all four blue proteins are shown in Figure 1, and plots of k_{obs} (normalized) vs. pH for all four proteins are shown in Figure 2. Table 1 presents a summary of some of the rate constants and Table 2 gives the activation parameters. All data are shown in the Supplementary Tables.

The discussion of these data is included in the general

presentation Chapter [1]. This work was done with Robert Holwerda and Robert Rosenberg.[10,11]

References

1. R. Malkin and B. G. Malmstrom, Adv. Enzymol., 33, 177 (1970).
2. R. A. Holwerda and H. B. Gray, J. Amer. Chem. Soc., in press.
3. H. L. Hodges, R. A. Holwerda, and H. B. Gray, J. Amer. Chem. Soc., 96, 3132 (1974).
4. B. Reinhammar, Biochim. Biophys. Acta, 205, 35 (1970).
5. P. R. Milne and J. R. E. Wells, J. Biol. Chem., 245, 1566 (1970).
6. a) R. P. Ambler and L. H. Brown, Biochem. J., 104, 784 (1969); b) R. P. Ambler and M. Wynn, Biochem. J., 131, 485 (1973).
7. O. Smithies, Adv. Prot. Chem., 14, 65 (1959).
8. R. A. Holwerda and H. B. Gray, J. Amer. Chem. Soc., 96, 6008 (1974).
9. D. Margerison in "Comprehensive Chemical Kinetics," Vol. I, C. H. Bamford and C. F. H. Tipper, Ed., Elsevier, Amsterdam, 1969, Chapter 5.
10. S. E. Wherland, R. A. Holwerda, R. C. Rosenberg, and H. B. Gray, J. Amer. Chem. Soc., 97, 5260 (1975).
11. R. C. Rosenberg, S. Wherland, and H. B. Gray, J. Amer. Chem. Soc., in press.

Table I Rate Constants

Protein	Dependence	$[Fe(EDTA)^{2-}]$ M	pH	μ (M)	k
Stellacyanin	Reducing Agent	-	6.9	0.5	$4.3(10^{5})\underline{M}^{-1}\,sec^{-1}$
	pH	$5.0(10^{-4})$	5.0	0.5	$272\pm10^{a}\ sec^{-1}$
		$5.0(10^{-4})$	7.8	0.5	$209\pm3\ sec^{-1}$
Plastocyanin	Reducing Agent	-	6.9	0.2	$8.2(10^{4})(4)^{b}\ \underline{M}^{-1}\,sec^{-1}$
	pH	$2.0(10^{-4})$	5.6	0.2	$8.4\pm0.2\ sec^{-1}$
		$2.0(10^{-4})$	7.4	0.2	$12.2\pm0.5\ sec^{-1}$
Azurin	Reducing Agent	-	7.0	0.2	$1.3(10^{3})(0.6)\underline{M}^{-1}\,sec^{-1}$
Laccase	Reducing Agent	-	6.9	0.5	$2.6(10^{2})(0.7)\underline{M}^{-1}\,sec^{-1}$
	pH	$1.0(10^{-3})$	4.9	0.5	$0.295\pm0.001\ sec^{-1}$
		$1.0(10^{-3})$	7.7	0.5	$0.166\pm0.001\ sec^{-1}$
	Ionic Strength	$1.0(10^{-3})$	6.9	0.06	$0.318\pm0.007\ sec^{-1}$
			7.1	0.52	$0.250\pm0.012\ sec^{-1}$
	$[Fe(EDTA)^{-}]^{c}$	$1.0(10^{-3})$	6.9	0.5	
	$4.96(10^{-4})\underline{M}$				$0.315\pm0.009\ sec^{-1}$
	$8.50(10^{-3})\underline{M}$				$0.404\pm0.036\ sec^{-1}$
	$[EDTA^{2-}]$	$1.0(10^{-3})$	6.9	0.5	
	$2.0(10^{-4})\underline{M}$				$0.31\pm0.02\ sec^{-1}$
	$5.0(10^{-3})\underline{M}$				$0.37\pm0.03\ sec^{-1}$

Footnotes to Table I

[a]The standard error of the mean of multiple determinations done on one filling of the drive syringes is designated as ±.

[b]The numbers in parentheses quoted here are the standard deviations of the slope as given by the weighted least squares analysis and are included as an indication of goodness of fit.

[c]These values for free $Fe(EDTA)^-$ are corrected from the amounts actually added for the amount of oxobridged dimer at pH 7 [see H. J. Schugar, A. T. Hubbard, F. C. Anson, and H. B. Gray, J. Amer. Chem. Soc., 91, 71 (1969)].

Table II Activation Parameters

Protein	$[Fe(EDTA)^{2-}]M$	pH	μ(M)	$\Delta H^{\ddagger}$(kcal/mole)	$\Delta S^{\ddagger}$(eu)
Stellacyanin	$5.0(10^{-4})$	7.0	0.1	3.0(0.003)[a]	−21 (0.1)
Plastocyanin	$8.0(10^{-4})$	7.0	0.2	1.9(0.01)	−30(0.02)
	$4.0(10^{-4})$	7.0	0.2	2.4(0.005)	−28(0.002)
Azurin	$7.5(10^{-4})$	7.0	0.2	2.4(0.01)	−36(0.04)
	$2.0(10^{-3})$	7.0	0.2	1.7(0.01)	−38(0.02)
Laccase	$1.09(10^{-3})$	7.0	0.1	13 (0.004)	−5.1(0.001)

[a]The numbers in parentheses are the standard deviations of the slope or intercept (or quantities directly proportional to these standard deviations) as given by the weighted least squares analysis and are included as a measure of goodness of fit.

Figure 1. Dependence of k_{obs} on the concentration of $Fe(EDTA)^{2-}$ for stellacyanin (A), plastocyanin (B), azurin (C), and laccase. Conditions are given in Table 1.

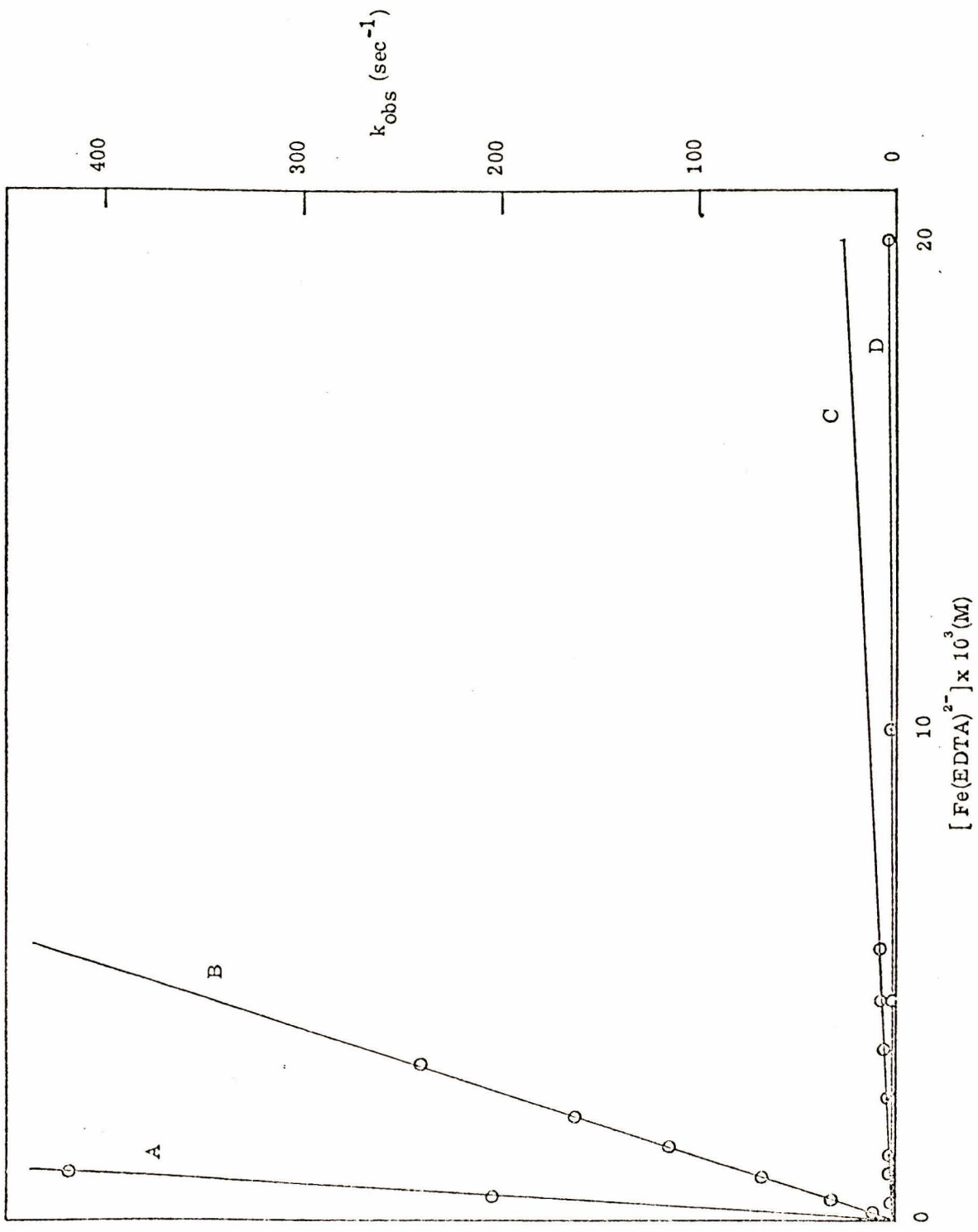
k_{obs} (sec^{-1})
400
300
200
100
0
A
B
C
D
0
10
20
[Fe(EDTA)$^{2-}$] x 10^{3}(M)

Figure 2. Dependence of the rate constants on pH. The rates for each protein are normalized to the mean of k_a and k_b as given in Table 2. The best-fit curves are shown for each protein. Data symbols are: laccase, □; azurin, ◇; plastocyanin, △; and stellacyanin, ○.

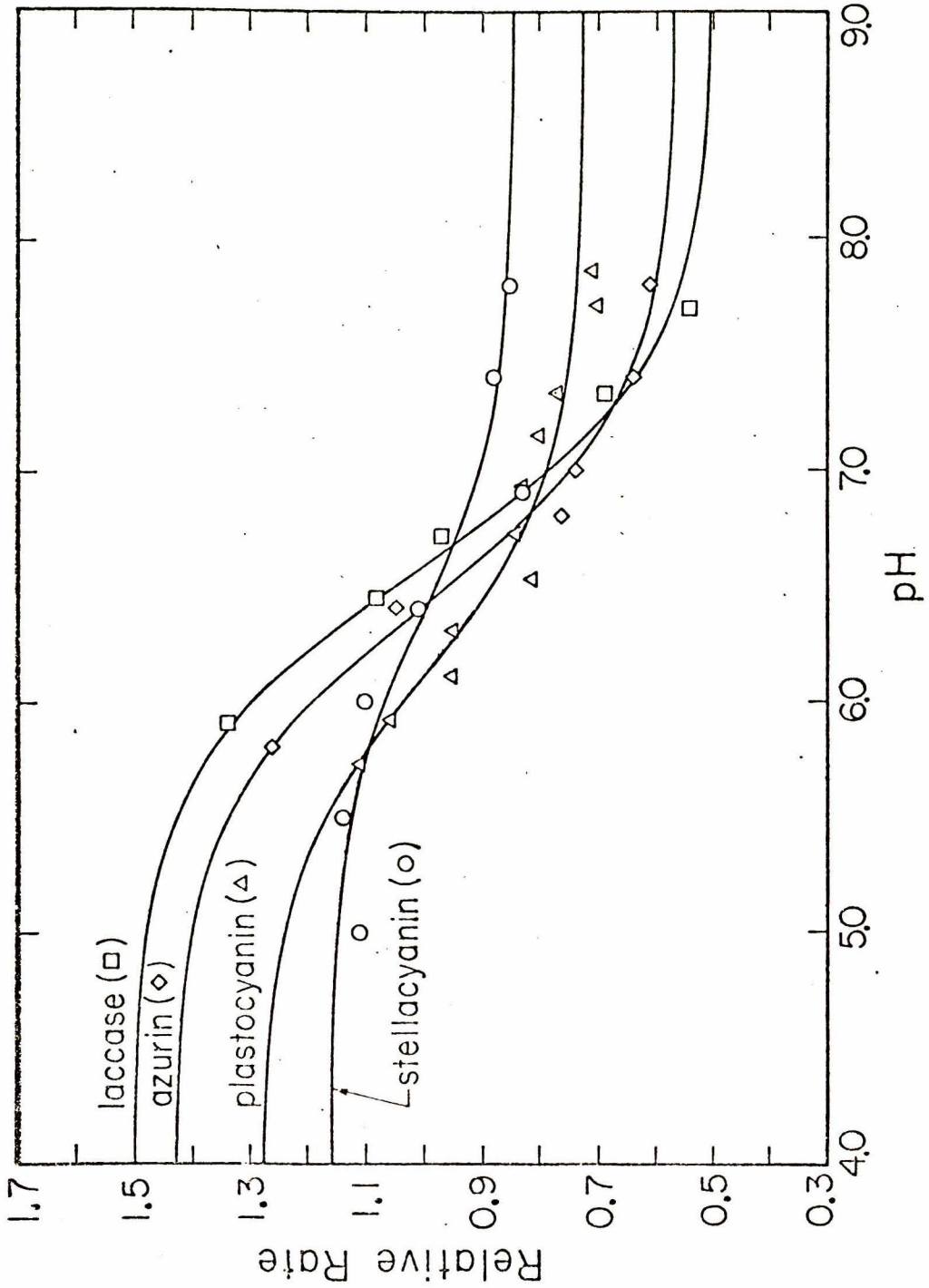
laccase (□)
azurin (◇)
plastocyanin (△)
stellacyanin (○)
Relative Rate
1.7
1.5
1.3
1.1
0.9
0.7
0.5
0.3
4.0
5.0
6.0
7.0
8.0
9.0
pH

Supplementary Table 1
$Fe(EDTA)^{2-}$ Reduction of Blue Proteins-Data

Protein	$k_{obs}(sec^{-1})$ Mean	Stand. Error	T(°C)	Ionic Strength (M) μ_{total}	μ_{buffer}	$[Fe(EDTA)^{2-}]$ mM	pH	λ	$[EDTA]_{free}$ (mM)	$[Fe(EDTA)^{-}]$ (mM)
stellacyanin	247	6.4	25.2	0.5	0.26	0.5	6.4	604		
	214	0.22	25.2	0.5	0.26	0.5	7.4	604		
	209	2.81	25.2	0.5	0.26	0.5	7.8	604		
	272	9.65	25.2	0.5	0.26	0.5	5.0	604		
	279	3.39	25.2	0.5	0.26	0.5	5.5	604		
	270	5.08	25.2	0.5	0.26	0.5	6.0	604		
	204	1.45	25.1	0.5	0.26	0.5	6.9	604		
	418	1.08	25.1	0.5	0.26	1.0	6.9	604		
	500	12.77	25.1	0.1	0.04	0.5	7.0	604		
	659	40.63	38.3	0.1	0.04	0.5	7.0	604		
	511	12.91	30.7	0.1	0.04	0.5	7.0	604		
	399	18.74	15.9	0.1	0.04	0.5	7.0	604		
	321	8.04	7.8	0.1	0.04	0.5	7.0	604		
	416	8.82	20.2	0.1	0.04	0.5	7.0	604		
laccase	0.0710	0.00223	25.1	0.5	0.3	0.5	6.9	614		
	0.215	0.00125	25.1	0.5	0.3	1	6.9	614		
	0.615	0.000270	25.1	0.5	0.3	2.5	6.9	614		
	1.23	0.0384	25.1	0.5	0.3	5	6.9	614		

Protein	k_{obs} (sec^{-1}) Mean	Stand. Error	T(°C)	Ionic Strength (M) μ_{total}	μ_{buffer}	$[Fe(EDTA)^{2-}]$ mM	pH	λ	$[EDTA]_{free}$ (mM)	$[Fe(EDTA)^{-}]$ (mM)
	2.25	0.0223	25.1	0.5	0.3	10	6.9	614		
	3.81	0.200	25.1	0.5	0.3	20	6.9	614		
	0.0661	0.000472	8.3	0.1	0.04	1.09	7.0	614		
	0.140	0.00135	16.7	0.1	0.04	1.09	7.0	614		
	0.255	0.00270	25.7	0.1	0.04	1.09	7.0	614		
	0.399	0.00270	31.6	0.1	0.04	1.09	7.0	614		
	0.666	0.00573	38.2	0.1	0.04	1.09	7.0	614		
	0.176	0.000337	8.3	0.1	0.04	2.73	7.0	614		
	0.380	0.00472	16.7	0.1	0.04	2.73	7.0	614		
	0.761	0.00135	25.7	0.1	0.04	2.73	7.0	614		
	1.21	0.0128	31.6	0.1	0.04	2.73	7.0	614		
	1.95	0.0438	38.2	0.1	0.04	2.73	7.0	614		
	0.295	0.00135	25.6	0.5	0.3	1	4.92	614		
	0.354	0.00902	25.6	0.5	0.3	1	5.40	614		
	0.421	0.00200	25.6	0.5	0.3	1	5.92	614		
	0.335	0.00606	25.6	0.5	0.3	1	6.32	614		
	0.300	0.00297	25.6	0.5	0.3	1	6.72	614		
	0.215	0.00147	25.6	0.5	0.3	1	7.33	614		
	0.166	0.000595	25.6	0.5	0.3	1	7.70	614		

Protein	k_{obs} (sec^{-1}) Mean	Stand. Error	T(°C)	Ionic Strength (M) μ_{total}	μ_{buffer}	$[Fe(EDTA)^{2-}]$ mM	pH	λ	$[EDTA]_{free}$ (mM)	$[Fe(EDTA)^{-}]$ (mM)
	1.54	0.0167	25.6	0.5	0.3	5	4.94	614		
	1.74	0.0200	25.6	0.5	0.3	5	5.39	614		
	1.78	0.0335	25.6	0.5	0.3	5	5.92	614		
	1.62	0.0521	25.6	0.5	0.3	5	6.33	614		
	1.33	0.0110	25.6	0.5	0.3	5	6.79	614		
	0.967	0.00888	25.6	0.5	0.3	5	7.36	614		
	0.853	0.00384	25.6	0.5	0.3	5	7.77	614		
	0.318	0.00740	25.6	0.06	-	1	6.87	614		
	0.279	0.0168	25.6	0.202	0.3	1	6.99	614		
	0.232	0.00898	25.6	0.304	0.3	1	7.02	614		
	0.257	0.00472	25.6	0.409	0.3	1	7.00	614		
	0.250	0.0119	25.6	0.521	0.3	1	7.06	614		
	0.310	0.0201	25.0	0.5	0.3	1	6.94	614	0.2	
	0.329	0.0347	25.0	0.5	0.3	1	6.94	614	0.5	
	0.328	0.0256	25.0	0.5	0.3	1	6.94	614	1.0	
	0.281	0.0117	25.0	0.5	0.3	1	6.92	614	3.0	
	0.372	0.0316	25.0	0.5	0.3	1	6.87	614	5.0	
	0.315	0.00868	25.0	0.5	0.3	1	6.98	614		0.496
	0.364	0.0395	25.0	0.5	0.3	1	6.96	614		0.985

Protein	$k_{obs}(sec^{-1})$ Mean	Stand. Error	T(°C)	Ionic Strength (M) μ_{total}	μ_{buffer}	$[Fe(EDTA)^{2-}]$ mM	pH	λ	$[EDTA]_{free}$ (mM)	$[Fe(EDTA)^{-}]$ (mM)
	0.330	0.00773	25.0	0.5	0.3	1	6.94	614		4.63
	0.404	0.359	25.0	0.5	0.3	1	6.94	614		8.5
	0.556	0.0121	25.0	0.5	0.3	1	6.94	614		13.2
plastocyanin	239	5.65	25.5	0.2	0.05	3.15	6.94	597		
	162	5.09	25.5	0.2	0.05	2.10	6.94	597		
	114	1.57	25.5	0.2	0.05	1.46	6.94	597		
	68.7	0.89	25.5	0.2	0.05	0.879	6.94	597		
	50.7	0.217	25.5	0.2	0.05	0.63	6.94	597		
	33.4	0.0595	25.5	0.2	0.05	0.42	6.94	597		
	19.8	0.469	25.5	0.2	0.05	0.28	6.94	597		
	12.0	0.287	25.5	0.2	0.05	0.175	6.94	597		
	8.35	0.192	25.0	0.2	0.05	0.2	5.6	597		
	6.14	0.205	25.0	0.2	0.05	0.2	6.2	597		
	10.4	0.198	25.0	0.2	0.05	0.2	6.75	597		
	12.61	0.290	25.0	0.2	0.05	0.2	7.25	597		
	12.2	0.507	25.0	0.2	0.05	0.2	7.40	597		
	55.93	0.210	24.4	0.2	0.05	0.8	7.04	597		

Protein	$k_{obs}(sec^{-1})$ Mean	Stand. Error	T(°C)	Ionic Strength (M) μ_{total}	μ_{buffer}	$[Fe(EDTA)^{2-}]$ mM	pH	λ	$[EDTA]_{free}$ (mM)	$[Fe(EDTA)^{-}]$ (mM)
	25.92	0.441	24.4	0.2	0.05	0.4	7.04	597		
	66.74	0.616	31.0	0.2	0.05	0.8	7.04	597		
	30.24	0.250	31.0	0.2	0.05	0.4	7.04	597		
	46.37	0.0954	19.8	0.2	0.05	0.8	7.04	597		
	25.08	0.264	19.8	0.2	0.05	0.4	7.04	597		
	47.09	0.162	14.0	0.2	0.05	0.8	7.04	597		
	19.84	0.209	13.9	0.2	0.05	0.4	7.04	597		
	41.11	0.169	7.5	0.2	0.05	0.8	7.04	597		
	19.43	0.0236	7.4	0.2	0.05	0.4	7.04	597		
azurin	0.517	0.00556	25.8	0.2	0.05	0.40	7.0	626		
	1.178	0.00981	25.8	0.2	0.05	0.90	7.0	626		
	1.94	0.0361	25.8	0.2	0.05	1.50	7.0	626		
	3.20	0.0146	25.8	0.2	0.05	2.50	7.0	626		
	4.68	0.0259	25.8	0.2	0.05	3.50	7.0	626		
	6.00	0.0639	25.8	0.2	0.05	4.50	7.0	626		
	7.30	0.0631	25.8	0.2	0.05	5.50	7.0	626		
	1.16	0.00956	25.5	0.2	0.05	0.75	7.0	626		
	0.765	0.00309	9.0	0.2	0.05	0.75	7.0	626		

Protein	$k_{obs}(sec^{-1})$ Mean	Stand. Error	T(°C)	Ionic Strength (M) μ_{total}	μ_{buffer}	$[Fe(EDTA)^{2-}]$ mM	pH	λ	$[EDTA]_{free}$ (mM)	$[Fe(EDTA)^{-}]$ (mM)
	0.987	0.00765	14.0	0.2	0.05	0.75	7.0	626		
	1.04	0.00919	18.2	0.2	0.05	0.75	7.0	626		
	1.30	0.00104	31.6	0.2	0.05	0.75	7.0	626		
	2.74	0.00126	25.3	0.2	0.05	2.00	7.0	626		
	2.04	0.00226	8.9	0.2	0.05	2.00	7.0	626		
	2.40	0.00326	14.0	0.2	0.05	2.00	7.0	626		
	2.60	0.00159	18.3	0.2	0.05	2.00	7.0	626		
	2.90	0.00237	31.5	0.2	0.05	2.00	7.0	626		

Supplementary Table 2. Ionic Strength and pH Dependences

A. pH Dependences

Protein	pH	k(sec^{-1})	σ^a
Azurin[b]	5.80	$2.25(10^3)M^{-1}$	0.00708
	6.40	$1.87(10^3)M^{-1}$	0.00113
	6.80	$1.36(10^3)M^{-1}$	0.00155
	7.00	$1.31(10^3)M^{-1}$	0.00102
	7.40	$1.19(10^3)M^{-1}$	0.000767
	7.80	$1.08(10^3)M^{-1}$	0.000515
Stellacyanin[c]	5.00	$2.72(10^2)$	9.65
	5.50	$2.79(10^2)$	3.39
	6.00	$2.70(10^2)$	5.08
	6.40	$2.47(10^2)$	6.40
	6.90	$2.04(10^2)$	1.45
	7.40	$2.14(10^2)$	0.22
	7.80	$2.09(10^2)$	2.81
Plastocyanin[d]	5.73	48.1	0.9
	5.93	45.9	1.3
	6.11	41.1	1.0
	6.31	41.3	1.0
	6.53	35.3	0.7
	6.74	36.4	0.6
	6.93	36.0	0.8
	7.15	34.5	0.8
	7.34	33.2	0.7
	7.72	30.3	0.8
	7.87	30.9	0.5
Laccase[e]	4.92	0.354	0.001
	5.40	0.421	0.009
	5.92	0.421	0.002
	6.32	0.335	0.006
	6.72	0.300	0.003
	7.33	0.215	0.001

Supplementary Table 2 (Continued)

	7.70	0.166	0.001
	4.94	1.54	0.02
	5.39	1.74	0.03
Laccase[f]	5.92	1.78	0.0034
	6.33	1.62	0.05
	6.79	1.33	0.01
	7.36	0.967	0.009
	7.77	0.853	0.004

B. Ionic Strength Dependences

Azurin (pH 6.8, 25.5 ± 0.1°, 5mM phosphate)

$[Fe(EDTA)^{2-}]$	μ	k_{obs}	σ
0.3 mM	0.01	0.349	0.007
	0.035	0.394	0.009
	0.075	0.416	0.018
	0.130	0.444	0.012
	0.200	0.453	0.014
	0.350	0.510	0.015
0.4 mM	0.010	0.452	0.014
	0.035	0.532	0.013
	0.075	0.558	0.014
	0.130	0.583	0.009
	0.200	0.612	0.017
	0.350	0.676	0.022

Plastocyanin (pH 6.9, 25.1 ± 0.2°, 3 mM phosphate)

1.0 mM	0.05	31.1	1.0
	0.10	49.5	1.7
	0.20	75.9	1.2
	0.30	89.1	4.0
	0.50	113.	4.0

[a] For the azurin data, the standard deviations of the second order rate constants are those of the slopes from the $1/\sigma^2$ weighted least squares fits of the concentration dependences at each pH. For the other proteins, the standard deviations are those from the mean of the multiple determinations performed.

Supplementary Table 2 (Continued)

[b] 25.0°, μ = 0.2 M, 0.05 M from buffer.

[c] 25.2°, μ = 0.5 M, 0.26 M from buffer, 0.5 mM $Fe(EDTA)^{2-}$.

[d] 25.0°, μ = 0.2 M, 0.18 M from buffer, 1.0 mM $Fe(EDTA)^{2-}$.

[e] 25.6°, μ = 0.5 M, 0.3 M from buffer, 1.0 mM $Fe(EDTA)^{2-}$.

[f] 25.6°, μ = 0.5 M, 0.3 M from buffer, 5.0 mM $Fe(EDTA)^{2-}$.